1964

Elastic and partially plastic instability of multi-story frames, PhD Dissertation, September 1964

Y. C. Yen

ELASTIC AND PARTIALLY PLASTIC INSTABILITY

OF

MULTI-STORY FRAMES

by

Yu-Chin Yen

A Dissertation

Presented to the Graduate Faculty

of Lehigh University

in Candidacy for the Degree of

Doctor of Philosophy

Lehigh University

1964

Approved and recommended for acceptance as a dissertation in partial fulfillment of the requirements for the degree of Doctor of Philosophy.

_____ (Date)

_____
George C. Driscoll, Jr.
Professor in Charge

Accepted, _____ (Date)

Special committee directing the doctoral work of Mr. Yu-Chin Yen

_____
Professor Cornie L. Hulsbos, Chairman

_____
Professor George E. Raynor

_____
Professor Charles C. Taylor

_____
Professor William J. Eney

_____
Professor George C. Driscoll, Jr.

ACKNOWLEDGMENTS

The author is greatly indebted to Dr. George C. Driscoll, Jr., Professor in charge of the dissertation, for his encouragement, advice, and valuable suggestions during the preparation of this dissertation. The guidance of Professors Cornie L. Hulsbos, George E. Raynor, Charles C. Taylor, and William J. Eney, chairman and members respectively of the Special Committee directing the author's doctoral work, is gratefully acknowledged.

The work described in this dissertation is part of a project on "Welded Continuous Frames and Their Components" sponsored jointly by the Welding Research Council and the U. S. Navy Department under an agreement with the Institute of Research of Lehigh University. Funds are supplied by the American Iron and Steel Institute, the American Institute of Steel Construction, Office of Naval Research, Bureau of Ships, and the Bureau of Yards and Docks. The Column Research Council of the Engineering Foundation acts in an advisory capacity. The work was done at Fritz Engineering Laboratory, Department of Civil Engineering, Lehigh University, Bethlehem, Pennsylvania. Professor William J. Eney is the Head of the Laboratory, and the Department and Professor Lynn S. Beedle is the Director of the Laboratory.

The author wishes to express his appreciation to Dr. T. R. Higgins, Director of Engineering and Research, American Institute of Steel Construction, for his continued interest in the progress of the research work reported herein.

Sincere gratitude is extended to all the author's associates at Fritz

Laboratory for helping to perform the test, especially to Dr. Theodore V. Galambos and Dr. Le-Wu Lu for fruitful discussion.

The help of Mr. Kenneth R. Harpel for preparing the test setups and specimens is gratefully appreciated, and acknowledgment is also due to Mr. Chin-Lian Chang for helping with the computations.

The manuscript was typed with care by Miss Rosalie R. Fischer. Her cooperation is appreciated.

TABLE OF CONTENTS

TABLES

FIGURES

ABSTRACT

A symmetrical multi-story frame under symmetrical vertical load may buckle sideways, if the load reaches the critical buckling load.

In this dissertation an energy method has been used to determine the buckling load of frames in the inelastic range as well as in the elastic range. The problem is solved by extending the Raleigh-Ritz method. Deformed shapes of beams and columns are assumed, boundary conditions at joints of members are imposed, and the total bending strain energy and potential energy of external loads of the frame are expressed as functions of deformation parameters. The buckling load of a frame is obtained by solving a buckling condition resulting from minimization of the total potential energy of the frame.

For a frame with slender columns, the frame buckles in the elastic range and the effect of primary bending moment upon buckling of the frame is not significant. Therefore the frame is assumed under concentric column loads.

For frames with medium slenderness of columns, the frame is likely to buckle in the inelastic range. In this case the inelastic energy method can be applied.

In building frames, however, columns are very stout. Therefore the frame might buckle when some plastic hinges have developed in the frame. The discontinuity due to hinge rotation is another burden to the buckling analysis of the building frame. Moreover, plastic hinges on one side of a frame undergo strain reversal and become elastic again at the instant of bifurcation. In this case the

frame under primary bending moments was not solved by exact method.

The frame was solved by introducing hinges on the ends of beams according to the concept of a deteriorated frame. Reductions of stiffnesses due to primary bending moments on beams and axial loads on columns were taken into account.

A computer program for inelastic buckling analysis of an eleven-story building frame under concentric column load is included. Another program for deformation analysis of the frame reveals the fact that the frame has a definite buckling mode.

Finally an experimental technique is shown to obtain the buckling load of a three-story frame. The results of a frame stability test are analyzed and compared with the results obtained from the proposed method and existing methods.

1. INTRODUCTION

1.1 Frame Instability and Method of Plastic Design

In plastic design of multi-story frames, the members are proportioned by a criterion based on the load leading to the formation of a failure mechanism. However, it is possible that the frame as a whole may buckle at a load much smaller than the ultimate load corresponding to the failure mechanism. Therefore, instability problems may govern the design of multi-story frames. According to the results of some single story rectangular frame tests[1.1], the load-carrying capacity of a frame is only 80 to 90% of the plastic load. For tall building frames the axial loads on the columns are much larger than the load on the beams. Under such a high axial load and small bending moment on the columns, the overall instability problem becomes critical and the frame as a whole may sway sideways in the lower story of the frame. On the contrary, for a single-story frame with distributed load on the beam, it is likely that the failure mechanism in the plastic design governs. Therefore, in the analysis of multi-story building frames, an important criterion should be satisfied, i. e. overall instability of the frame due to high axial loads on columns should be examined. The criteria concerning the limitation and capacity of deformation, lateral torsional buckling, local buckling and plastic strength of a member are discussed in detail elsewhere[1.2][1.3][1.4][1.5][1.6].

1.2 Statement of the Problem

There are many factors which affect the buckling load of a frame. It is essential to understand clearly each of these variables before the

type of the frame instability problem can be classified. Once the individual type of problem is formulated, suitable variables can be chosen for investigation according to practical necessity and their importance.

The factors affecting frame instability loads are the following:

(1) Slenderness ratio of columns. This is the most important factor governing the buckling load of a frame as can be seen from load vs. slenderness curve of a frame in Fig. 5.2.

(2) Stiffness of beams. The stiffness of beams is an important factor affecting the buckling load of a frame. A stiffer beam introduces more restraint on columns at the instant of buckling.

(3) Degree of restraint at supports. Pinned, partial-fixed or fix-ended conditions have substantial influence on the critical load of a frame. As shown in Table 6.2 and 6.3, effective length factor K's for fix-ended frames are more than twice as much as those of pin-ended frames. However, K values of practical structures should fall somewhere between these two extreme values.

(4) Types of steel. Since the stress-strain curves and moment-curvature relations vary with different types of materials, the buckling loads of frames differ accordingly.

(5) Cross-sectional shapes. With adequate lateral bracing, a cross-section of a member with a larger moment of inertia is more efficient in resisting buckling of a frame. When a frame is loaded into the inelastic range, the re-

sidual stresses and yielding patterns of a member are quite different depending on the cross-sectional shape of the member.

(6) Loading conditions. Whether the loads are symmetrically applied or whether they produce primary bending moment in the frames are factors affecting the instability of frames. The structure might be in the most critical state when possible dynamic loads are applied. The method of analysis presented in this dissertation can be regarded as the first step toward the analysis of stability problem including the effect of dynamic load on the frame.

(7) Loading sequence. In the inelastic range, the behavior of a structure is non-conservative in its nature. When a structure is non-conservative, the structure may have more than one deformed configuration under the same intensity of load. Under strain reversal, mechanical energy is transformed into dissipated heat. The process is not reciprocal. Therefore, the final status of the structure depends on the loading history. For proportionally increasing vertical and horizontal loads on a frame, no strain reversal would occur in its members. However, a structure may undergo unloading in some part of the members, if the vertical loads are applied first and then the horizontal loads follow.

(8) Existence of shear wall or bracing. In actual building frames, the walls or even partitions help resist sway considerably. The effect of bracing can enforce the frames to buckle in symmetrical modes which result in much higher critical loads than anti-symmetrical modes.

Types of frame instability are classified according to their loading conditions in Fig. 1.1.

Type A is characterized by the bifurcation of equilibrium position at the critical load. If the loads are not symmetrical, horizontal deflection develops immediately after the vertical loads are applied as shown in type B. Type C is characterized by the application of proportional horizontal and vertical loads. This is a typical problem to be found in most of the literature. However, type D is a more practical situation. The frames under vertical loads are subjected to gradually increasing horizontal loads. The windward corners will undergo considerable strain reversal. To neglect this effect would result in a conservative analysis. However, its quantitative picture is totally unknown in the analysis of multi-story frames.

When the frame is prevented from sidesway by adequate bracing, the instability mode is symmetrical which is shown as type E.

1.3 Review of Literature

More than 200 years ago Euler solved the elastic buckling problem of compression members. Unfortunately the theory he developed cannot coincide with experimental values obtained in the case of short columns in the inelastic range. Because at the time relatively low strength material such as wood was predominant, the instability problem was not of primary importance. These are major reasons why the instability

problem has been neglected by engineers for a long time.

Since steels and aluminum alloys became the major structural material, the stability problems have become the decisive factors in the modern design of buildings, bridges, and aircraft. In general, these structures are composed of some members under axial compression and bending.

The theory and experiments on the instability of individual members are well developed both in the elastic and the inelastic ranges. However, there is much to be done in the field of rigid-jointed trusses and frames. A brief description of the historical development of frame stability theory and experimental work is included in this article.

As early as 1913, Müller-Breslau[1.7] was the first to use the three moment equation modified for axial thrust. F. Bleich[1.8][1.9] extended the modified three moment equation to the stability analysis of rigid-jointed structures for practical application. The modified four moment equation was first applied by Bleich to calculate the buckling stress of compression members in trusses. The results of the analysis led to the proposal of an approximate formula which was first adopted in German Specification DIN 1050 and DIN 4114 and later in almost every country in the world.

Zimmermann[1.10][1.11][1.12], in a series of papers, developed the determinant criterion for frame buckling by considering the frame as a continuous column with intermediate elastic supports.

The energy method was applied by Kasarnowsky and Zetterholm[1.13] for the solution of continuous columns with intermediate elastic support. In 1936, J. Ratzersdorfer solved the buckling load of trusses by the

method of virtual work. Almost one year later a more general solution by the energy method was presented by F. Bleich and H. Bleich[1.14]. At the same time Lundquist[1.15] developed the stiffness criteria for stability analysis of frames with rigid joints based on the moment distribution principle. By the energy method, Hoff[1.16][1.17][1.18][1.19] proved the convergence of the moment distribution method and of the uniqueness of the results obtained by this method for stable equilibrium. The proof also resulted in Hoff's criterion for stability.

In 1938, Chwalla[1.20] made a pioneer study on antisymmetrical buckling of a pin-ended single-story frame with primary bending moments on the frame. However, the method is very complicated. Perhaps this is the reason why most of the efforts were directed toward modification of the moment distribution method, three-moment equation method and slope-deflection method to solve axially loaded frames for almost 20 years. Among these are the contributions made by Loh[1.21], Winter[1.22] et al, Perri[1.23], Kavanagh[1.24], Masur[1.25], Livesley and Chandler[1.26], Wood[1.27], and Merchant[1.28].

Since the primary bending moment is not always an important factor in the buckling of an elastic frame, Chwalla[1.29] and Jokisch applied the modified slope deflection method to calculate critical buckling loads of two-bay two-story frames with concentrated load on their column tops. Several buckling loads were obtained corresponding to the different buckling modes of the frame.

In 1960, Galambos[1.30] pointed out the importance of the effect of partial base fixity upon buckling of a frame. Using the column deflection curves developed by Ojalvo[1.31], Lu[1.32] solved

the inelastic buckling of single-story frames based on the moment distribution method due to Winter[1.33], et al. At the same time Johnson[1.34] developed an energy method with the aid of the moment distribution method to solve anti-symmetrical buckling of multi-story frames.

In 1961, the most complete solution of sidesway buckling of single-story frame in the elastic range was presented by Masur[1.35], et al. The authors generalized the modified slope-deflection method and moment distribution method to include the effect of primary bending moments on the frame prior to buckling.

Within the last few years, the high-speed digital computer has made possible a completely new approach to the complicated instability analysis of frames. Livesley[1.36][1.37] developed a digital computer program to solve elastic-plastic structures in 1959. In this dissertation a more direct approach with different assumptions is given with the aid of digital computer.

A good summary of elastic buckling solutions of frames was published by the Japanese Column Research Council[1.38] in 1960. A general outline on recent developments in the frame stability problem was presented by Horne[1.39]. A survey of literature on the stability of frames up to 1962 was made by Lu[1.40]. In Ref. (1.4), Levi presented the methods of design and a check against instability of multi-story frames based on the concept of subassemblages. Some charts and domains are developed to check against local buckling, and lateral-torsional buckling of a member in braced multi-story frames.

Since the turning of the sixty's, many efforts have been directed toward the energy method. In 1962 Rawlings[1.41] pointed out the appli-

cability of energy methods in plastic frame analysis. Careful study has been made of relationships among the various components of energy involved when a rectangular member is bent beyond the yield points. The energy relationships derived are applied to examine deformation of a single-story frame in the inelastic range. Jennings[1.42] extends Rayleigh's[1.43] principle to solve the elastic buckling of two-story frames. In his paper six functions are used to define the buckling mode of a member. This results in the evaluation of large matrices which is not very practical for highly indeterminate multi-story frames. On the other hand, Johnson[1.34] simply assumed a third degree polynomial as the buckling mode of a member. The results of analysis are very satisfactory. However, Johnson's method is only applicable for simple structure with the aid of moment distribution method.

In this dissertation, an energy method has been used to solve the buckling of multi-story frames in the inelastic as well as elastic range. For general reference, the books by Timoshenko[1.44], Bleich[1.45], Hoff[1.46], and LaSalle[1.47] are particularly helpful.

Above is a brief description of theoretical developments in the field of frame stability. From the standpoint of experimental investigation, very few test results are available due to the complex and expensive nature of tests.

In 1938, Chwalla[1.48] conducted experiments on the elastic buckling of single-story frames to check the validity of his theory. Similar tests with box sections were conducted by Lu[1.49]. In recent years the plastic method of structural analysis has been rapidly developed. As a consequence, the phenomenon of instability of partially plastic frames has to be explored experimentally.

Among these are the tests conducted by Bolton[1.50], Gurney[1.51], Salem[1.52], Wood[1.53], and Low[1.54]. In 1961 Yen et al[1.1] completed some inelastic instability tests of single-story frames made of small wide-flange sections. Similar sections were used for three-story frame tests as described in Chapter 7 of this dissertation.

1.4 Scope of Investigation

As pointed out in Article 1.1, in tall building frames axial loads on columns of the lower storeis are relatively large compared to the primary bending moments introduced by distributed loads on beams. The high axial loads on columns give rise to a possibility of a dangerous phenomenon of overall frame instability. When column loads reach the critical loads the frame may sway sideways suddenly. This phenomenon can occur at any stage, whether the frame is in the elastic range or inelastic range, depending on the stiffness of columns and beams.

For a single- or two-story frame, when the primary bending moments are relatively large compared to the axial loads, it is likely that the frame should fail by excessive bending stress. In other words, beam mechanisms develop before the frame buckles. A previous single-story frame test result can support this argument. For example, Frame W-1 with column slenderness $\frac{h}{r_x} = 40$, failed by beam mechanism rather than instability[1.1].

Therefore, in this dissertation methods are presented to analyze the instability of elastic and inelastic multi-story frames under high axial loads on columns. On the other hand, an experimental technique is shown for investigation of the instability of three-story frames.

2. GENERAL PRINCIPLES OF STABILITY ANALYSIS

2.1 Methods of Frame Stability Analysis

(1) Differential Equation Method

A differential equation which determines a deflection curve can be set up for each member of the frame[1.20]. Imposing the boundary conditions, the differential equation can be solved in relatively few cases. For the solution of multi-story frames, the method becomes too complicated for practical use.

(2) Energy Method

For exact analysis, the basic principle is: the second variation of the total potential energy of the system should be vanishing when the system passes from stable to unstable equilibrium[1.46], (Art. 2.3). However, the rigorous establishment of the neutral state of equilibrium by means of variational calculus is far too complex in many cases of practical importance. Therefore, a much simpler and very practical method due to Lord Rayleigh[1.43] can be used to advantage.

For stability analysis of highly indeterminate structures such as multi-story building frames, the benefit of simplicity by Rayleigh's method becomes more evident as can be seen in the analysis of an eleven-story frame in Chapter 8.

(3) Simultaneous Equation and Matrix Method

The axial thrust, bending moment, rotation and displacement are the variables to express load-deformation characteristics of a member. A number of simultaneous equations corresponding to each variable can be set up by modified slope deflection method, three-moment equation method and four-moment equation method. The vanishing of the stiffness

matrix leads to the buckling condition[1.45].

(4) Convergence Method

This is the method of successive approximation. The method of moment distribution is modified to take into account the effect of axial load. For buckling condition there are Lundquist's Series Criterion and Hoff's Convergence Method[1.46].

(5) Graphical Method

By numerical integration method, Ojalvo[2.1] developed a series of inelastic column curves based on the moment-curvature-thrust relationships of 8WF31 sections developed by Ketter[2.2]. An exact method of elastic-plastic solution of a simply frame was shown.

(6) Mixed Method

Any method mentioned above can be combined for the solution of frame stability problem so far as the basic requirements shown in the next article are satisfied[1.38].

2.2 Basic Requirements in Theoretical Analysis

As mentioned in the previous article, there are different methods of analysis. However, any theory of the static behavior of structures is an elaboration, in one form or another, of the following requirements that have to be satisfied by any theoretical state.

(1) Equilibrium

The internal stresses in the structure shall be in statical equilibrium with externally applied loads.

(2) Compatibility

Since the structure is statically indeterminate, equilibrium condition alone is not enough.

The displacements of the structure shall be geometrically compatible with the internal strains, the internal strains being in turn compatible with each other.

(3) Conformity with Stress-Strain Relations

In an inelastic structure the internal stresses and the strains, or moment and curvature are related according to the characteristics of the materials. If the actual moment-curvature-thrust curves are used, the effect of residual stresses is automatically taken into account.

However, the stress-strain relationships given hold good for a "loading" process only. A "loading" process is defined as a process under which the strain increases under increasing stress. As the stress in a member decreases, the strain may decrease linearly even if the member is in the inelastic range. In this case the member is unloading elastically. When part of the structure has to undergo an "unloading" process, the strains in this part might not be unique. In this case the structure no longer obeys the specified stress-strain law. Rather the stress-strain relationships are the function of the deformation status at the time of unloading. In the analysis of a highly indeterminate structure, it becomes extremely complicated if the effect of strain reversal is taken into account. The effect of strain reversal on instability of a column under equal end moment has been shown in Chapter 8 of Ref. (2.3). Qualitatively it is on the safe side to neglect the effect, however, quantitative analysis has not been done in any literature. Therefore, unique moment-curvature-thrust curves of a typical wide flange section are used in the subsequent development of the theory.

However, for frames designed by the plastic method, the plastic hinges undergo an unloading process and become elastic again at the instant of bifurcation. The solution of this type of frame is shown in Art. 8.2.

2.3 Criteria of Instability

Whether a structure in a given equilibrium state is stable, can be tested by introducing any infinitesimal disturbing force or deformation. If the infinitesimal distrubing force or deformation causes the structure to depart a finite amount from that state, the structure is said to be stable, and the structure could in practice remain under the given loading and boundary conditions. By considering the effect of a small disturbance, it is possible to determine whether the resulting changes in the internal resistance of the structure are statically sufficient to balance the changes in equilibrium conditions due to the incremental deflections and external forces. When the structure is unstable under this test, an external horizontal force contrary to the direction of sidesway has to be introduced in order to satisfy the equilibrium condition. While simple problems may be treated thus, it is usually more consistent to use the concept of total potential energy for a criterion of stability. The total potential energy must be a minimum with respect to any incremental state of deformation if the structure is to be stable. If the potential energy is not a minimum, then an infinitesimal distrubing force will produce changes in deformation that result in a net release of energy, and the structure will acquire finite velocities. Therefore, the criterion that infinitely small disturbing forces produce only infinitely small deflections will then be violated.

As usually expressed, the concept of minimum total potential energy is applicable only to conservative structures. A conservative structure is defined as a structure which has a unique final state of deformation regardless of the loading process. In order to be a conservative structure, both stress-strain and load-displacement relationships of the structure must be single-valued functions. The potential energy of an external load is defined by the product of the magnitude of the load and its altitude. The strain energy is defined as the sum of the internal work which is the product of the magnitude of the stress and incremental strain. Total potential energy is the sum of these two terms. In non-conservative structures, the energy is continuously being expended irreversibly due to plastic deformation and strain reversal in some part of the structure. By adopting a modified potential energy concept it is, however, possible to stipulate a form of the minimum energy criterion for stability that is applicable to non-conservative structures as shown in Ref. (1.39).

In this case the modified total potential energy $(U_n + V_n)$ should be used. Let U_n be the modified strain energy and V_n the potential energy of inelastic structure. $(U_n + V_n)$ consists of the potential energy of the applied loads V, the elastic strain energy in the structure U_e and the energy absorbed in permanent deformation U_p.

The energy absorbed in plastic deformation depends on the loading part for the structure, and it is assumed that the path taken is that represented by the load-deformation curve. Then the modified total potential energy is

$$\Sigma (U_n + V_n) = \Sigma U_e + \Sigma U_p + \Sigma V \qquad (2.1)$$

According to Theorem 13 in Reference (1.46), the equilibrium condition is: the first-order change in total potential must vanish for every virtual displacement when an elastic body is in equilibrium. This corresponds to the condition:

$$\frac{\partial \Sigma (U_n + V_n)}{\partial \rho} = 0 \qquad (2.2)$$

Where ρ is one of sidesway displacements of the system*.

Equilibrium condition Eq. (2.2) is analogous to a ball on uneven ground. The ball is in a position of equilibrium when the slope of the potential surface vanishes. Stable equilibrium is analogous to a ball on the bottom of a concave surface. A certain amount of work is required to produce any displacement away from this equilibrium position. In the same manner the potential energy of a structure in stable equilibrium increases for any displacement from the position of equilibrium. Therefore, the curvature of the potential energy surface must be a positive value if the structure is in stable equilibrium.

$$\frac{\partial^2 \Sigma (U_n + V_n)}{\partial \rho^2} > 0 \qquad (2.3)$$

On the other hand, unstable equilibrium can be compared to a ball on a convex surface with a negative curvature of potential surface. If a structure under loads is in unstable equilibrium, and displacement causes the structure to displace further which results in a release of potential energy as a form of kinetic energy. This decrease of potential energy of the structure for any displacement ρ, corresponds to

$$\frac{\partial^2 \Sigma (U_n + V_n)}{\partial \rho^2} < 0 \qquad (2.4)$$

*All symbols are defined in Chapter 10 NOMENCLATURE.

When the system passes from stable to unstable equilibrium the curvature of the potential surface vanishes. Therefore, the buckling condition for neutral equilibrium is

$$\frac{\partial^2 \Sigma (U_n + V_n)}{\partial \rho^2} = \frac{\partial^2 \Sigma\, U_e}{\partial \rho^2} + \frac{\partial^2 \Sigma\, U_p}{\partial \rho^2} + \frac{\partial^2 \Sigma\, V}{\partial \rho^2} = 0 \qquad (2.5)$$

When total potential energy is a function of several displacement parameters, Eq. (2.2) and Eq. (2.5) must be satisfied for every displacement.

Since the bending moment becomes a constant value at a plastic hinge, $\frac{\partial^2 \Sigma\, U_p}{\partial \rho^2} = 0$. The buckling condition is similar to that of an elastic structure except for replacing the plastic hinges by ordinary hinges. The critical load obtained this way is called the deteriorated critical load introduced by Wood[1.53].

3. MATERIAL PROPERTIES AND SECTION GEOMETRY OF A MEMBER UPON BUCKLING

3.1 Section Geometry and Residual Stresses

Euler's buckling formula suggests that the critical buckling load is proportional to the moment of inertia of the column section. Provided local buckling can be prevented, an increase in the moment of inertia of column section of a given cross-sectional area results in an economical design. Therefore, a solid section is rarely used. Since most of the rigid frames in practice are made of wide flange sections, the efforts in this dissertation are directed toward the investigation of the load carrying capacity of frames made of such sections.

Due to different cooling rates after rolling of parts of a wide-flange section, residual stresses are developed in the section. The pattern of the residual stresses is rather regular throughout the range of wide-flange sections. The transition curves seen in Fig. 2.1 between the elastic and plastic regions in the load-deformation curves are partially due to the action of residual stresses. Unfortunately the buckling strength of columns in the inelastic range is so sensitive to the effect of residual stresses that the effect can no longer be neglected. The moment-curvature-thrust curves of a typical wide flange section (8WF31) shown in Article 3.3 have been used in the development of the energy method. The effect of residual stresses is automatically included in the energy method. Since the effect of residual stress tends to shift the moment-curvature-thrust curve downward, this results in reducing the capacity of the member to absorb strain energy.

3.2 Material Properties

The moment-curvature-thrust curves and load-deformation curve represent the section and material properties of the members. As material properties the modulus of elasticity and yield stress will be discussed here.

In the elastic range the modulus of elasticity of ordinary A7 steel is about E = 30 ksi and the yield stress σ_y = 33 ksi. However, for prediction of the buckling load of the model frames discussed in Chapter 7, E = 31, 370 ksi and σ_y = 42.7 ksi according to results obtained from stub column tests. The sectional properties of the test specimens are summarized in Table 3.1 and Table 3.2.

3.3 Moment-Curvature-Thrust Curves of Wide-Flange Section

The bending properties of a section under various axial load intensities can be regarded as the backbone of the analysis of a structure beyond the elastic range. Figure 2.1 shows typical moment-curvature-thrust curves of an 8WF31 section. The curve is non-dimensionalized with respect to the yield moment and curvature of the section.

A computer program has been developed for calculation of moment-curvature-thrust curves of WF sections[3.2]. Close comparison between the two results obtained for 14WF246 and 8WF31 sections shows that the $\overline{M}$ - $\overline{\phi}$ - $\overline{P}$ curves obtained can be used for other WF sections.

3.4 Strain Energy vs. Curvature Relationships of Wide-Flange Sections

Take a unit length of WF shape with yield moment M_y and corresponding curvature ϕ_y. Referring to Fig. 2.1, the bending strain energy u stored in a unit length of the beam during a curvature change from 0 to ϕ can be obtained by integration of the area under the moment-curva-

ture curve between the ϕ/ϕ_y limits of 0 and ϕ/ϕ_y for the particular value of thrust. The strain energy may be non-dimensionalized by dividing u by the unit strain energy at yielding $u_y = M_y\phi_y$. The non-dimensional strain energy u/u_y is designated $\bar{u}$. Numerically this area $\bar{u}$ is the sum of non-dimensional elastic strain energy and the energy absorbed in plastic deformation. As an example, for a beam-column bent in the same curvature $\phi = \phi_y$, the areas under an $\bar{M} - \bar{\phi} - \bar{P}$ curve with $\bar{p} = 0$ and with $\bar{p} = 0.8$ are 0.496 and 0.182 respectively. This indicates that the high axial load on column reduces tremendously the capacity for energy absorption. Another fact worthy of mentioning here is that the elastic strain energy is rather small compared to the plastic strain energy. In other words, after the first yielding the structural member can still absorb strain energy several times as much. In order to carry out area integration under $\bar{M} - \bar{\phi} - \bar{P}$ curves in Fig. 2.1, the abscissa ϕ/ϕ_y was divided into intervals of 0.2. The ordinates of M/M_y for each P/P_y were measured at $\phi/\phi_y = 0.2, 0.4, 0.6 \ldots$ up to 1.6. The non-dimensional strain energy $\bar{u}$ was obtained as the cumulative sum of each incremental strain energy. The results of numerical integration of the strain energy of $\bar{M} - \bar{\phi} - \bar{P}$ curves are plotted as $\bar{u} - \bar{\phi}$ curves in Fig. 3.1.

In order to render the analytical method possible, strain energy vs. curvature relationships under various axial loads should be expressed in mathematical forms. Therefore, $\bar{u} - \bar{\phi}$ curves are fitted into two sets of curves. Two sets of curves are used instead of one, for the sake of accuracy. In general

$$\bar{u} = f(\bar{p})\,\bar{\phi}^2 \qquad (3.1)$$

where the coefficient of bending strain energy

$$f(\bar{p}) = 0.4509 - 0.1363\,\bar{p} - 0.0425\,\bar{p}^{\,2} \qquad (3.2a)$$

is good for axial load $\bar{p} < 0.4$ and

$$f(\bar{p}) = 0.4354 + 0.0242\,\bar{p} - 0.3471\,\bar{p}^{2} \qquad (3.2b)$$

for axial load $\bar{p} \geqslant 0.4$.

A maximum of $\bar{\phi} = 1.5$ was a limiting value in the $\bar{u} - \bar{\phi}$ curve fitting. Beyond this point, $\bar{u} - \bar{\phi}$ relationships are simply a parabolic extension of the curve fitted. However, in reality plastic hinges can be introduced for curvatures larger than limiting values. The $\bar{M} - \bar{\phi} - \bar{P}$ curves beyond points $\bar{\phi} = 1.5$, 1.4, 1.2, and 0.8 for $\bar{P} = 0$, 0.2, 0.4, 0.6, and 0.8 respectively are very flat. Therefore, beyond these points, the section can be assumed fully yielded. Several values from fitted curves are plotted and compared with actual $\bar{u} - \bar{\phi}$ curves in Fig. 3.1.

$\bar{u} - \bar{\phi}$ relationships are used for evaluation of bending strain energy of columns and beams in the following Chapters. In general the strain energy for a member can be derived as follows:

Let ℓ = length of the member

M_y = yield moment of the member

ϕ_y = curvature at first yield of the member

P_y = axial yield load of the member

u = bending strain energy per unit length

$\bar{u}$ = nondimensional bending strain energy

$\bar{\phi}$ = nondimensional curvature

$\bar{p}$ = nondimensional axial load

U = total strain energy of the member

$f(\bar{p})$ = coefficient of bending strain energy

Then the bending strain energy of unit length of a member

$$u = u_y \bar{u} = M_y \phi_y \cdot f(\bar{p}) \bar{\phi}^2 \qquad (3.3)$$

where $\bar{u} = f(\bar{p}) \bar{\phi}^2$ from eq. (3.1). Therefore the total bending strain energy for a member can be obtained by integration of the unit strain energy u throughout the length of a member ℓ.

$$U = \int_\ell u \, dx = \int_\ell M_y \phi_y \cdot f(\bar{p}) \bar{\phi}^2 dx = M_y \phi_y f(\bar{p}) \int_\ell \bar{\phi}^2 \, dx \qquad (3.4)$$

For a given member under a given axial thrust, the coefficient $M_y \phi_y f(\bar{p})$ is specified. Once the variation of curvatures along the member is known, the total bending strain energy can be obtained by integration of eq. (3.4).

4. POTENTIAL ENERGY OF A MEMBER

4.1 Basic Assumptions

A column in a frame may be bent in single curvature or double curvature. The top of the column may sway considerably from its upright position. For any combined bending and sidesway, a third degree polynomial can be assumed to represent the deformed shape of a column in a multi-story frame. By assigning appropriate values for the four constants in a third degree polynomial, the deformed shape of the actual column can reasonably be approximated.

Since the effect of strain reversal is neglected, the deformed shape is independent of the loading history. Therefore, the bending moment corresponding to the deformed shape can be uniquely determined.

If the differential settlement of column tops is neglected, the deformed shape of a beam can be assumed as a three-term sine curve. The first term takes care of the deflection due to uniform load on the beam. The second term is superimposed to simulate the antisymmetrical deformation. For the compensation due to restraining moment at both ends of the beam, the third term is added. If a third degree polynomial is assumed as a beam deflection curve, the effect of differential shortening of columns can be included. In Rayleigh's method an approximate deflection curve with unknown deflection coefficients is assumed. To determine the instant of buckling, these unknown deflection coefficients are adjusted and given values such that the total potential energy of the system becomes a minimum. By assuming a load P the stiffness matrix composed of unknown deflection coefficients can be evaluated. The buckling load of a frame is obtained when the assumed

load P makes the stiffness matrix vanishing.

It is well known that the change in the value of the total potential is insensitive to the particular choice of the deflected shape of members[1.43]. Therefore, good approximate values of the buckling load can be obtained by Rayleigh's method if a reasonable deflected shape is chosen.

4.2 Bending Strain Energy of a Column

Figure 4.1 shows the deflected shape of a column. The shape is assumed to be the same third degree polynomial in Johnson's[1.34] paper.

$$W(x) = s\left[A + B\left(\frac{x}{s}\right) + C\left(\frac{x}{s}\right)^2 + D\left(\frac{x}{s}\right)^3\right] \tag{4.1}$$

Slope equation

$$\frac{d\,W(x)}{dx} = B + 2C\left(\frac{x}{s}\right) + 3D\left(\frac{x}{s}\right)^2 \tag{4.2}$$

Curvature equation

$$\phi = \frac{d^2W(x)}{dx^2} = \frac{2C}{s} + 6D\frac{x}{s^2} \tag{4.3}$$

The boundary conditions are:

$$x = s,\ W(x) = \rho h \tag{4.4}$$

$$x = s,\ \frac{d\,W(x)}{dx} = \Psi_j \tag{4.5}$$

$$x = -s,\ W(x) = 0 \tag{4.6}$$

$$x = -s,\ \frac{d\,W(x)}{dx} = \Psi_i \tag{4.7}$$

The constants A, B, C, and D can be obtained by solution of the above simultaneous equations.

$$A = \frac{\Psi_i}{4} - \frac{\Psi_j}{4} + \rho \tag{4.8}$$

$$B = \frac{-\Psi_i}{4} - \frac{\Psi_j}{4} + \frac{3}{2}\rho \tag{4.9}$$

$$C = \frac{-\Psi_i}{4} + \frac{\Psi_j}{4} \tag{4.10}$$

$$D = \frac{\Psi_i}{4} + \frac{\Psi_j}{4} - \frac{1}{2}\rho \tag{4.11}$$

Substitute equation (4.10) and (4.11) into (4.3),

$$\phi = \frac{1}{s}\left[-\frac{\Psi_i}{2} + \frac{\Psi_i}{2} + \left(\frac{3}{2}\Psi_i + \frac{3}{2}\Psi_j - 3\rho\right)\frac{x}{s}\right] \tag{4.12}$$

Substitute equation (4.12) into (3.4) and integrate from $-\frac{h}{2}$ to $\frac{h}{2}$, bending strain energy of a column

$$U_c = \frac{4M_y f(\bar{p})}{\phi_y h}\left(\Psi_i^2 + \Psi_j^2 + \Psi_i\Psi_j - 3\Psi_i\rho - 3\Psi_j\rho + 3\rho^2\right) \tag{4.13}$$

For given sectional properties, column height, and axial thrust, the total bending strain energy of the column U_c can thus be specified by joint rotations Ψ_i and the sidesway ρ of the column.

4.3 Potential Energy of a Column

Potential of the axial load P on the column[1.46] is

$$V_c = -P\Delta_c \tag{4.14}$$

where the axial shortening of the column[1.46]

$$\Delta_c = \int_{-s}^{s} \frac{1}{2}\left(\frac{dW}{dx}\right)^2 dx \tag{4.15}$$

Substitute equations (4.9), (4.10), and (4.11) in (4.2)

$$\frac{dW}{dx} = -\frac{1}{4}\Psi_i - \frac{3}{8}\Psi_i + \frac{3}{2}\rho - \frac{1}{2}(\Psi_i - \Psi_j)\frac{x}{s} + \left(\frac{3}{4}\Psi_i + \frac{3}{4}\Psi_j - \frac{3}{2}\rho\right)\left(\frac{x}{s}\right)^2 \tag{4.16}$$

Integrate (4.15) through the column height h,

$$\Delta_c = \frac{h}{30}(2\,\Psi_i^2 + 2\,\Psi_j^2 + 18\,\rho^2 - 3\,\Psi_i\,\rho - 3\,\Psi_j\,\rho - \Psi_i\,\Psi_j) \quad (4.17)$$

Therefore, potential energy of the column

$$V_c = -\frac{Ph}{30}(2\,\Psi_i^2 + 2\,\Psi_j^2 + 18\,\rho^2 - 3\,\Psi_i\,\rho - 3\,\Psi_j\,\rho - \Psi_i\,\Psi_j) \quad (4.18)$$

Similar to eq. (4.13), given the axial thrust and column height, the potential energy of the column can be calculated in terms of the joint rotations and the sidesway of the column. The total potential energy of a column is the sum of strain energy U_c and potential energy V_c, or $U_c + V_c$.

4.4 Bending Strain Energy of a Beam

The deflected shape of a beam is assumed to be

$$W(x) = \ell\left(a \sin\frac{\pi x}{\ell} + b \sin\frac{2\pi x}{\ell} + c \sin\frac{3\pi x}{\ell}\right) \quad (4.19)$$

where a, b, and c are amplification constants corresponding to each mode. By differentiating (4.19), slope and curvature of the beam can be obtained

$$\frac{dW(x)}{dx} = \pi\left(a \cos\frac{\pi x}{\ell} + 2\,b \cos\frac{2\pi x}{\ell} + 3\,c \cos\frac{3\pi x}{\ell}\right) \quad (4.20)$$

$$\frac{d^2W(x)}{dx^2} = \frac{-\pi^2}{\ell}\left(a \sin\frac{\pi x}{\ell} + 4\,b \sin\frac{2\pi x}{\ell} + 9\,c \sin\frac{3\pi x}{\ell}\right) \quad (4.21)$$

The deformed shape and loading condition is shown in Fig. 4.2. In order to eliminate the second and the third amplification constants, two boundary conditions, one at each end of the beam are imposed in the equation (4.20)

$$x = 0, \quad \frac{dW}{dx} = \Psi_i \quad (4.22)$$

$$x = \ell, \frac{dW}{dx} = \Psi_j \tag{4.23}$$

Therefore,

$$\Psi_i = \pi a + 2\pi b + 3\pi c \tag{4.24}$$

$$\Psi_j = -\pi a + 2\pi b - 3\pi c \tag{4.25}$$

solve (4.24) and (4.25) for b and c.

$$b = \frac{1}{4\pi}(\Psi_i - \Psi_j) \tag{4.26}$$

$$c = \frac{1}{3\pi}\left(\frac{\Psi_i}{2} - \frac{\Psi_j}{2} - \pi a\right) \tag{4.27}$$

Substitute equation (4.26) and (4.27) in (4.19), (4.20), and (4.21),

$$W(x) = a\ell \sin\frac{\pi x}{\ell} + \frac{\ell}{4\pi}(\Psi_i + \Psi_j)\sin\frac{2\pi x}{\ell} + \frac{\ell}{6\pi}(\Psi_i - \Psi_j - 2\pi a)\sin\frac{3\pi x}{\ell} \tag{4.28}$$

$$\frac{dW(x)}{dx} = \pi a\cos\frac{\pi x}{\ell} + \frac{1}{2}(\Psi_i - \Psi_j)\cos\frac{2\pi x}{\ell} + \frac{1}{2}(\Psi_i - \Psi_j - 2\pi a)\cos\frac{3\pi x}{\ell} \tag{4.29}$$

$$\phi = \frac{d^2W(x)}{dx^2} = \frac{-\pi^2}{\ell} a\sin\frac{\pi x}{\ell} - \frac{\pi}{\ell}(\Psi_i + \Psi_j)\sin\frac{2\pi x}{\ell} - \frac{3\pi}{2\ell}(\Psi_i - \Psi_j - 2\pi a)\sin\frac{3\pi x}{\ell} \tag{4.30}$$

Substitute (4.30) in (3.4).

Strain energy of a beam

$$U_B = \frac{M_y \pi^2 f(\bar{H})}{8\phi_y \ell}(13\Psi_i^2 + 13\Psi_i^2 + 40\Psi^2 a^2 - 10\Psi_i\Psi_j - 36\pi\Psi_i a + 36\pi\Psi_j a) \tag{4.31}$$

where $\bar{H}$ is a nondimensional axial thrust on the beam. Equation (4.31)

is to be used for a beam without unequal settlement at both ends. Strain energy of the beam V is expressed as functions of joint rotations Ψ_i, Ψ_j, and magnification factor a.

For an elastic beam under the configuration of antisymmetrical buckling, $\Psi_j = \Psi_i$ and $a = 0$, Eq. (4.31) becomes

$$U_B = \frac{\pi^2 EI}{\ell} \Psi_i^2 \tag{4.32}$$

If a third degree polynomial is assumed as the deflected shape of the beam, Eq. (4.13) gives

$$U_B = \frac{6 E I}{\ell} \Psi_i^2 \tag{4.33}$$

The exact solution of the bending strain energy of an elastic beam is

$$U_B = \frac{6 E I}{\ell} \Psi_i^2 \tag{4.34}$$

Therefore, Eq. (4.13) results in an exact solution in this particular case, while Eq. (4.31) gives a poor approximation. Another fault of the trigonometric series is that, Eq. (4.19) gives a vanishing curvature at both ends of the beam which is not the actual case. However, the results of single[1.1] and three-story frame tests showed that the deformed shapes of beams were very close to single wave sine curves. This is the reason why the trigonometric series Eq. (4.19) was assumed as a deflected shape of a beam.

4.5 Potential Energy of a Beam-Column

Potential of a beam-column is composed of two parts: V_w, the potential of uniform load w on the beam and V_H, potential of axial thrust H on the beam-column.

$$V_w = -\int_0^{\ell} w\, W(x)\, dx \tag{4.35}$$

Substitute (4.28) in (4.32)

$$V_w = -\frac{w\ell^2}{9\pi^2}(\Psi_i - \Psi_j + 16\pi a) \tag{4.36}$$

Potential of axial thrust

$$V_H = -H\,\Delta_B \tag{4.37}$$

Where axial shortening of the beam

$$\Delta_B = \frac{1}{2}\int_o^{\ell}\left(\frac{d\,W(x)}{dx}\right)^2 dx \tag{4.38}$$

Substitute (4.29) in (4.38)

$$\Delta_B = \frac{\ell}{8}(\Psi_i^2 + \Psi_j^2 + 4\pi^2a^2 - 2\pi a\,\Psi_i - 2\pi a\,\Psi_j) \tag{4.39}$$

Hence

$$V_H = -\frac{H\ell}{8}(\Psi_i^2 + \Psi_j^2 + 4\pi^2a^2 - 2\pi a\,\Psi_i - 2\pi a\,\Psi_j) \tag{4.40}$$

Potential energy of the beam is $V_B = V_w + V_H$ and total potential energy of the beam is $U_B + V_B = U_B + V_w + V_H$.

5. BUCKLING ANALYSIS OF PARTIALLY PLASTIC FRAMES

5.1 Assumptions

The method of buckling analysis presented in this dissertation is oriented toward the solution of highly indeterminate tall frames. The objective of the development of the method lies in the exploration of overall instability phenomenon of the structure as a whole under unified assumptions made on each member. In order to render the analysis possible, some of the following assumptions are essential.

(1) On the lower story of tall frames, the load on the beam is small compared to the high axial load on the columns. Therefore, the effect of primary bending moment is negligible. In the upper stories, the failure is likely due to simple plastic mechanism because of the relatively low axial loads on columns. In other words, the loads are assumed to be applied on column tops.

(2) At the instant of sidesway buckling, the infinitesimal deformations are not enough to develop plastic hinges in the frame. In case of strong column and weak beam design, plastic hinges might be developed on both ends of the beams. When the frame buckles sidewise, the leeward ends remain as plastic hinges while the windward ends "unload" elastically. Therefore, hinges on one end of beams can be introduced according to the concept of a deteriorated structure as shown in Art. 2.3.

(3) The deformed shape of the member can be represented by third degree polynomials and three term sine curves.

(4) The effect of strain reversal at the instant of buckling is neglected. To neglect the effect, the buckling load obtained is on

the safe side[2.3].

5.2 Total Potential of a Whole System

Total potential energy of a frame is the sum of the potential energy and strain energy of beams and columns of which the frame is composed. Therefore, total potential energy of the system is

$$\Sigma(U + V) = \Sigma(U_c + V_c) + \Sigma(U_B + V_B) \qquad (5.1)$$

In general, for a single-bay nth-story frame subjected to concentrated loads on its column tops, the total potential of the system can be developed as follows. Referring to Fig. 5.1, when the load reaches the critical load, the frame buckles in an antisymmetrical mode. Let subscript i denote the ith floor of the frame. Δ_i indicates the shortening of the column on the ith floor. Then the total settlement at the top of the ith column is

$$\Delta h_i = \sum_{1}^{i} \Delta_i \qquad (5.2)$$

Since at the top of each column, $\frac{P}{n}$ concentrated load is applied, the total potential of all $\frac{P}{n}$ loads

$$\Sigma V_c = -\frac{2P}{n} \sum_{i=1}^{i=n} \sum_{i=1}^{i} \Delta_i = -\frac{2P}{n} \sum_{i=1}^{n} (n + 1 - i)\,\Delta_i \text{ , or}$$

$$\Sigma V_c = -\frac{Ph}{15n} \sum_{i=1}^{n} (n - i + 1)(2\psi_{i-1}^2 + 2\psi_i^2 + 18\rho_i^2 - \psi_{i-1}\psi_i - 3\psi_i\rho_i) \qquad (5.4)$$

where p is the vertical reaction at a support of a column. The axial thrusts on beams are saml1 compared with those of columns, hence neglected

$$\Sigma V_B = 0$$

The strain energy of the ith column is

$$\frac{8\,(M_{yc})_i \overline{f}(\overline{P}_i)}{(\phi_{yc})_i\, h}\,(\psi_{i-1}^2 + \psi_i^2 + \psi_{i-1}\psi_i - 3\psi_{i-1}\rho_i - 3\psi_i\rho_i - 3\rho_i^2)$$

For all the columns in the frame

$$\Sigma U_c = \sum_{i=1}^{n} \frac{8\,(M_{yc})_i \overline{f}(\overline{P}_i)}{(\phi_{yc})_i\, h}\,(\psi_{i-1}^2+\psi_i^2+\psi_{i-1}\psi_i-3\psi_{i-1}\rho_i-3\psi_i\rho_i+3\rho_i^2) \qquad (5.5)$$

As a nature of antisymmetric deformation

$$\psi_i = \psi_j \quad \text{and} \quad a = 0$$

From equation (4.31), total strain energy of beams

$$\Sigma U_B = \frac{2\pi^2 \overline{f}(0)}{\ell^2} \sum_{i=1}^{n} \frac{(Myb)_i}{(\phi yb)_i}\,\psi_i^2 \qquad (5.6)$$

Therefore, total potential energy of a frame is

$$\Sigma (U+V) = \frac{8}{h} \sum_{i=1}^{n} \left(\frac{M_{yc}}{\phi_{yc}}\right)_i \overline{f}(\overline{P}_i)\,(\psi_{i-1}^2+\psi_i^2+\psi_{i-1}\psi_i-3\psi_{i-1}\rho_i-3\psi_i\rho_i+3\rho_i^2)$$
$$+ \frac{2\pi^2 \overline{f}(0)}{\ell^2} \sum_{i=1}^{n} \left(\frac{M_{yb}}{\phi_{yb}}\right)_i \psi_i^2$$
$$-\frac{Ph}{15n}\sum_{i=1}^{n}(n-i+1)(2\psi_{i-1}^2+2\psi_i^2+18\rho_i^2-\psi_{i-1}\psi_i-3\psi_{i-1}\rho_i+3\psi_i\rho_i) \qquad (5.7)$$

Applying the criterion of instability described in Article 2.3 the critical buckling load can be obtained from the condition

$$\frac{\partial \Sigma (U+V)}{\partial (\psi_i, \rho_i)} = 0 \qquad (5.8)$$

Equation (5.8) can be arranged in matrix form

$$[A][\psi] = 0 \qquad (5.9)$$

For a given member size and geometry of a frame, matrix [A] is a function of load P. For any value of P deformation matrix [ψ] cannot vanish. Therefore, the critical buckling load P_{cr} can be obtained when $[A] = 0$ is satisfied. This can best be done by assuming

P values and computing $[A]$. The critical load P_{cr} is obtained by interpolation between the two loads when the determinant changes its sign.

5.3 Buckling Analysis of Three-Story Frames by Inelastic Energy Method

As shown in Article 7.1, some three-story model frames were proposed for stability tests[5.1]. In this article, the proposed method of anlysis together with the assumptions made in the theory is to be demonstrated by the computation of the buckling loads of the model frames under concentric column loads.

The geometry, size and loading condition of the frames are shown in Fig. 5.2. A small wide-flange shape designated No. M-2362 of Bethlehem Steel Company was adopted as the member size of the frame. The sectional properties are shown in Table 3.1. The compression yield load P_y = 44.27 kips was adopted from the results of stub column tests. As determined from control beam tests, the full plastic moment was 47 kip-in. With a shape factor of 1.16, a yield moment M_y = 40.5 ksi was used in the calculation of buckling loads.

The total potential energy of the frame is tabulated in Table 5.1, where Y1, Y2, Y3, Z, and X are determined by sectional properties, length of members, and axial load on column. The parameters are defined in Chapter 10. Buckling condition of the frame is obtained by differentiation of the total potential energy with respect to deformation ψ's and ρ's as tabulated in Table 5.2.

In order to obtain the relationship between the buckling load of the frame and slenderness of columns, slenderness ratio was varied from $\frac{h}{r_x}$ = 15 to $\frac{h}{r_x}$ = 160, while M_y = 40.5 kip-in., ϕ_y = 0.001023 in.$^{-1}$, P_y = 44.26 kip and L = 60 in. were kept constant as

input in the computer for the solution of the determinant in Table 5.2. The value of the determinant was evaluated by assuming an axial load P, and hence, an energy coefficient $f(\bar{P})$, on a column. By increasing the axial load P, the value of the determinant changed its sign at the critical buckling load. Therefore, the critical buckling loads of the frame were the results of the solution of buckling conditions. They are tabulated in Table 5.3 and plotted as a cross-dotted line in Fig. 5.2. A maximum buckling load of $\bar{P} = 1$ was obtained when the slendernesses of columns were about 19. For a frame with slendernesses of columns smaller than 19, the columns were assumed fully yielded with $\bar{P} = 1$. A GE225[5.2] digital computer was used for the computation.

5.4 Applicability and Limitations of the Method

It is not likely that a structural engineer can find a method which is universally the best for analysis of any structures and loading conditions so far as the accuracy and simplicity of the method are concerned. In order to attain some margin of accuracy in structural analysis, the chances are that the additional computational effort to achieve this accuracy be multiplied several times. This renders the buckling analysis of complicated multi-story frames impracticable if not impossible.

Since Rayleigh's method is widely used in practice as a quick approximate method for a simple structure, there is no reason why the method cannot be extended to analyze multi-story frames. In fact the energy method has an advantage of simplicity over other methods when the degree of indeterminancy of the structure increases.

When the number of stories increases the axial load on the lower columns is much larger than the uniform load on the beams. Therefore the initial bending moment generated by the uniform load on the beams is almost negligible, so far as no plastic hinge develops on beams. However, for buckling analysis of single or two-story frames with primary bending moment, neglect of the effect of primary bending moment can be serious in the inelastic range. Finally it should be pointed out that the method is designed for rather tall multi-story frame analysis. The greater the number of stories, the better the result should be. However, the number of unknown deformation quantities increases with the increasing number of stories and bays.

For a symmetrical structure,

Let n = number of stories

b = number of bays

m = total maximum unknown variables of the frame of n-stories and b-bays.

$m = b(n + 1) - 1$ for multi-bay frame.

$m = 2n + 1$ for single-bay frame.

The capacity of the computer should be large enough to evaluate a square matrix $[m] \times [m]$.

6. BUCKLING ANALYSIS OF ELASTIC FRAMES

6.1 Derivation of the Theory

Elastic energy method may be regarded as a particular case of the inelastic energy method developed in Chapter 5. With slender columns, the frame should fail in elastic range and the results obtained by energy methods can be compared with the existing method of modified slope deflection. Tables and charts are not necessary for solution of frame instability by the energy method. Moreover, the elastic solution can be used to predict frame instability in plastic range such as Rankine's formula $\frac{1}{P_{cr}} = \frac{1}{P_e} + \frac{1}{P_p}$ recommended by Merchant[6.1].

To develop a pure elastic energy method, a slight alteration is necessary in the previous Chapter on the inelastic method. Consider a unit length of beam-column subjected to end moments M bent in curvature ϕ, then the elastic strain energy

$$u = \frac{1}{2} M \phi \tag{6.1}$$

Since $M = EI\phi$, $\phi = \bar{\phi}\,\phi_y$

$$u = \frac{EI}{2}\phi^2 = \frac{EI\phi_y^2}{2}\bar{\phi}^2 \tag{6.2}$$

Equation (6.2) can be considered as a special case of Eq. (3.3), which is valid both in the inelastic as well as in the elastic ranges. Equate Eq. (3.3) to Eq. (6.2) and solve for $f(\bar{P})$.

$$M_y \phi_y f(\bar{P})\bar{\phi}^2 = \frac{EI}{2}\phi_y^2\bar{\phi}^2$$

$$\therefore \quad f(\bar{P}) = \frac{\phi_y EI}{2M_y} = \frac{1}{2}$$

Therefore, the energy expression developed in Chapter 5 can be used for the buckling analysis of elastic structures by substituting the energy coefficient $f(\bar{p}) = \frac{1}{2}$. In order to avoid duplication, no further derivation of elastic energy formula is shown.

Finally, it should be pointed out that tables and charts are not necessary for solution of frame instability problems by the energy method; the method is a convenient tool in frame analysis when a computer is available.

6.2 Elastic Instability Analysis of Three-Story Frames

The same frame analyzed in Chapter 5 has been chosen as an example to demonstrate the method of elastic instability analysis. The dimensions of the frame and its loading condition are shown in Fig. 5.2.

Total potential energy of the frame is

$$\Sigma(U+V) = \sum_{i=1}^{3} \frac{4EiIi}{h} (\psi_{i-1}^2 + \psi_i^2 + 3\rho_i^2 + \psi_{i-1}\psi_i - 3\psi_{i-1}\rho_i - 3\psi_i\rho_i) + \frac{\pi^2}{\ell} \sum_{i=1}^{3} E_i I_i \psi_i^2$$

$$- \frac{Ph}{45} \sum_{i=1}^{3} (4-i)(2\psi_{i-1}^2 + 2\psi_i^2 + 3\rho_i^2 + \psi_{i-1}\psi_i - 3\psi_{i-1}\rho_i - 3\psi_i\rho_i) \qquad (6.3)$$

Differentiating the total energy with respect to each of the deformation parameters, $\psi_0, \psi_1, \psi_2, \psi_3, \rho_1, \rho_2$, and ρ_3 leads to a buckling condition shown in Table 6.1 as seven homogeneous simultaneous equations.

Elastic critical buckling loads of the frame are plotted in Fig. 5.2 as a round-dotted line.

6.3 Comparison of Energy Method with Existing Method of Modified Slope Deflection

In order to evaluate the accuracy of the elastic energy method, some computations have been made on elastic buckling loads of one-, two-, and three-story frames by the elastic energy method and the modified slope deflection method. The results are tabulated in Table 6.2, 6.3, and 5.3. They are plotted in Fig. 6.1, 6.2, and 5.2. The solid curves in Fig. 6.2 and Fig. 6.3 indicate the effective length factor k vs. stiffness ratio γ relationships obtained from the energy method, when the specified structures buckle in antisymmetrical modes. The dotted curves correspond to the solutions which appeared in Tables 20, 21, and 22 of Ref. (1.45). Close comparison between the results of the two methods can be observed for smaller stiffness ratio γ. For practical building frames, γ is about 1. For larger γ values, the frame should fail in the inelastic range. In this case both methods are not valid. For $\gamma = \infty$, k values obtained from both methods are almost the same, as can be seen from Tables 6.2 and 6.3. When the floor system has an infinite stiffness, $\gamma = 0$, difference in k values is less than 1/2%. As shown in Fig. 6.1 and Fig. 6.2, the error involved in the energy method is due to the inferior beam curve assumed. According to a sample computation for a single-story frame by assuming a third degree polynomial instead of a three-term sine curve, the results obtained were within an error of 1/2%.

7. TESTS ON THE STABILITY OF THREE-STORY FRAMES

There are two objectives for the test of three-story frames. First, the phenomenon of inelastic instability in multi-story building frames is to be explored with relatively simple examples of three-story frames. Second, the energy method developed can be compared with the test results. At this writing tests were completed only on Frame U-2 shown in Table 7.1. Two separate tests were conducted on Frame U-2. The first tests did not give reliable data on frame stability because accidental restraints in the loading system prevented sway. The second test was conducted after alterations were made to the loading system. The two tests designated as "first test" and "second test" are reported herein. Recommended further tests are discussed in Chapter 9.

7.1 Description of Model Frames

The frame U-2 which was tested and is reported in this dissertation is one of four which were originally proposed. The frames and loading condition are summarized in Table 7.1. In order that the frames would simulate practical building frames as much as possible WF sections were adopted both for columns and beams.

The columns were fabricated from 2-5/8" x 1-1/2" wide flange shapes designated No. M-2362 by Bethlehem Steel Company. The cross sectional dimensions were measured with the aid of a micrometer and actual properties of the section were compared with those given by Bethelehem Steel Company. Both the actual and nominal properties are shown in Table 3.1.

The material properties of the member were determined by tension coupon test and stub column test. Coupons cut from the flanges and from the web of the section gave quite different yield levels. Therefore, a stub-column test was made to find the compressive stress-strain curve of a full cross-section of the member of the frames. This was an axial compression test which gave the integrated effect of different web and flange strengths in one test. The main purpose of the test was to obtain a compressive yield value to use in predicting the theoretical buckling load. The average yield stress level of flange coupons was very close to the result obtained from the stub column test. Therefore, the average value of 42.7 ksi was adopted as the yield stress level in theoretical predictions.

Slendernesses of columns and beams were chosen as variables and they were within the proportions of practical building frames. For practical frames, the end condtion should fall somewhere between the two extreme cases-pin-ended and fix-ended. However, pin-ended support was chosen to be on the safe side. A roller bearing system was attached at each column support to eliminate rotation friction as much as possible.

Past experience in testing rigid frames into the plastic range had shown that adequate lateral support was essential if the theoretical ultimate load was to be attained. In this investigation two frames connected by a lateral bracing system were tested at the same time. This would prevent any premature lateral torsional buckling of the members.

The bracing system was composed of welded purlins and girts made from 1-1/2" x 3/4" channels and cross braces. The cross braces were made of 1/4" diameter threaded steel rods and 2-1/2" long turnbuckles. The cross sectional properties of the purlins are given in Table 3.2. The spacing of purlins was less than $35r_y$ of the main frame member[7.1].

As shown in Fig. 7.1, a concentrated load $\frac{P}{3}$ was applied at both quarter points of each floor beam. The maximum design load was obtained by assuming a beam mechanism. Base fittings and welded connections were designed accordingly. The frames were fabricated by a local industrial firm.

Typical plans of model frame U-2 are shown in Fig. 7.2 and Fig. 7.3.

7.2 Loading System and Test Apparatus

Similar to the setup used in previous single-story frame tests[1.1], loads were applied by dead weights and lever systems. However, the design principles of the loading system were quite different from those of the single-story frame tests so that the application of floor loads could be easily controlled.

The key to a successful test of bifurcation type instability in a multi-story frame lies in adequate control over the alignment of the model frame and loading system as a whole in each story.

There are two causes leading to misalignment of a whole system, i. e. misfits in the model frame and eccentricity of the loading system. The former cannot be eliminated while the latter can be adjusted. Following are features of the test setup illustrated

in Fig. 7.7.

(1) Each floor has its own loading system

(2) A system of H-shaped spreader beams hung on the floor beams is adjustable in both directions in the plane of each floor. Therefore an applied load on each floor can be distributed symmetrically on four loading points on the floor beams.

(3) Total floor loads can be measured accurately through a dynamometer hung beneath the H-shaped beams.

(4) A magnification lever hung on the dynamometer is used to magnify dead load on a basket or loading platform. The magnification results in a load on the specimen about fifteen times the amount of dead weight applied to the loading basket.

(5) A tie-down wire on one end of the magnification lever keeps the lever in a horizontal position. Since the wire is connected to movable rollers on the base beams the wire can be kept in an upright position.

(6) High-strength steel beams with a yield stress of 65 ksi were used in the loading system to reduce the dead weight and member sizes of the loading system.

The test setup shown in Fig. 7.4 through Fig. 7.6 was designed according to the above requirements.

7.3 Strain Measurement

Strain in the frame was measured by attached strain gages. All strain gages were electric resistance SR-4 type A-1 linear gages. The location of the gages on the frame is shown in Fig. 7.8. A pair of strain gages was attached at the center of the outer surface

of each flange at each of the gage locations. There were 36 gages throughout the frame. The gage readings were used to align the loading system to assure a symmetrical strain picture in the columns. From the strain readings on both sides of a member, the thrust as well as bending moment of the member can be obtained. A strain gage similar to the 36 strain gages on the frame was attached on a steel plate separated from the frame. The gage is defined as a reference gage to record any accidental drift of the measuring circuit during the test. No appreciable difference in strain reading was recorded from the reference gage throughout the test. Therefore, the 36 active gage readings were used to compute the strain in the frame without any correction. A single dummy gage was included in the strain indicator bridge circuit for temperature compensation.

A total of 37 gages were connected to two "19 Channel Switch and Balance Boxes". The switch boxes were connected to a "Budd Digital Strain Indicator". The strain readings were directly shown in the dial without a balancing and reducing process. For the purpose of automatic data reducing, strain readings were punched on IBM data cards.

7.4 Deflection Measurement

The purpose of the frame stability test is to obtain sidesway deflection versus load relationships. The frame is considered buckled when the horizontal deflection increased without additional load. Therefore, deflection has to be measured precisely.

The deflection was measured by six-inch steel scales attached on the frame and surveyor's transits. The position of the scales is

shown in Fig. 7.9. Five transits were mounted on a scaffold twenty feet away from the frame. Two sets of column deflections and three sets of beam deflections were taken through the transits. Some transits mounted on the scaffold can be seen in Fig. 7.10.

For the purpose of test control, load-deflection curves at the center of a beam and at the top of the first story column were plotted during the test. They are shown in Fig. 7.11 and Fig. 7.12. At first test the frame was restrained from sidesway, while during the second test the same frame was not restrained by the loading system. Fig. 7.11 is the load-deflection curve of the first test. The frame did not sway when the load reached the critical buckling load, instead the center portion of one of the top beams yielded considerably at a total load of 75 kips. Therefore, the test was temporarily suspended. Fig. 7.12 shows the load-deflection curve of the frame for the second test. The first story swayed eight inches suddenly at a total load of 71 kips.

7.5 Test Procedure

After the frame was fabricated, the loading system was attached to the frame. The frame was white-washed and the loading system painted in blue. Three dynamometers were connected to a strain indicator. Strain gage readings before and after attachment of the loading system were taken as initial readings. Several fifty-pound steel blocks were put on the third floor basket. Unsymmetrical strain-readings on the top floor columns were adjusted by changing the position of the cross bar of the H-shaped spreader beam system. Then the position of the cross beam was fixed by two pairs of bolts

on the ends of the beam. After completion of the alignment of the top story, the second and then the bottom floor were aligned. The alignment was surprisingly easy and accurate compared to that of previous single-story frame tests.

Since the weight of magnification lever on each story was different, the initial loads on each story were not equal. Therefore, the loading system was balanced by putting additional weights on two baskets to assure equal application of loads on all stories. From then on increments of about five kips on the whole frame were applied. Dynamometer readings, strain gage readings and deflection measurements were taken after each increment. The load-deflection curves at the mid-span of a beam and the sidesway deflection at the top of the first story were plotted to compare with the analytical results.

After the load on the frame exceeded 46 kips, yielding was observed at both ends of the second story beams. Therefore, the load increment was reduced.

When the load reached 75 kips, which is slightly lower than the simple plastic load of 76 kips, a beam mechanism was observed on a top floor beam. The test was suspended.

During earlier single-story frame tests[1.1] it was found to be difficult to adjust for excessive elongations of tie-down wire ropes. Therefore, as shown in Fig. 7.6, 7/8" diameter steel rods were used to tie down the magnification levers in the first test of Frame U-2. It was believed that the tie down rods introduced some restraint so that the frame did not buckle when it otherwise should have. A tie-down rod and a magnification lever formed a hinge plane

which was perpendicular to the expected direction of motion rather than in it. Therefore, some alterations were made. The model frame was raised six feet by placing it on a pair of 36WF300 grillage beams and a pair of pedestals as shown in Fig. 7.13. A longer set of wire ropes was installed in order to cause a smaller horizontal restraining force at the instant of frame buckling. Shackles were inserted between the dynamometer and magnification lever. Another test was run using a proceudre similar to the original one. The test was satisfactory after these minor alterations. When a total load on the frame reached 68 kips, the tie-down wire ropes on the first and the second stories were adjusted by tightening the turn-buckles. This resulted in slightly changed lever ratios of the two magnification levers. The total load on the frame was increased to 71 kips. About two minutes after adjustment of the levers, the frame swayed suddenly. It is believed that the load of 71 kips represented a good approximation of actual buckling load because of the following reasons:

(1) The sudden bifurcation of the frame is evidence that little restraint of the loading system was imposed on the model frame.

(2) The magnification levers pivoted about the axes of the tie-down wire ropes and moved with the frame.

(3) Before frame buckling, small increments of load were actually applied by gradual adjustment of lever ratios. This experimental load of 71 kips, is only 4% lower than the predicted load of 74 kips calculated by the inelastic energy method on the deterioted frame. The failure mode of the frame was similar to a sidesway panel

mechanism on the first story as expected. Figure 7.14 shows a general view after the frame buckled.

7.6 Test Results and Their Comparison with Analytical Methods

In general the test was satisfactory and the frames behaved as expected. The two frames performed almost identically. No lateral-torsional buckling was observed. Adequate bracing was supplied to prevent this. However, some of the diagonal braces preventing out-of-plane sway of the structure were buckled due to a sudden bifurcation of the first story. The welded rigid joints were adequate throughout the frame. No cracks or local buckling could be observed after test. A buckling mode similar to a panel mechanism of the first story was obtained. Very little inelastic permanent deformation was observed throughout the frame except the drastic sway rotations at the tops of the first-story columns.

From the strain gage readings, the bending moments and thrusts throughout the frame were computed and they are shown in Fig. 7.15 through Fig. 7.20.

Relative load-deflection curves of columns at each floor level are plotted in Fig. 7.21 and Fig. 7.22. The relative sidesway deflections of the second and the third floors Δ_2 and Δ_3 are very small compared to the sway deflection of the first floor Δ_1.

Deformed shapes of the frame at different loading are plotted in Fig. 7.23, 7.24, and 7.25. Figure 7.26 shows the buckled shape of the frame after testing. A comparison between Fig. 7.25 and Fig. 7.26, the deformed shape before and after buckling, indicates that the frame has a marked buckling mode with the first story as a critical story.

The buckling load of 71 kips obtained from the test was compared with the predicted load of 74 kips according to the method outlined in Article 8.2. The predicted load was only 4% higher than the test result.

8. PRACTICAL APPLICATION OF THE THEORY

8.1 Analysis of Tall Building Frames Neglecting the Effect of Primary Bending Moments.

In order to look into the phenomenon of frame buckling in actual building frame, an eleven-story frame was chosen for analysis. The frame was designed by George C. Driscoll, Jr. Beams are proportioned according to the simple plastic theory and columns by an elastic method according to the 1947 AISC specification.

The dimensions, member sizes and loading condition of the frame are shown in Fig. 8.1. The modulus of elasticity E=30,000 ksi and yield stress σ_y = 33 ksi were adopted in the calculation. Some notations convenient for a computer program are tabulated in Table 8.1. The total energy of the frame is shown in Table 8.2. The buckling condition of the frame was obtained by minimization of the expression $\Sigma(U + V)$ with respect to deformation parameters ψ's and ρ's, as shown in Table 8.3. Figure 8.2 is a flow chart for buckling analysis of the frame using a G. E. 225 computer. The imput data were axial yield loads and yield moments of columns and beams, span length, story height and applied load on the structure. Within 3.4 minutes the computer printed out the nondimensional critical load $\overline{P}cr = 0.63$. From this the buckling load on the frame is predicted as $2P = 2 \times 0.63 \times P_y = 2 \times 0.63 \times 1960 = 2470$ kips.

In order to analyze the deformation configulation of the frame after buckling, another program was set up for calculation of deformation parameters ψ's and ρ's. The side sway of the first floor was assumed to be within a value of $\rho_1 = 0.005$ radians. An arbitrary side

sway of 0.005 radian was chosen to be somewhat greater than the order of magnitude of design sidesway of typical building frames. Given ρ_1 value at the critical load, the rest of the deformation quantities can be obtained by solving the simultaneous equations for $\Psi_1, \Psi_2, \cdots \Psi_{11}$, and $\rho_2, \rho_3, \cdots \rho_{11}$. Since the deformation of the frame is not unique after a frame has swayed sidewise, the absolute value of deformation quantities are not meaningful; rather their relative deformations are more significant. Figure 8.3 shows the flow chart for deformation analysis of the eleven-story frame. The results of the deformation analysis are shown in Fig. 8.4. Evidently the largest sway would occur on the second floor and the third floor would come next. The first floor should be rather stable due to a larger column size and its fixed-ended condition. Programs for buckling analysis and deformation analysis are shown in Appendix A and Appendix B respectively.

8.2 Buckling of Frame with Plastic Hinges Developed on Beams due to Primary Bending Moments.

As shown in Article 2.3, plastic hinges can be replaced by actual hinges in the stability analysis of frames to obtain the deterioted critical load. Therefore, zero moments were assumed at the locations of plastic hinges on the deteriorated structure. In the case of a frame with a very strong floor system, it is not likely that plastic hinges will develop in beams. For this type of the frame, the method outlined in the previous article can be used.

However, the frame becomes more critical if the beams are designed according to the simple plastic mechanism. In this weak beam design, plastic hinges develop at both ends of beams prior to the

formation of beam mechanisms. To start with, the applied load on the deteriorated structure can be assumed. A load equal to the load at the formation of the first plastic hinge may be assumed. Then the load is gradually increased for the tests of stability condition. Discontinuity in boundary condtion is introduced at the joints having plastic hinges. At this stage, the frame becomes more susceptible to buckling failure due to reduction of the degree of indeterminacy by introducing plastic hinges. When the frame sways sidewise, plastic hinges on one end of all beams undergo unloading and become elastic again. The plastic hinges on the other ends continue to rotate. Therefore, hinges may be introduced on one end of beams and buckling of the frame maybe analyzed accordingly. An example of analysis is shown in Fig. 7.1. The frame U-2 has dimensions and sectional properties shown in Fig. 7.1(a). The frame can almost carry the load corresponding to the simple beam mechanism. Prior to the development of beam mechanism some plastic hinges must have formed at both ends of the beams. Though some of the end moments of beams might not reach the full plastic moment, they are very close to the plastic moment in plastically designed frames. It is on the safe side to assume that hinges form at the end of each beam as shown in Fig. 7.1(b). Therefore, the frame analyzed is weaker than the actual frame under the same loading condition. At the instant of sidesway buckling, the frame has the configuration of Fig. 7.1(c). The plastic hinges at one end of all beams become elastic while the hinges on the other ends cause continuous rotation. Because of the discontinuity, three hinges and corresponding hinge rotations Ψ_8, Ψ_9,

and ψ_{10} are introduced. The loads are applied on the column tops of the deteriorated frame. Therefore, the analysis takes into account the effect of yielding throughout the frame and the effect of unloading at the joints.

The method of analysis is similar to that of the previous three-story frame. The nondimensional critical buckling load of the frame is $\bar{P}cr = 0.42$ as shown in Appendix C. The total buckling load on the frame $4P = 4 \times 0.42 \times 44.26 = 74$ kips.

8.3 Merchant's Approximate Formula

In 1954, Merchant[6.1] proposed a generalized Rankine's formula to estimate the failure load of elastic-plastic structures. The ultimate load of the frame $\bar{P}$ can be expressed in terms of the simple plastic load $\bar{P}_p$ and the elastic buckling load $\bar{P}cr$ as in the following formula:

$$\frac{1}{\bar{P}} = \frac{1}{\bar{P}_p} + \frac{1}{\bar{P}_{cr}}$$

A series of thirty-four model tests on three-, five-, and seven-story frames[1.54] indicated that Merchant's formula is too conservative. The buckling load of the three-story model frames has been calculated by Merchant's formula.

From Table 5.3, the elastic critical load is $\bar{P}cr = 0.782$. The simple plastic load $\bar{P}_p = 0.425$ can be obtained from the simple beam mechanism shown in Fig. 7.1. The critical buckling load of the frame U-2 is

$$\bar{P} = \frac{\bar{P}cr \cdot \bar{P}_p}{\bar{P}cr + \bar{P}_p} = \frac{0.782 \times 0.425}{0.782 + 0.425} = 0.275$$

For the frame of four columns, the total buckling load on the frame is

$$4P = 4 \times 0.275 \times 44.26 = 49 \text{ kips}$$

8.4 Effective Length Factor Method

The load carrying capcity of centrally loaded columns and simple frame can be expressed in terms of the effective length of the columns $K\ell$, where K is effective length factor[8.1]. The K value is dependent on the G values which define the end conditions of the column. By definition

$$G = \frac{\Sigma \frac{Ic}{Lc}}{\Sigma \frac{Ig}{Lg}}$$

in which Σ indicated a summation for all members rigidly connected to that joint and lying in the plane of buckling. Ic is the moment of inertia and Lc the unsupported length of a column section, and Ig is the moment of inertia and Lg the unsupported length of a girder or other restraining member.

For the frame U-2, $G_o = \infty$

$$G_1 = \frac{\Sigma \frac{Ic}{Lc}}{\Sigma \frac{Ig}{Lg}} = \frac{\frac{I}{44} + \frac{I}{44}}{\frac{I}{60}} = 2.72$$

where subscripts o and 1 indicate the joints at bottom and top of the first story column. The alignment charts in Reference (8.1) give a K value of 2.9. According to Table 2.5 of Reference 8.1 the non-dimensional buckling load of the column is $\overline{P} = 0.64$. The total buckling load of frame U-2 is

$$4P = 4 \times 0.64 \times 44.26 = 113 \text{ kips}$$

8.5 Buckling Analysis of Frames with Tapered Columns.

For frames with tapered columns, the energy method has an advantage of simplicity over conventional method. Results of the buckling analysis of a portal frame with linearly tapered columns showed that additional effort over that of uniform columns is practically negligible. In this case the total strain energy of a column can be obtained by integration of Eq. (6.2), except moment of inertia of the column I be replaced by a linear function.

8.6 Comparison Among Analytical Methods

Results of buckling analysis of the model frame U-2 by different analytical methods are summarized in Table 8.4. Since model frame U-2 was proportioned according to the geometry and member size of practical building frames, the numerical values appearing in Table 8.4 reveal the quantitative picture of the assumptions made in the different analytical methods. Some comparisons among the methods are significant in drawing the conclusions in the following chapter.

(a) Comparison between the effective length factor method and the concentric inelastic energy method shows that the effective length factor method recommended by the Column Research Council can effectively predict the buckling load of a concentrically loaded frame. More details are shown in Table 8.5 and Fig. 8.5.

(b) Merchant's Formula is overconservative.

(c) The results obtained by simple plastic analysis, Merchant's solution, the inelastic energy method with plastic hinges, and the tests are drastically different from those obtained by effective length factor, concentric modified slope-deflection and concentric

energy methods. This indicates the significance of the effect of primary bending moment upon the buckling of one- to three- story frames.

8.7 Buckling Analysis of Single-Story Frames and Their Comparison with Exact Solution and Test Results.

The inelastic energy method was designed for the stability analysis of tall building frames. The effect of primary bending moment due to loads on beams is relatively small compared with the high axial load on the lower stories. However, the inelastic energy method was applied to compute the buckling loads of single-story model frames W-1 and W-2. Results of exact analysis and tests are summarized in Table 5 of Reference (1.1).

For frame W-1, the critical buckling load and ultimate load from test were 9.22 kips and 11.17 kips on each column. A buckling load of 9.74 kips was computed by the inelastic energy method compared with the result of 10.65 kips obtained by Lu.

For frame W-2, 8.79 kips was the critical buckling load and 10.14 kips was the ultimate load obtained from the test, while 9.73 kips was the buckling load calculated by the inelastic energy method compared with 10.18 kips obtained by Lu.

9. SUMMARY AND CONCLUSIONS

In this dissertation an energy method has been used for the anti-symmetrical buckling analysis of multi-story frames in the elastic and inelastic ranges. Elastic buckling loads of one- two-, and three-story frames with varied slenderness of columns were computed by the proposed elastic energy method. Their results were compared with those obtained by the existing method of modified slope deflection. The method developed in this dissertation is valid for determining the tangent modulus load of axially loaded frames. The problem of a frame subjected to primary bending moments was not solved exactly. However, an approximate buckling load was obtained by applying the inelastic energy method to a deteriorated frame taking into account the effect of yielding on beams and columns. A technique for experimental investigation of the instability of three-story frames is shown. A practical sample of a buckling analysis of an eleven-story building frame is given.

Finally a three-story frame is analyzed by existing methods and the proposed method. The results of analysis are compared with a test result.

The contribution of this dissertation can be summarized as follows.

(1) A method to determine the elastic buckling load of multi-story frames under concentric column loads was shown. The advantage of the method over conventional methods lies in its simplicity because trigonometric functions no longer exist in the buckling condition. Therefore, the buckling load of a frame can be obtained without tables of

trigonometric functions or stability functions.

(2) The method is extended to analyze frames in the inelastic as well as the elastic range. Frames partially yielded due to axial load and residual stresses can be analyzed.

(3) An experimental technique to investigate the phenomena of instability in multi-story frames is shown. The test setup is effective both for small deflections and large deflections of model frames. Therefore, the test setup can be used to investigate the instability of frames under combined vertical and horizontal loads.

(4) A digital computer program is developed to solve the anti-symmetrical buckling of an actual building frame. The imput data are geometry of the frame, bending characteristics of members and axial yield strength of columns. The computer can print out the critical buckling load within several minutes for the analysis of an eleven-story frame.

(5) The deformed shape of the frame at the instant of buckling is investigated. After obtaining the critical buckling load, another program has been developed to solve the angular rotation at each joint and sidesway at each story. The results of the analysis reveal a clear picture of failure mode of the frame. The design can be revised accordingly to increase the ultimate strength of the frame.

The following conclusions can be drawn from the results of the investigation contained in this dissertation.

(1) The elastic energy method developed in this dissertation can be used to predict the elastic instability load of frames more

directly than the modified slope-deflection method. The error involved in this method is within the order of magnitude of those due to the irregularity of material properties, loading conditions and construction methods.

(2) Close comparions between the results obtained by the inelastic energy method and the method recommended by the Column Research Council[8.1] indicate that the CRC method is very effective for practical analysis of low building frames under concentric column loads.

(3) The predicted buckling load is only 4% higher than the test result. However, more tests are necessary to confirm the accuracy of the inelastic energy method.

(4) The inelastic instability analysis of an eleven-story building frame showed that the reduction of load-carrying capcity is more than one-third of the full yield load of the columns. Therefore, a check against instability may be necessary in the lower story of high multi-story frames.

(5) The results of deformation analysis reveal some important facts about the buckling mode of practical building frames. The frame has a definite failure mode with the largest sidesway in a lower story of the frame. The magnitude of the sidesway tapers off rapidly away from this critical story.

(6) A revised design against overall instability of a frame can be made by increasing the member sizes in the critical story of the frame. This might result in an economical design so far as the overall instability load is the critical load of the frame.

(7) The buckling load obtained by Merchant's method was only two-

thirds of the buckling load obtained from the test. Therefore, Merchant's method is too conservative for a frame of these proportions and loading.

(8) The design of the model frame and test setup were satisfactory as evidenced by the test result. A sudden bifurcation of the frame at buckling indicates that the function of the H-shaped spreader beams was very satisfactory for the alignment of the frame and the loading system imposed little restraint to sidesway movement of the frame.

(9) The agreement between the theoretical failure mode and buckled shape of the test frame can be regarded as additional evidence that the inelastic energy method is adequate and can be used for deformation analysis of frames.

Based on the theoretical and experimental studies contained in this dissertation, some additional research work still needed is suggested in the following.

(1) Investigation of the effect of beam stiffness upon buckling of a frame can be made by conducting the proposed test of Frame U-4 in Table 7.1.

(2) In order to investigate the structural behavior at the lower stories of a tall building frame, two additional loads can be applied on the column tops of Frame U-1 and U-3 in Table 7.1.

(3) The buckling behavior of an isolated portion of the lower several stories of the eleven-story frame must be studied. From the results of computation, a decision can be made as to what extent the top stories can be disregarded for a buckling analysis.

(4) Results of the above theoretical and experimental studies should be able to lead to the establishment of specifications in the design of multi-story frames against instability of bifurcation type.

(5) The effect of partial base fixity upon the buckling of multi-story frames must be studied.

The energy method for stability analysis presented in this dissertation constitutes a possible first step in obtaining the critical load of the structure under both static and dynamic loads. Further studies in this field by the energy method are strongly recommended.

10. NOMENCLATURE

A = Cross-sectional area

a = Magnification parameter of beam deflection curve

b = Number of bays

d = Depth of cross-section

E = Elastic modulus

$f(\bar{P})$ = Coefficient of bending strain energy

H = Axial thrust on a beam

$H=\frac{H}{Py}$ = Non-dimensional axial thrust on a beam

h = Column height

I = Moment of inertia

I_i = Moment of inertia of the i^{th} story member

i = Subscript of story number or left joint

j = Subscript of right joint

K = Effective length factor

ℓ = Span length

$\bar{M}=\frac{M}{M_y}$ = Non-dimensional bending moment

My = Yield bending moment

$(M_{yb})_i$ = Yield moment of i^{th} floor beam

$(M_{yc})_i$ = Yield moment of i^{th} story column

m = Total maximum unknown variables of the frame

n = Number of stories

P = Axial load on a column

$\bar{P} = \frac{P}{P_y}$ = Non-dimensional axial load

$\bar{P}_i = (\frac{P}{P_y})_i$ = Non-dimensional axial load on the i^{th} story column

P_{cr} = Critical buckling load of a frame

P_e = Elastic buckling load of a frame

P_p = Ultimate load by simple plastic method

P_y = Axial yield load

r_y = Radius of gyration about weak axis

S = Section modulus

s = Half length of a column

U = Total strain energy of a member

U_B = Total strain energy of a beam

U_c = Total strain energy of a column

U_e = Elastic strain energy of a member

U_n = Modified strain energy

u = Bending strain energy of a unit length

$u = \frac{u}{u_y}$ = Non-dimensional bending strain energy

u_y = Unit bending strain energy at yield

V = Potential energy of a member

V_B = Potential energy of a beam

V_C = Potential energy of a column

V_H = Potential energy of axial thrust on a beam

V_w = Potential energy of uniform load on a beam

V_n = Modified potential energy

w = Uniform load on a beam

$X = \frac{4\pi^2 My \, f(0)}{\phi_y \ell}$ = in Table 5.1 and Table 5.2

$Y1 = \frac{8 \, My \, f(\bar{P})}{\phi_y h}$ = in Table 5.1 and Table 5.2

$Y2 = \frac{8 \, My \, f(2/3 \, \bar{P})}{\phi_y h}$ = in Table 5.1 and Table 5.2

$Y3 = \frac{8 \, My \, f(1/3\bar{P})}{\phi_y h}$ = in Table 5.1 and Table 5.2

$Z = \frac{\bar{P} \, Py \, h}{45}$ = in Table 5.1 and Table 5.2

γ = Stiffness ratio

Δ_B = Axial shortening of a beam

Δ_C = Axial shortening of a column

Δ_i = Axial shortening of the i^{th} story column

Δh_i = Total settlement at the top of the i^{th} story column

δ_i = Sidesway deflection at the i^{th} floor

ρ_i = Sidesway rotation of the i^{th} story column

σ = Stress

σ_y = Yield stress

ϕ = Curvature

$\bar{\phi} = \frac{\phi}{\phi_y}$ = Nondimensional curvature

ϕ_y = Curvature at yield

$(\phi_{yb})_i$ = Yield curvature of i^{th} floor beam

$(\phi_{yc})_i$ = Yield curvature of i^{th} story column

Ψ_i = Angular rotation of joint i

Ψ_j = Angular rotation at joint j

11. TABLES AND FIGURES

Table 3.1

Table 3.1 SECTIONAL PROPERTIES OF TEST SPECIMENS

	Area of Section A, $in.^2$	Depth of Section d, in	Flange Width b, in.	Flange Thickness t, in.	Flange Thickness W, in.	I_x $in.^4$	S_x $in.^3$	r_x in.	Z $in.^3$	f	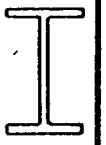
Nominal	1.085	2.625	1.840	0.201	0.156	1.236	0.942	1.062	1.086	1.16	
Measured	1.043	2.625	1.813	0.207	0.156	1.251	0.953	1.095	1.067	1.12	

Table 3.2

Table 3.2 SECTIONAL PROPERTIES OF PURLIN

Area of Section A, $in.^2$	Depth of Section d, in.	Flange Width b, in.	Flange Thickness t, in.	Web Thickness W, in.	I_x $in.^4$	S_x $in.^3$	r_x in.	r_y in.	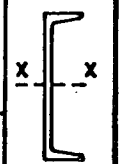
0.34	1.5	0.75	0.188	0.125	0.11	0.15	0.56	0.22	

Table 5.1

Table 5.1 TOTAL POTENTIAL ENERGY OF THREE-STORY FRAMES

COLUMN U_c (0-1;4-5)	$Y1\left[\psi_0^2+\psi_1^2+\psi_0\psi_1-3\psi_0\rho_1-3\psi_1\rho_1+3\rho_1^2\right]$
U_c (1-2;5-6)	$Y2\left[\psi_1^2+\psi_2^2+\psi_1\psi_2-3\psi_1\rho_2-3\psi_2\rho_2+3\rho_2^2\right]$
U_c (2-3;6-7)	$Y3\left[\psi_2^2+\psi_3^2+\psi_2\psi_3-3\psi_2\rho_3-3\psi_3\rho_3+3\rho_3^2\right]$
V_c	$-3Z\left[2\psi_0^2+2\psi_1^2+18\rho_1^2-3\psi_0\rho_1-3\psi_1\rho_1-\psi_0\psi_1\right]$
	$-2Z\left[2\psi_1^2+2\psi_2^2+18\rho_2^2-3\psi_1\rho_2-3\psi_2\rho_2-\psi_1\psi_2\right]$
	$-Z\left[2\psi_2^2+2\psi_3^2+18\rho_3^2-3\psi_2\rho_3-3\psi_3\rho_3-\psi_2\psi_3\right]$
BEAM U_B (1-5)	$\frac{X}{2}\psi_1^2$
U_B (2-6)	$\frac{X}{2}\psi_2^2$
U_B (3-7)	$\frac{X}{2}\psi_3^2$

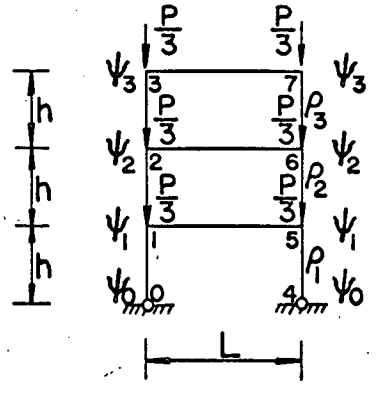

Table 5.2

Table 5.2 INELASTIC BUCKLING CONDITION OF THREE-STORY FRAMES

	ψ_0	ψ_1	ψ_2	ψ_3	ρ_1	ρ_2	ρ_3
$\frac{\partial\Sigma(U+V)}{\partial\psi_0}$	2Y1 −12Z	Y1 +3Z			−3Y1 +9Z		
$\frac{\partial\Sigma(U+V)}{\partial\psi_1}$	Y1 +3Z	2Y1+2Y2 −20Z+X	Y2 +2Z		−3Y1 +9Z	−3Y2 +6Z	
$\frac{\partial\Sigma(U+V)}{\partial\psi_2}$		Y2 +2Z	2Y2+2Y3 −12Z+X	Y3 +Z		−3Y2 +6Z	−3Y3 +3Z
$\frac{\partial\Sigma(U+V)}{\partial\psi_3}$			Y3 +Z	2Y3 −4Z+X			−3Y3 +3Z
$\frac{\partial\Sigma(U+V)}{\partial\rho_1}$	−3Y1 +9Z	−3Y1 +9Z			6Y1 −108Z		
$\frac{\partial\Sigma(U+V)}{\partial\rho_2}$		−3Y2 +6Z	−3Y2 +6Z			6Y2 −72Z	
$\frac{\partial\Sigma(U+V)}{\partial\rho_3}$			−3Y3 +3Z	−3Y3 +3Z			6Y3 −36Z

Table 5.3

Table 5.3 RESULTS OF ANTI-SYMMETRIC BUCKLING ANALYSIS OF THREE-STORY FRAMES

Method	$\frac{h}{r_x}$	15	20	25	30	40	60	80	120	160	
Modified slope Deflection	$\frac{P}{P_y}$	3.719	2.403	1.693	1.262	0.782	0.388	0.232	0.110	0.064	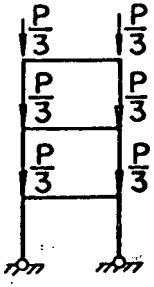
Elastic Energy	$\frac{P}{P_y}$	4.684	2.940	2.025	1.482	0.895	0.429	0.251	0.116	0.067	
Inelastic Energy	$\frac{P}{P_y}$	1.060	0.987	0.899	0.803	0.616	0.351	0.215	0.103	0.060	

Table 6.1

Table 6.1 ELASTIC BUCKLING CONDITION OF THREE-STORY FRAMES

	ψ_0	ψ_1	ψ_2	ψ_3	ρ_1	ρ_2	ρ_3
$\frac{\partial\sum(U+V)}{\partial\psi_0}$	$\frac{8EI_c}{h} - \frac{12Ph}{45}$	$\frac{4EI_c}{h} + \frac{3Ph}{45}$			$-\frac{12EI_c}{h} + \frac{9Ph}{45}$		
$\frac{\partial\sum(U+V)}{\partial\psi_1}$	$\frac{4EI_c}{h} + \frac{3Ph}{45}$	$\frac{16EI_c}{h} - \frac{20Ph}{45} + \frac{2\pi^2EI_b}{L}$	$\frac{4EI_c}{h} + \frac{2Ph}{45}$		$-\frac{12EI_c}{h} + \frac{9Ph}{45}$	$-\frac{12EI_c}{h} + \frac{6Ph}{45}$	
$\frac{\partial\sum(U+V)}{\partial\psi_2}$		$\frac{4EI_c}{h} + \frac{2Ph}{45}$	$\frac{16EI_c}{h} - \frac{12Ph}{45} - \frac{2\pi^2EI_b}{L}$	$\frac{4EI_c}{h} + \frac{Ph}{45}$		$-\frac{12EI_c}{h} + \frac{6Ph}{45}$	$-\frac{12EI_c}{h} + \frac{3Ph}{45}$
$\frac{\partial\sum(U+V)}{\partial\psi_3}$			$\frac{4EI_c}{h} + \frac{Ph}{45}$	$\frac{8EI_c}{h} - \frac{4Ph}{45} + \frac{2\pi^2EI_b}{L}$			$-\frac{12EI_c}{h} + \frac{3Ph}{45}$
$\frac{\partial\sum(U+V)}{\partial\rho_1}$	$-\frac{12EI_c}{h} + \frac{9Ph}{45}$	$-\frac{12EI_c}{h} + \frac{9Ph}{45}$			$\frac{24EI_c}{h} - \frac{108Ph}{45}$		
$\frac{\partial\sum(U+V)}{\partial\rho_2}$		$-\frac{12EI_c}{h} + \frac{6Ph}{45}$	$-\frac{12EI_c}{h} + \frac{6Ph}{45}$			$\frac{24EI_c}{h} - \frac{72Ph}{45}$	
$\frac{\partial\sum(U+V)}{\partial\rho_3}$			$-\frac{12EI_c}{h} + \frac{3Ph}{45}$	$-\frac{12EI_c}{h} + \frac{3Ph}{45}$			$\frac{24EI_c}{h} - \frac{36Ph}{45}$

Table 6.2

Table 6.2 RESULTS OF ANTI-SYMMETRIC BUCKLING ANALYSIS OF SINGLE-STORY FRAMES

Method	γ	0	0.1	0.2	0.5	1.0	5.0	∞	
Modified slope Deflection	k	2.00	2.03	2.07	2.17	2.33	3.38	∞	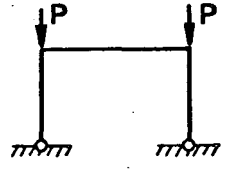
Elastic Energy	k	1.992	2.013	2.033	2.095	2.197	2.926	∞	
Modified slope Deflection	k	1.000	1.016	1.030	1.082	1.156	1.501	2.000	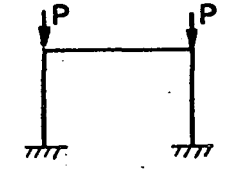
Elastic Energy	k	0.993	1.004	1.014	1.045	1.093	1.369	1.991	

Table 6,3

Table 6.3 RESULTS OF ANTI-SYMMETRIC BUCKLING ANALYSIS OF TWO-STORY FRAMES

Method	γ	0	0.1	0.5	1.0	2.0	∞	
Modified slope Deflection	k	2.000	2.033	2.166	2.328	2.634	∞	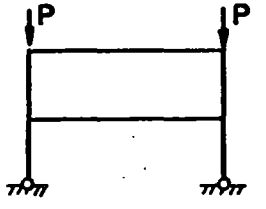
Elastic Energy	k	1.992	1.995	2.075	2.189	2.353	∞	
Modified slope Deflection	k	1.000	1.033	1.160	1.310	1.515	4.000	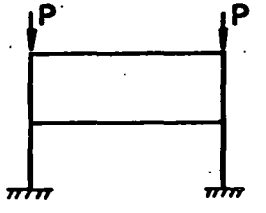
Elastic Energy	k	0.993	1.020	1.126	1.237	1.447	4.000	

Table 7.1

Table 7.1 PROPOSED TESTS OF UNBRACED FRAMES UNDER VERTICAL LOADS

Frame No.	Beam			Column				
	Span L (in)	Size	r_x (in)	$\frac{L}{r_x}$	Height h (in)	Size	r_x (in)	$\frac{h}{r_x}$
U-1	60	$2\frac{5}{8}$ I3.7	1.095	54.8	33	$2\frac{5}{8}$ I3.7	1.095	30
U-2	60	$2\frac{5}{8}$ I3.7	1.095	54.8	44	$2\frac{5}{8}$ I3.7	1.095	40
U-3	60	3I5.7	1.230	48.8	33	$2\frac{5}{8}$ I3.7	1.095	30
U-4	60	3I5.7	1.230	48.8	44	$2\frac{5}{8}$ I3.7	1.095	40

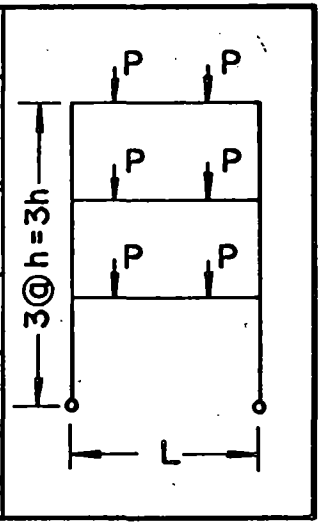

Tbl 8.1

Table 8.1 NOTATIONS IN COMPUTER PROGRAM

F(N) = -0.0425*P(N)*P(N)-0.1363*P(N)+0.4509 ForP(N)<0.4

G(N) = -0.3471*P(N)*P(N)+0.0242*P(N)+0.4354 ForP(N)>0.4

H = Height of a column

L = Span Length

MYB(N) = Yielding moment of the N^{th} floor beam

MYC(N) = Yielding moment of the N^{th} story column

N = Story or floor number

P = Non-dimensional axial load wrt. the first story column

PC = Non-dimensional critical buckling load

P(N) = Non-dimensional axial load on the N^{th} story column

PYC(N) = Axial yielding load of the N^{th} story column

RYB(N) = Yielding curvature of the N^{th} floor beam

RYC(N) = Yielding curvature of the N^{th} story column

$$X(N) = \frac{10.8216*MYB(N)}{L*RYB(N)}$$

$$Y(N) = \frac{8*F(N)*MYC(N)}{H*RYC(N)} \quad \text{For } P(N) < 0.4$$

$$Y(N) = \frac{8*G(N)*MYC(N)}{H*RYC(N)} \quad \text{For } P(N) > 0.4$$

$$Z = \frac{P*H*PYC(1)}{165}$$

PSI(N) = ψ_i

RHO(N) = ρ_i

Table 8.2

Table 8.2 TOTAL POTENTIAL ENERGY OF AN ELEVEN-STORY FRAME

Column	
U_C	$\sum_{N=1}^{11} Y(N) * (\psi_{N-1}^2 + \psi_N^2 + \psi_{N-1}\psi_N - 3\psi_{N-1}\rho_N - 3\psi_N\rho_N + 3\rho_N^2)$
V	$-66 * Z * (2\psi_1^2 + 18\rho_1^2 - 3\psi_1\rho_1)$
	$-55 * Z * (2\psi_1^2 + 2\psi_2^2 + 18\rho_2^2 - 3\psi_1\rho_2 - 3\psi_2\rho_2 - \psi_1\psi_2)$
	$-45 * Z * (2\psi_2^2 + 2\psi_3^2 + 18\rho_3^2 - 3\psi_2\rho_3 - 3\psi_3\rho_3 - \psi_2\psi_3)$
	$-36 * Z * (2\psi_3^2 + 2\psi_4^2 + 18\rho_4^2 - 3\psi_3\rho_4 - 3\psi_4\rho_4 - \psi_3\psi_4)$
	$-28 * Z * (2\psi_4^2 + 2\psi_5^2 + 18\rho_5^2 - 3\psi_4\rho_5 - 3\psi_5\rho_5 - \psi_4\psi_5)$
	$-21 * Z * (2\psi_5^2 + 2\psi_6^2 + 18\rho_6^2 - 3\psi_5\rho_6 - 3\psi_6\rho_6 - \psi_5\psi_6)$
	$-15 * Z * (2\psi_6^2 + 2\psi_7^2 + 18\rho_7^2 - 3\psi_6\rho_7 - 3\psi_7\rho_7 - \psi_6\psi_7)$
	$-10 * Z * (2\psi_7^2 + 2\psi_8^2 + 18\rho_8^2 - 3\psi_7\rho_8 - 3\psi_8\rho_8 - \psi_7\psi_8)$
	$-6 * Z * (2\psi_8^2 + 2\psi_9^2 + 18\rho_9^2 - 3\psi_8\rho_9 - 3\psi_9\rho_9 - \psi_8\psi_9)$
	$-3 * Z * (2\psi_9^2 + 2\psi_{10}^2 + 18\rho_{10}^2 - 3\psi_9\rho_{10} - 3\psi_{10}\rho_{10} - \psi_9\psi_{10})$
	$-Z * (2\psi_{10}^2 + 2\psi_{11}^2 + 18\rho_{11}^2 - 3\psi_{10}\rho_{11} - 3\psi_{11}\rho_{11} - \psi_{10}\psi_{11})$
Beam	
U_B	$\sum_{N=1}^{11} \frac{1}{2} * X(N) * \psi_N^2$

Table 8.3

Table 8.3 INELASTIC BUCKLING CONDITION OF AN ELEVEN-STORY FRAME

	ψ_1	ψ_2	ψ_3	ψ_4	ψ_5	ψ_6	ψ_7	ψ_8	ψ_9	ψ_{10}	ψ_{11}	ρ_1	ρ_2	ρ_3	ρ_4	ρ_5	ρ_6	ρ_7	ρ_8	ρ_9	ρ_{10}	ρ_{11}
$\frac{\partial\Sigma(U+V)}{\partial\psi_1}$	X1+2×Y1 +2×Y2 -484×Z	Y2 +55×Z										-3×Y1 +198×Z	-3×Y2 +165×Z									
$\frac{\partial\Sigma(U+V)}{\partial\psi_2}$	Y2 +55×Z	X2+2×Y2 +2×Y3 -400×Z	Y3 +45×Z										-3×Y2 +165×Z	-3×Y3 +135×Z								
$\frac{\partial\Sigma(U+V)}{\partial\psi_3}$		Y3 +45×Z	X3+2×Y3 +2×Y4 -324×Z	Y4 +36×Z										-3×Y3 +135×Z	-3×Y4 +108×Z							
$\frac{\partial\Sigma(U+V)}{\partial\psi_4}$			Y4 +36×Z	X4+2×Y4 +2×Y5 -256×Z	Y5 +28×Z										-3×Y4 +108×Z	-3×Y5 +84×Z						
$\frac{\partial\Sigma(U+V)}{\partial\psi_5}$				Y5 +28×Z	X5+2×Y5 +2×Y6 -196×Z	Y6 +21×Z										-3×Y5 +84×Z	-3×Y6 +63×Z					
$\frac{\partial\Sigma(U+V)}{\partial\psi_6}$					Y6 +21×Z	X6+2×Y6 +2×Y7 -144×Z	Y7 +15×Z										-3×Y6 +63×Z	-3×Y7 +45×Z			
$\frac{\partial\Sigma(U+V)}{\partial\psi_7}$						Y7 +15×Z	X7+2×Y7 +2×Y8 -100×Z	Y8 +10×Z										-3×Y7 +45×Z	-3×Y8 +30×Z			
$\frac{\partial\Sigma(U+V)}{\partial\psi_8}$							Y8 +10×Z	X8+2×Y8 +2×Y9 -64×Z	Y9 +6×Z										-3×Y8 +30×Z	-3×Y9 +18×Z		
$\frac{\partial\Sigma(U+V)}{\partial\psi_9}$								Y9 +6×Z	X9+2×Y9 +2×Y10 -36×Z	Y10 +3×Z										-3×Y9 +18×Z	-3×Y10 +9×Z	
$\frac{\partial\Sigma(U+V)}{\partial\psi_{10}}$									Y10 +3×Z	X10+2×Y10 +2×Y11 -16×Z	Y11 +Z										-3×Y10 +9×Z	-3×Y11 +3×Z
$\frac{\partial\Sigma(U+V)}{\partial\psi_{11}}$										Y11 +Z	X11+2×Y11 -4×Z											-3×Y11 +3×Z
$\frac{\partial\Sigma(U+V)}{\partial\rho_1}$	-3×Y1 +198×Z											6×Y1 -2376×Z										
$\frac{\partial\Sigma(U+V)}{\partial\rho_2}$	-3×Y2 +165×Z	-3×Y2 +165×Z											6×Y2 -1980×Z									
$\frac{\partial\Sigma(U+V)}{\partial\rho_3}$		-3×Y3 +135×Z	-3×Y3 +135×Z											6×Y3 -1620×Z								
$\frac{\partial\Sigma(U+V)}{\partial\rho_4}$			-3×Y4 +108×Z	-3×Y4 +108×Z											6×Y4 -1296×Z							
$\frac{\partial\Sigma(U+V)}{\partial\rho_5}$				-3×Y5 +84×Z	-3×Y5 +84×Z											6×Y5 -1008×Z						
$\frac{\partial\Sigma(U+V)}{\partial\rho_6}$					-3×Y6 +63×Z	-3×Y6 +63×Z											6×Y6 -756×Z					
$\frac{\partial\Sigma(U+V)}{\partial\rho_7}$						-3×Y7 +45×Z	-3×Y7 +45×Z											6×Y7 -540×Z				
$\frac{\partial\Sigma(U+V)}{\partial\rho_8}$							-3×Y8 +30×Z	-3×Y8 +30×Z											6×Y8 -360×Z			
$\frac{\partial\Sigma(U+V)}{\partial\rho_9}$								-3×Y9 +18×Z	-3×Y9 +18×Z											6×Y9 -216×Z		
$\frac{\partial\Sigma(U+V)}{\partial\rho_{10}}$									-3×Y10 +9×Z	-3×Y10 +9×Z											6×Y10 -108×Z	
$\frac{\partial\Sigma(U+V)}{\partial\rho_{11}}$										-3×Y11 +3×Z	-3×Y11 +3×Z											6×Y11 -36×Z

Table 8.4

Table 8.4 COMPARISON AMONG ANALYTICAL METHODS

	Methods of Analysis	Ultimate Load on a Column ($\bar{P}$)	Ultimate Load on the Frame U-2 (kips)
(1)	Simple Plastic Analysis	0.43	76
(2)	Effective Length Factor (CRC)	0.64	113
(3)	Merchant's Formula	0.28	49
(4)	Concentric Modified Slope Deflection	0.78	138
(5)	Concentric Elastic Energy	0.89	157
(6)	Concentric Inelastic Energy	0.62	110
(7)	Inelastic Energy with Plastic Hinges	0.42	74
(8)	Test Result	0.40	71

Table 8.5

Table 8.5 COMPARISON BETWEEN INELASTIC ENERGY METHOD AND CRC METHOD FOR BUCKLING LOADS OF THREE-STORY FRAMES

Method	$\frac{h}{r_x}$	15	20	25	30	40	60	80	120	
C. R. C.	$\frac{P}{P_y}$	0.905	0.857	0.810	0.745	0.627	0.354	0.230	—	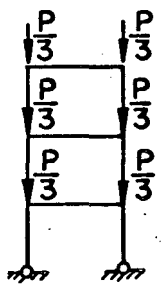
Inelastic Energy	$\frac{P}{P_y}$	1.060	0.987	0.899	0.803	0.616	0.351	0.215	0.103	
% Error	$\frac{P}{P_y}$	14.62	13.19	9.89	7.22	-1.78	-0.85	-6.96	—	

(A) Symmetrical vertical loads

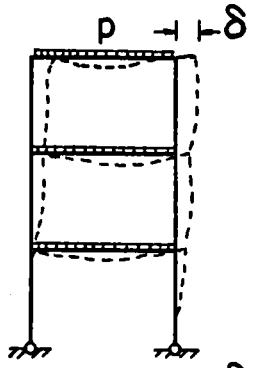

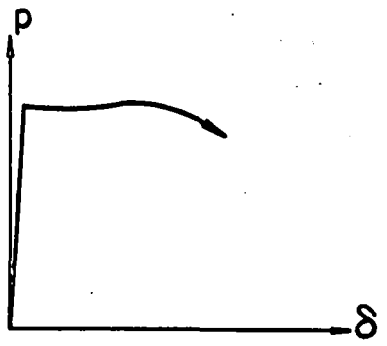

(B) Unsymmetrical vertical loads

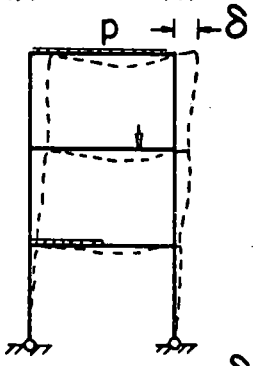

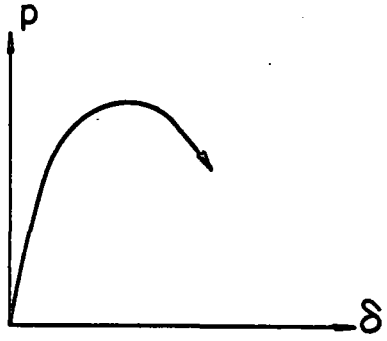

(C) Proportional application of vertical and horizontal loads

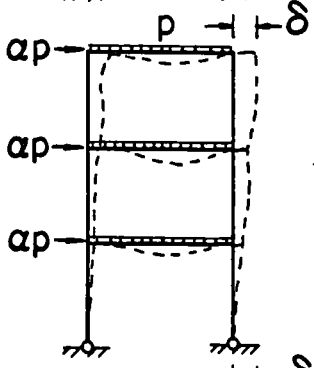

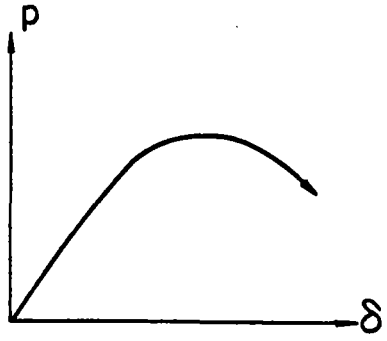

(D) Constant vertical loads with varying horizontal loads

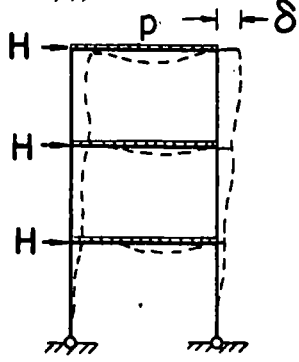

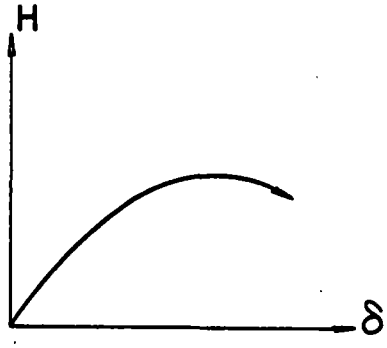

(E) Braced frame under vertical loads

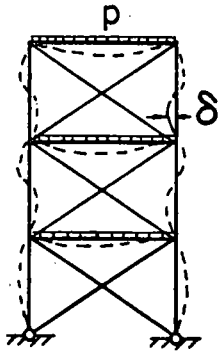

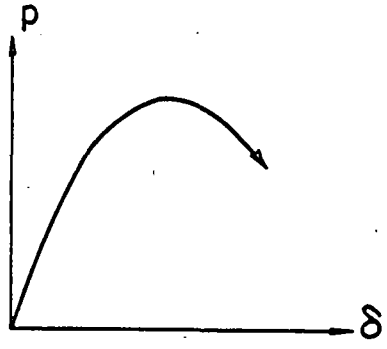

Fig. 1.1 TYPES OF FRAME INSTABILITY

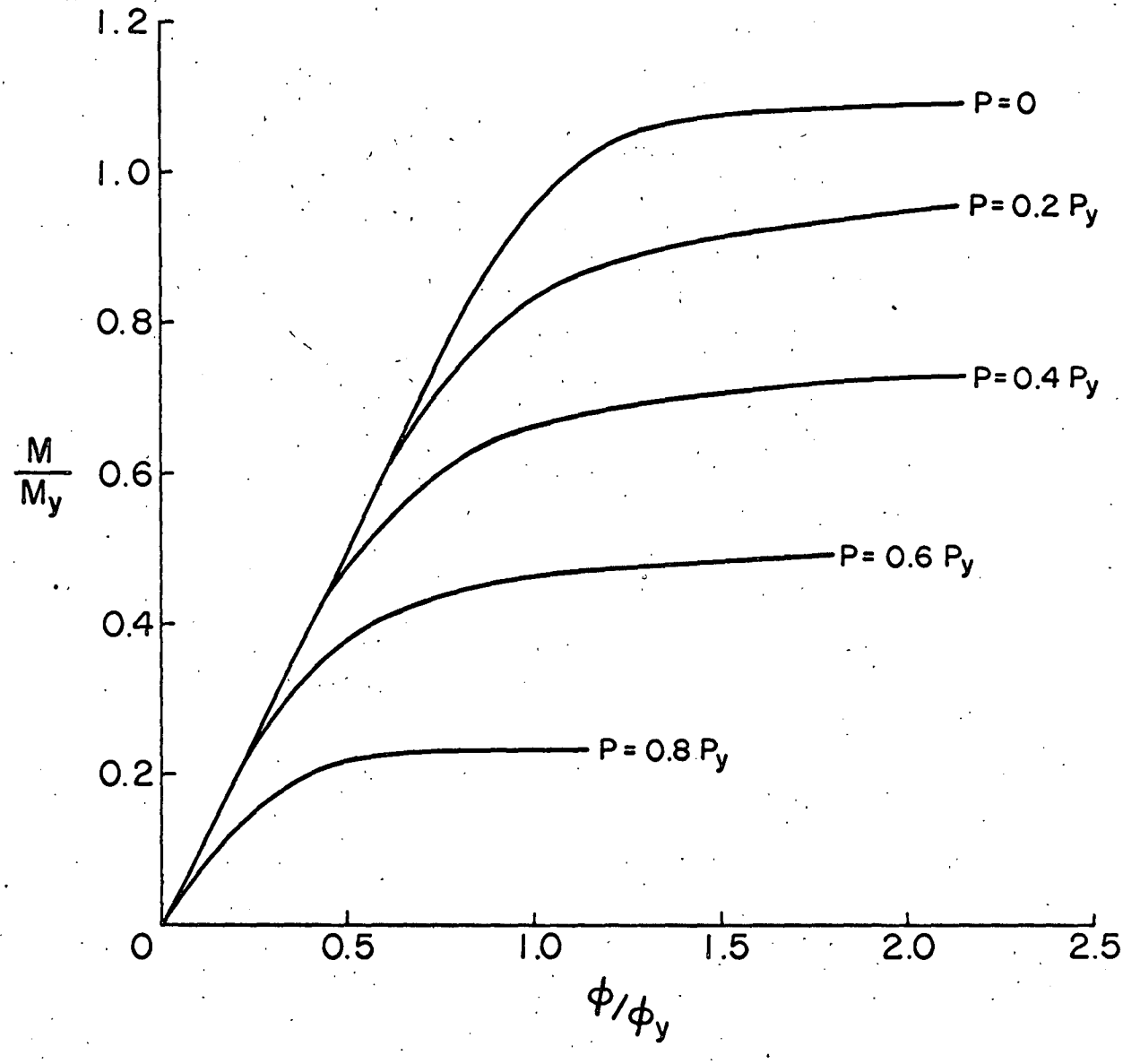

Fig. 2.1 MOMENT-CURVATURE-THRUST RELATIONSHIPS

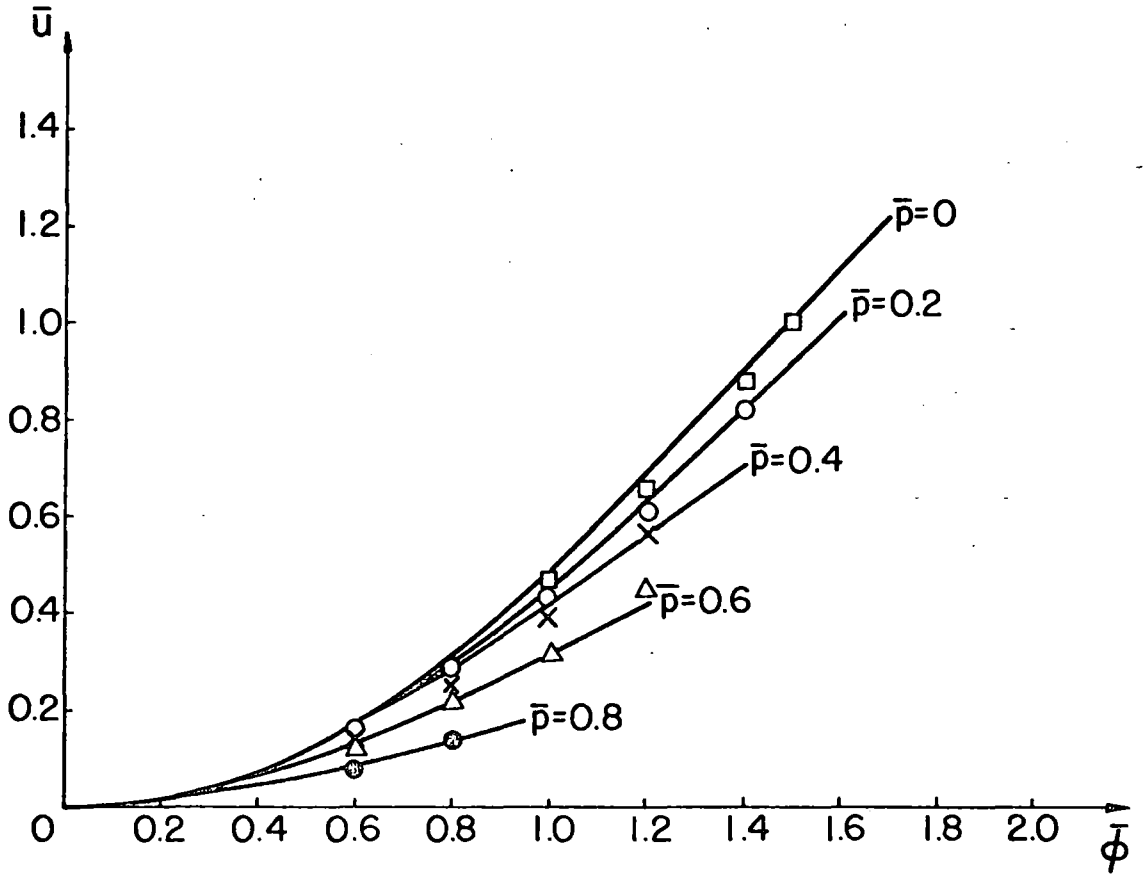

Fig. 3.1 BENDING STRAIN ENERGY VS. CURVATURE RELATIONSHIPS

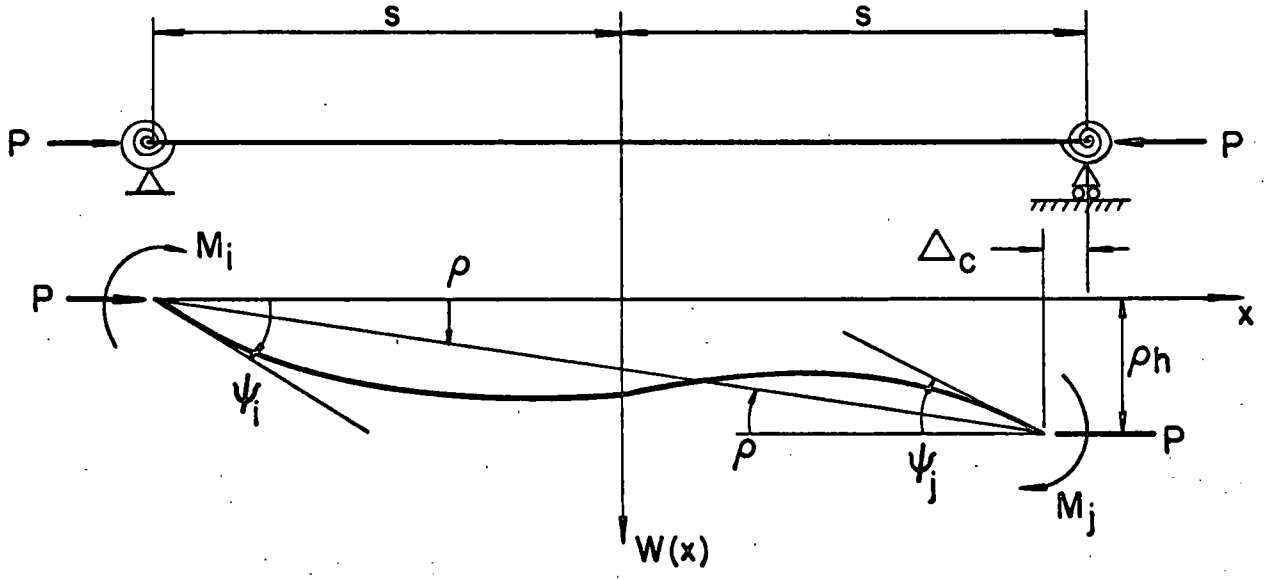

Fig. 4.1 DEFLECTED SHAPE OF A COLUMN

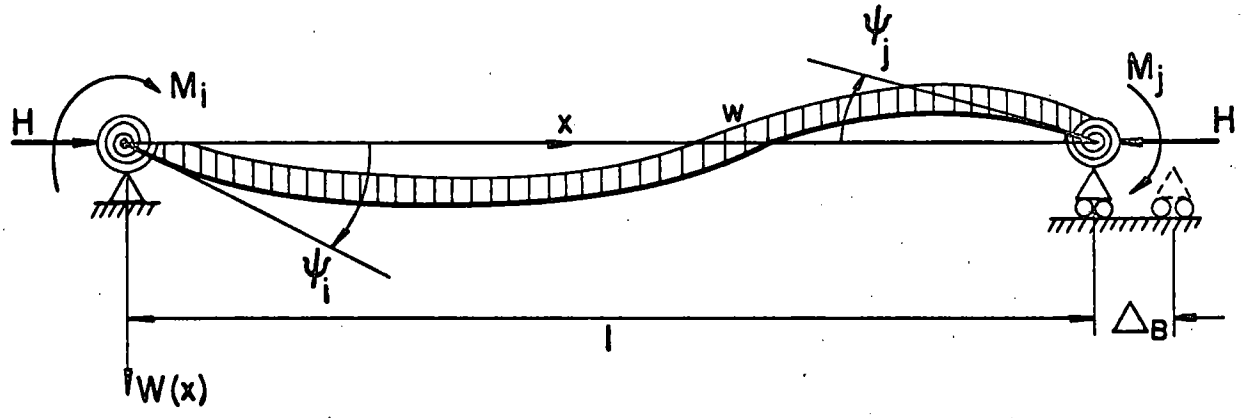

Fig. 4.2 DEFLECTED SHAPE OF A BEAM

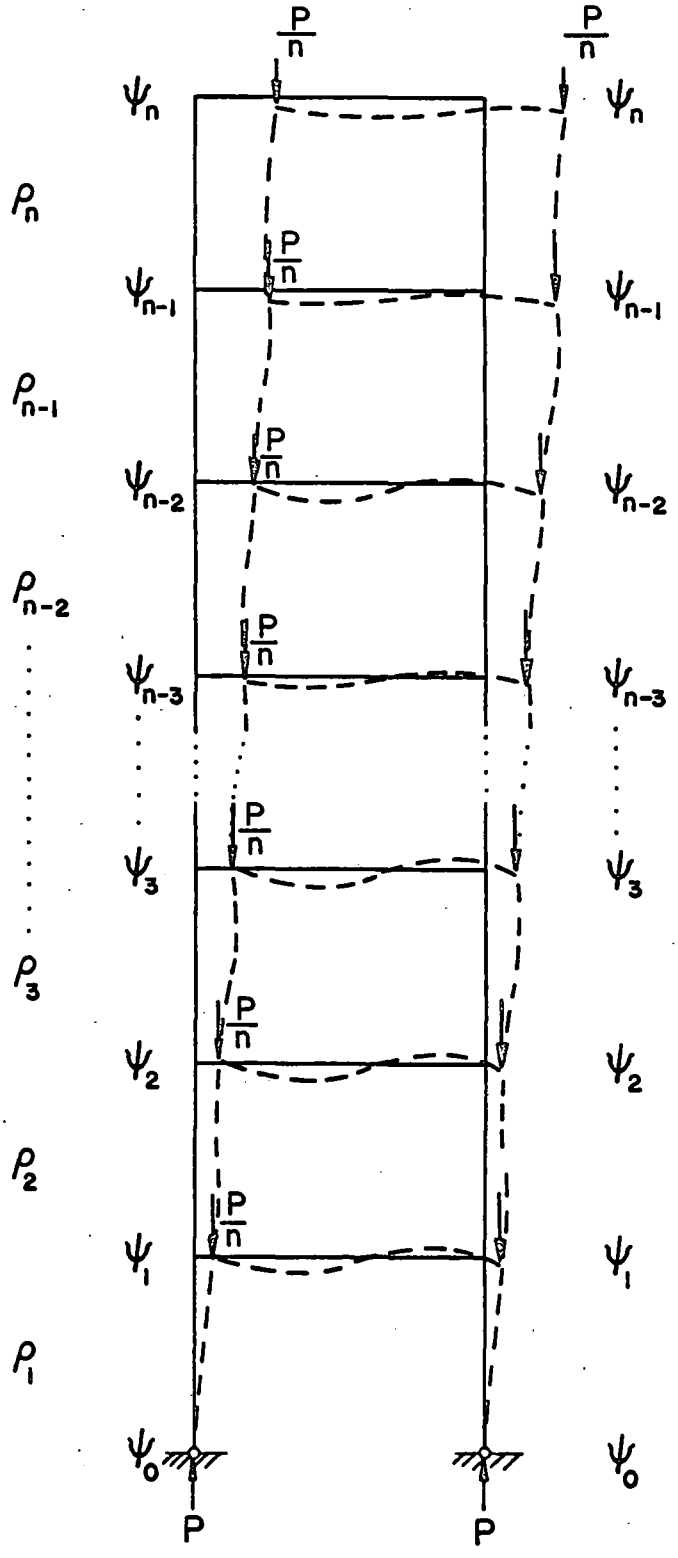

Fig. 5.1 ANTISYMMETRICAL BUCKLING MODE OF A FRAME

Fig. 5.2

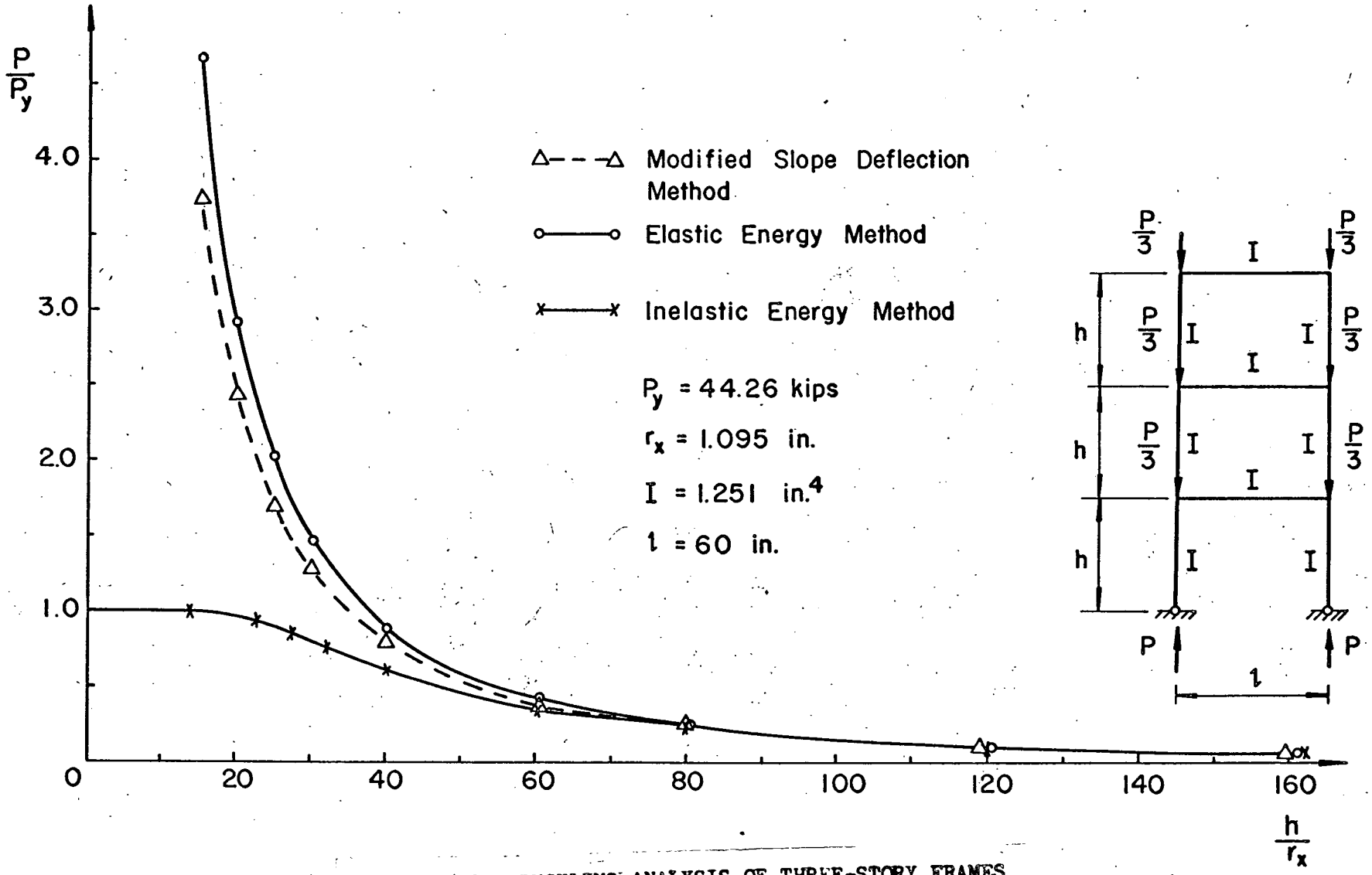

Fig. 5.2 BUCKLING ANALYSIS OF THREE-STORY FRAMES

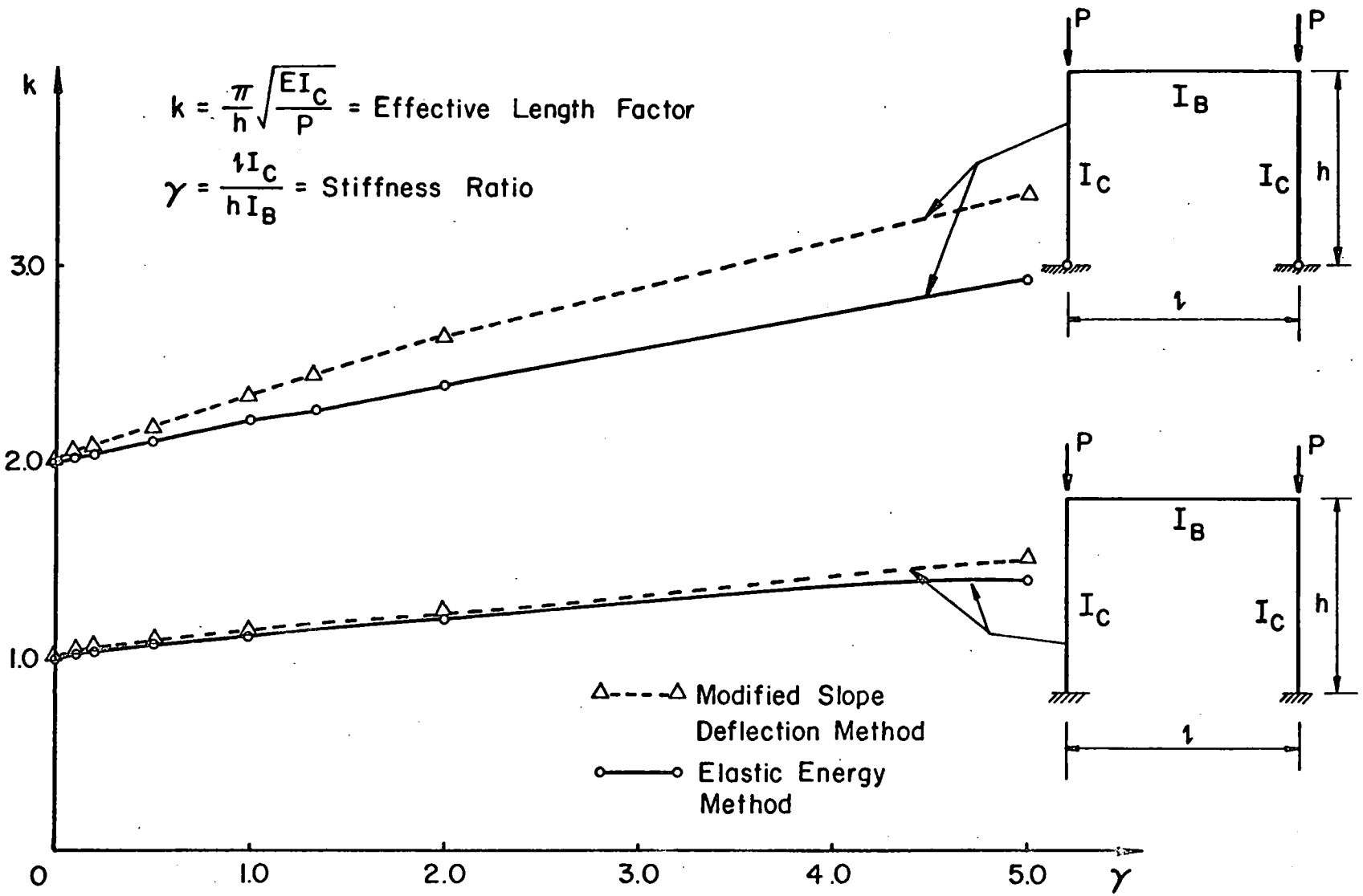

Fig. 6.1 BUCKLING ANALYSIS OF SINGLE-STORY FRAMES

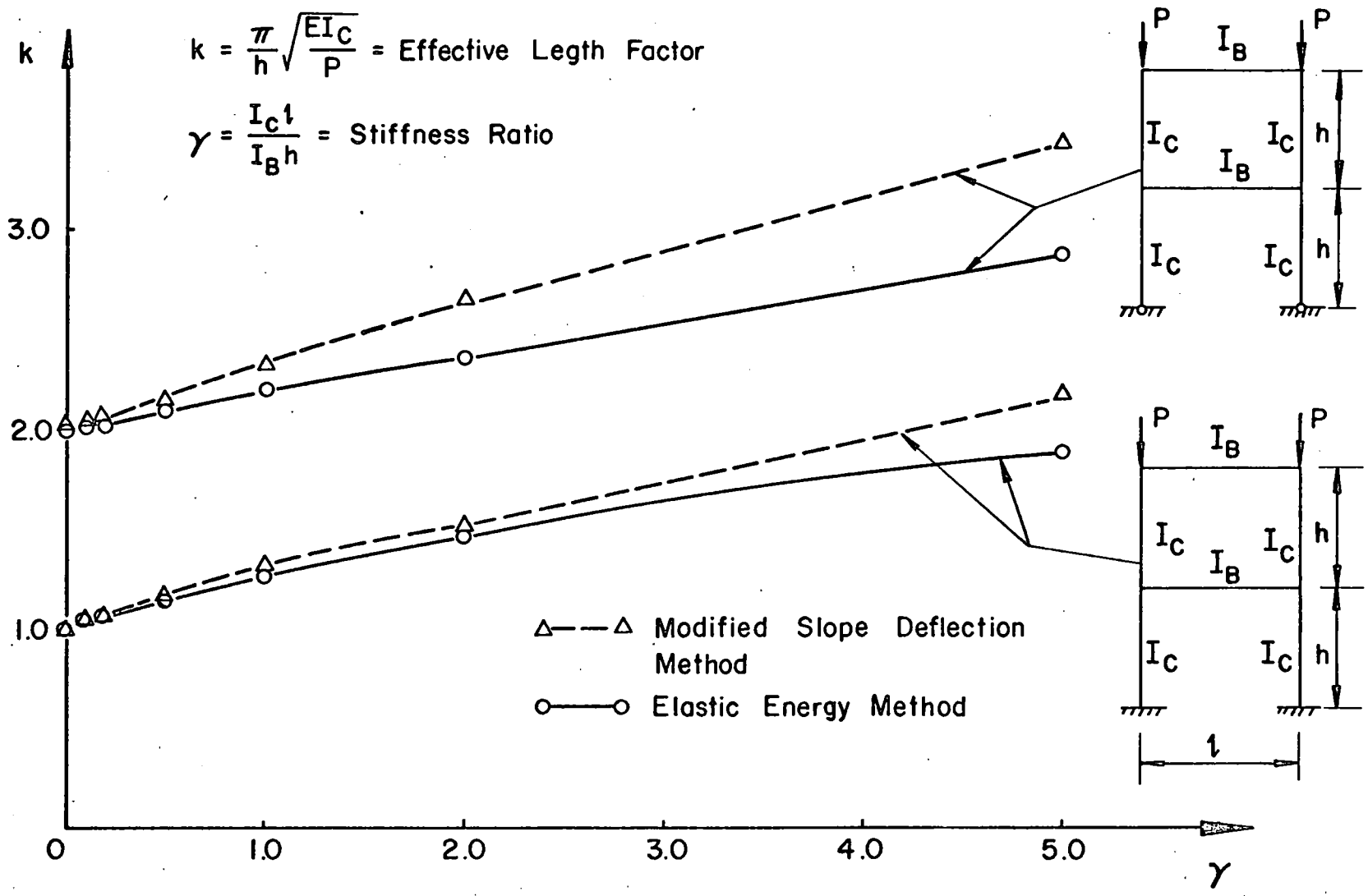

Fig. 6.2 BUCKLING ANALYSIS OF TWO-STORY FRAMES

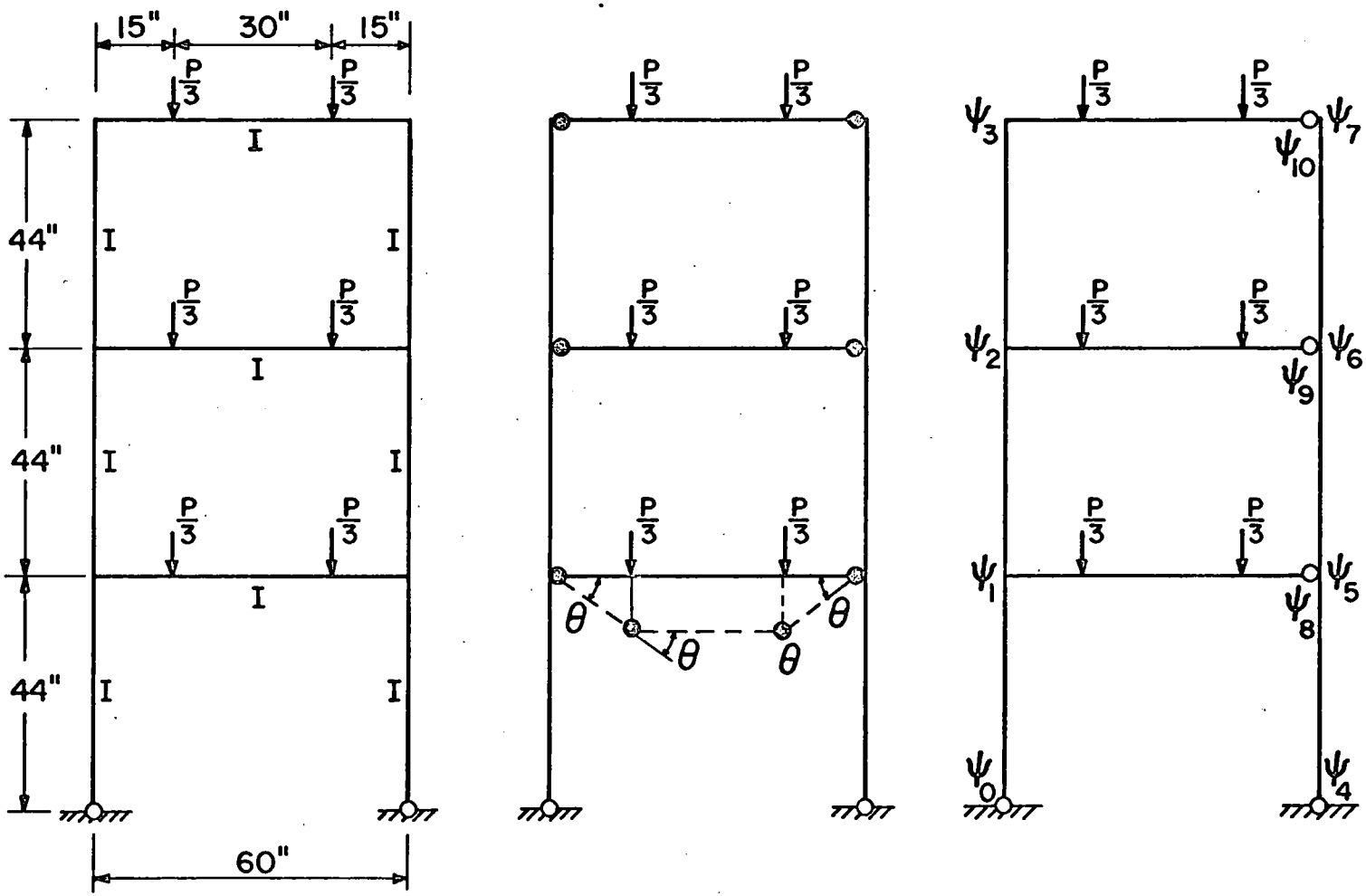

Fig. 7.1 INSTABILITY ANALYSIS OF FRAME WITH PLASTIC HINGES

Fig. 7.2

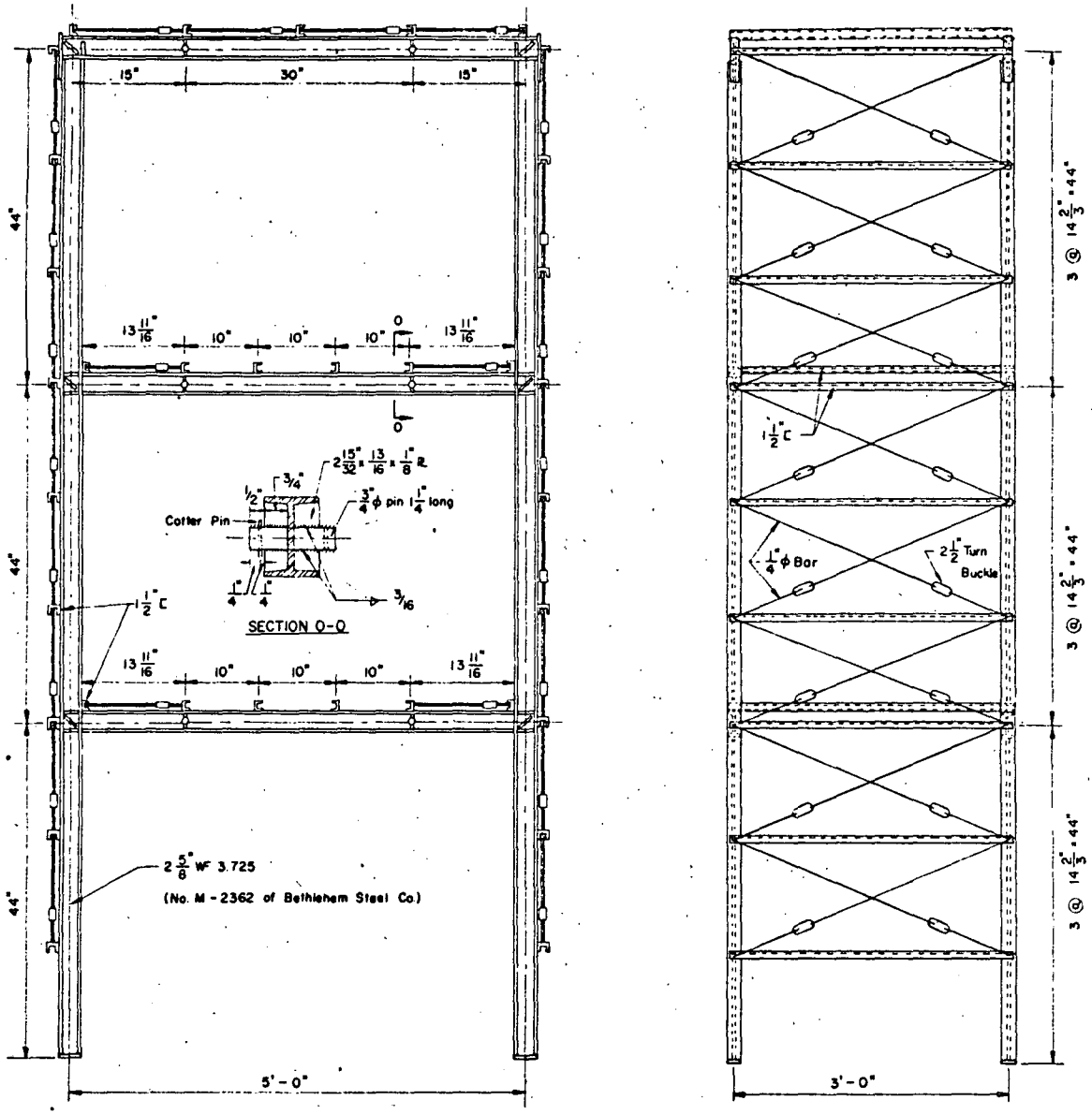

Fig. 7.2 MODEL FRAME - ELEVATION AND SIDE VIEW

Fig. 7.3

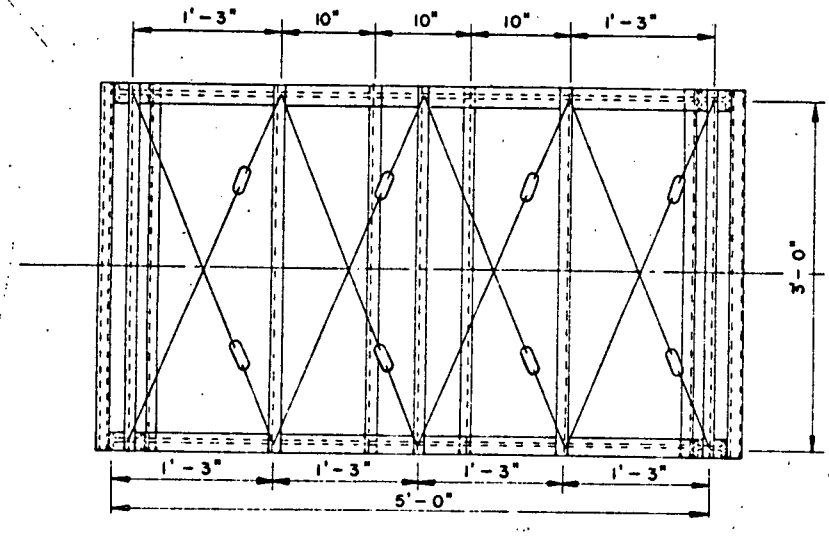

PLAN

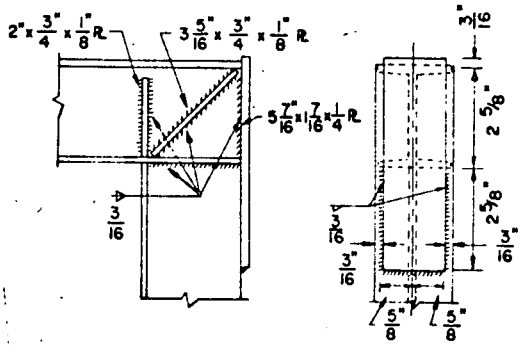

CORNER CONNECTION

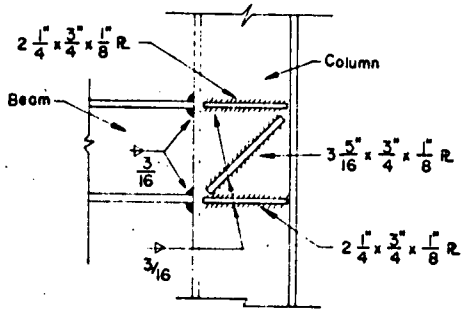

BEAM – COLUMN CONNECTION

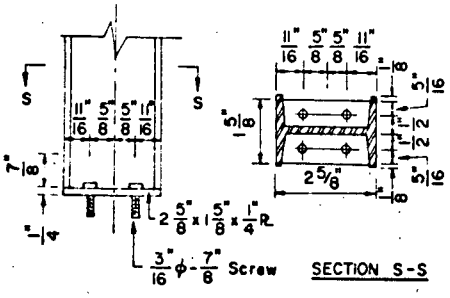

COLUMN BASE CONNECTION

Fig. 7.3 MODEL FRAME - PLAN AND CONNECTIONS

Fig. 7.4

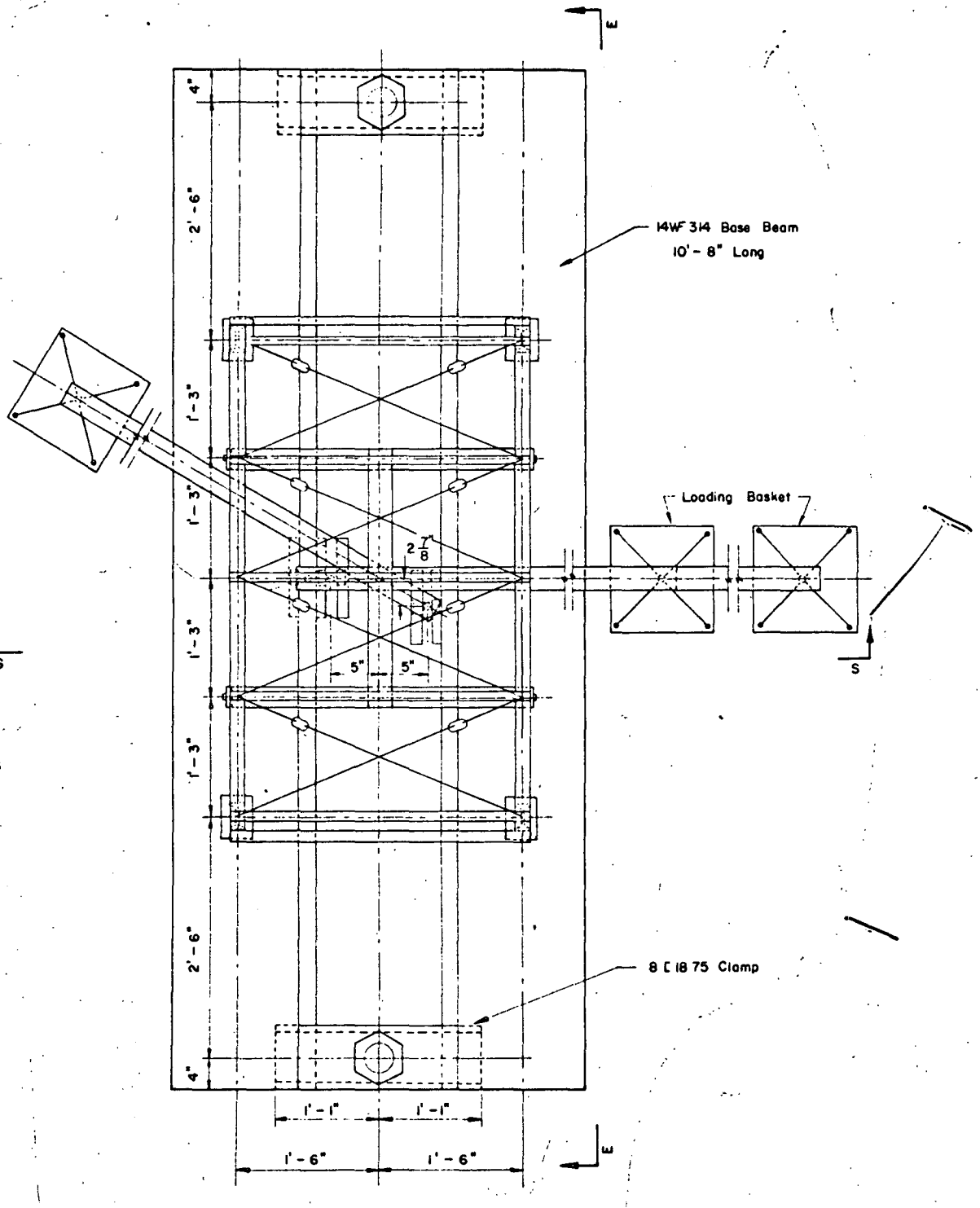

Fig. 7.4 MODEL FRAME TEST SETUP - PLAN

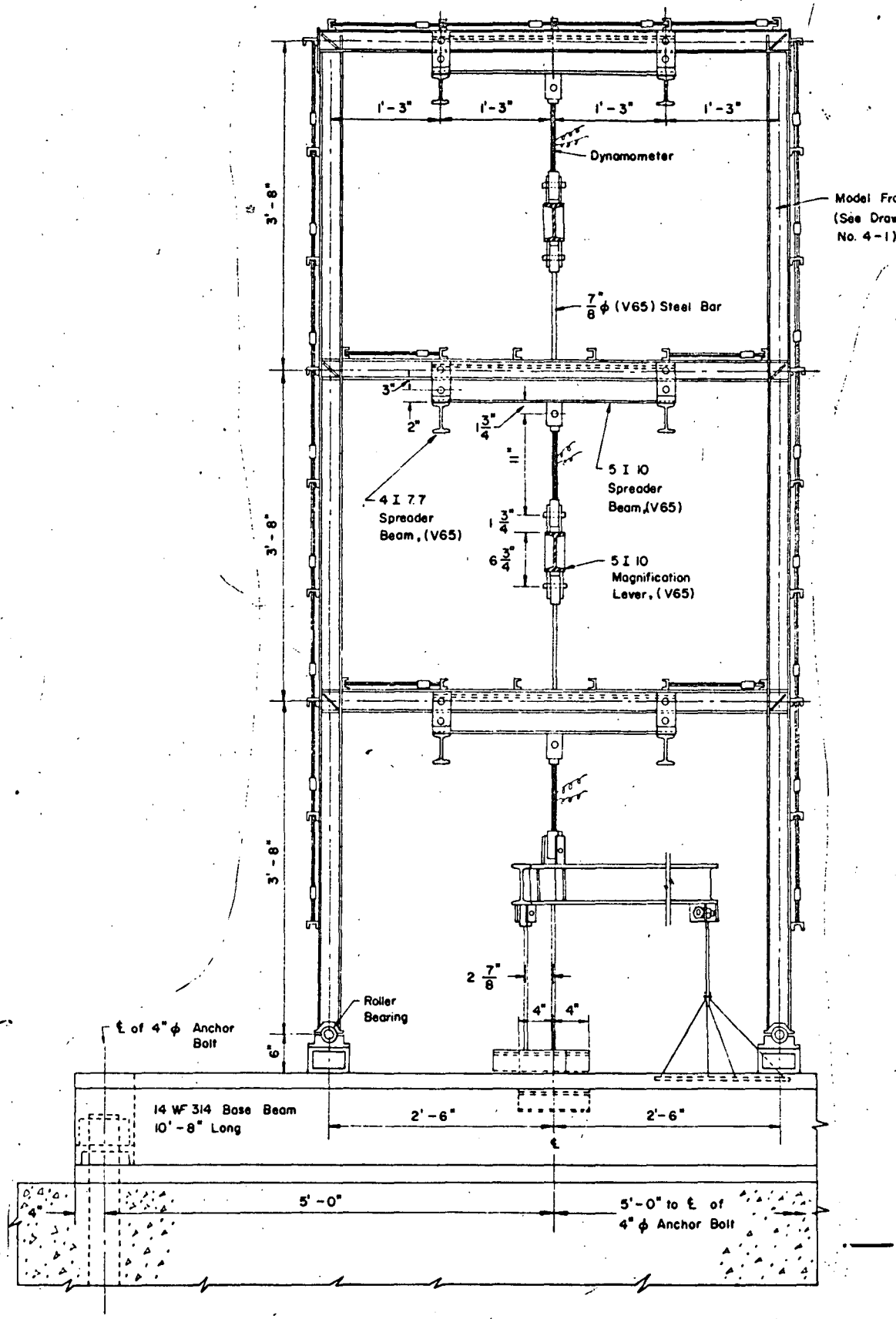

Fig. 7.5 MODEL FRAME TEST SETUP - SECTION E-E

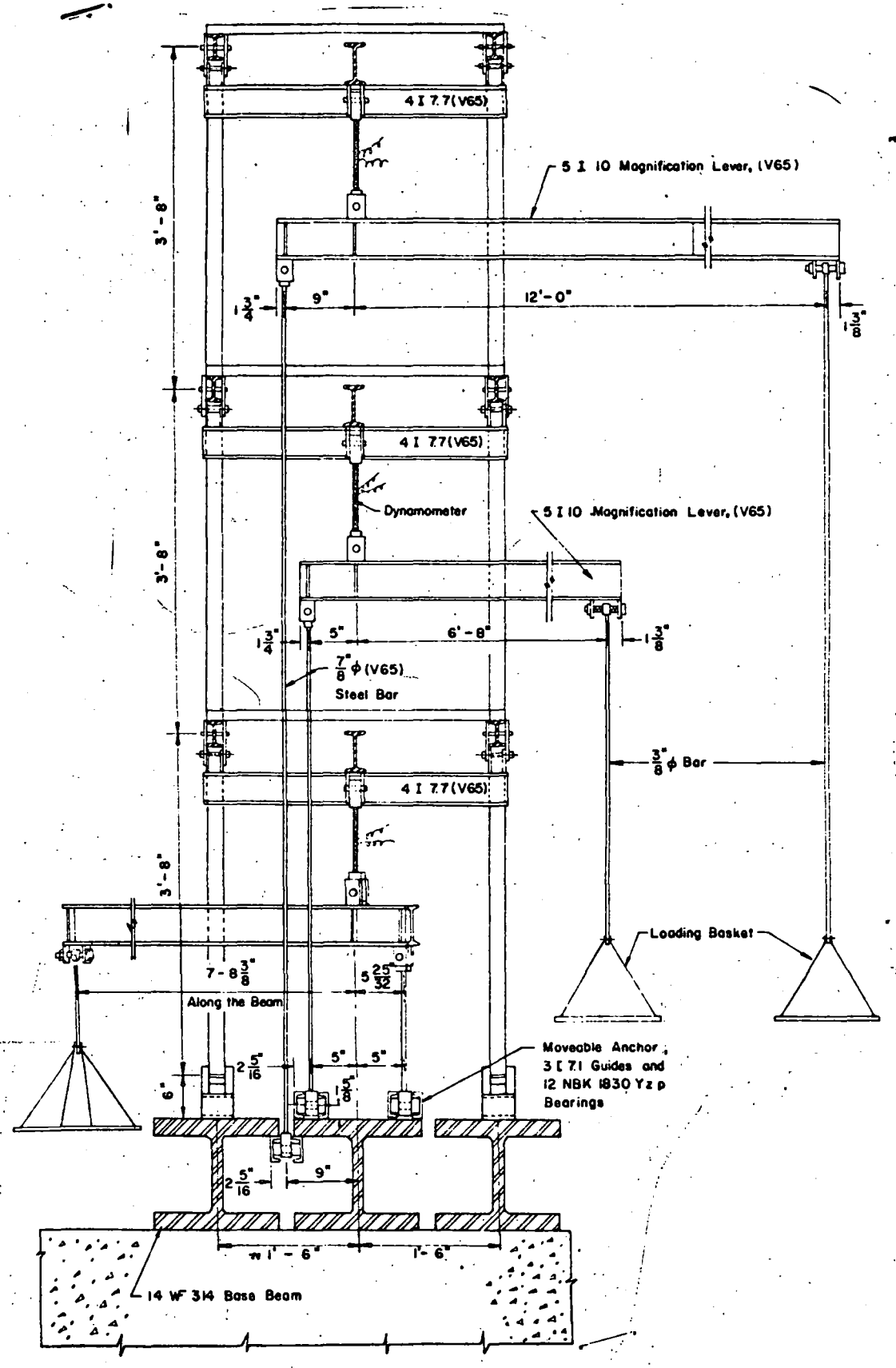

Fig. 7.6 MODEL FRAME TEST SETUP - SECTION S-S

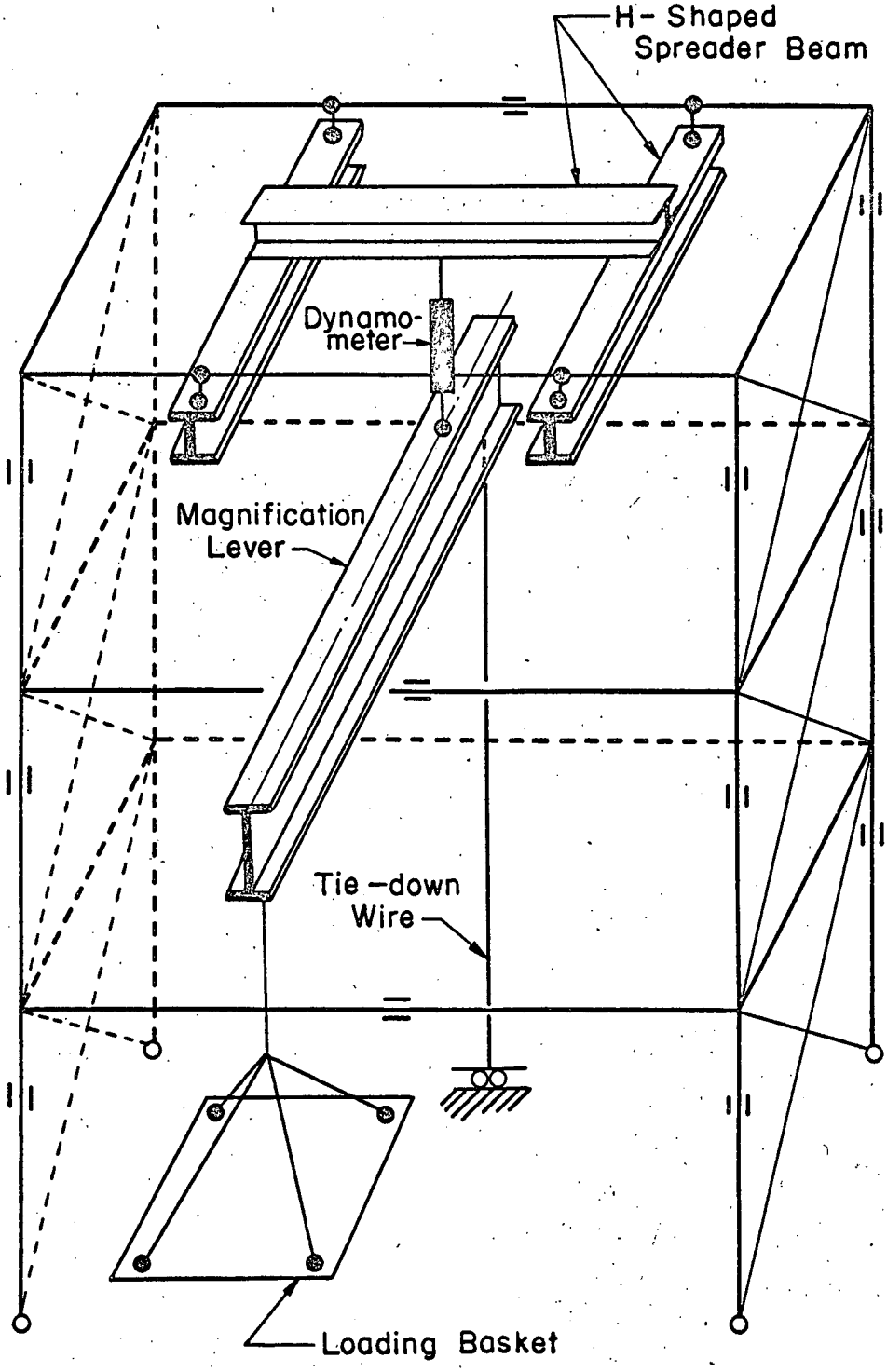

Fig. 7.7 MODEL FRAME LOADING SYSTEM

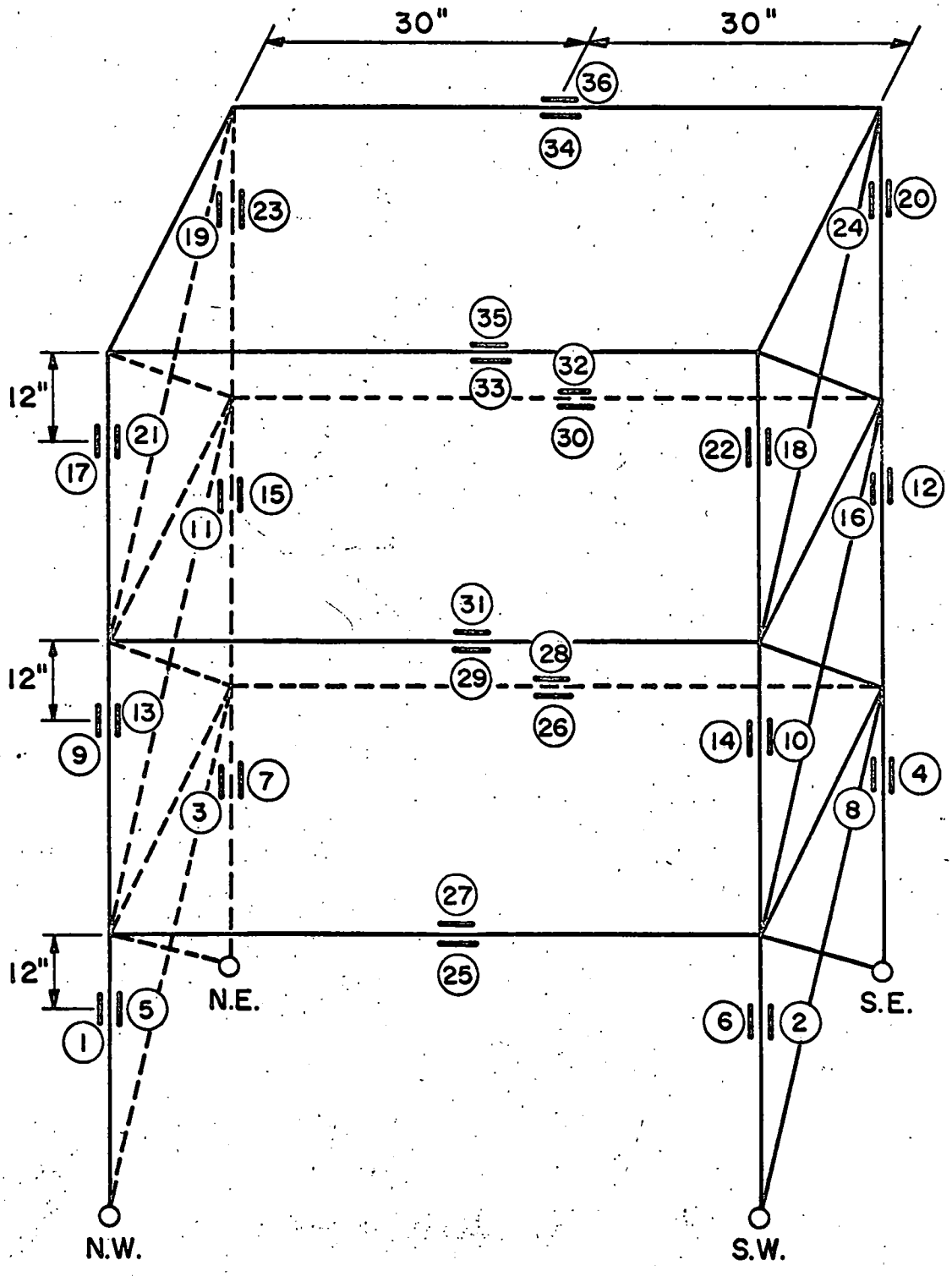

Fig. 7.8 STRAIN GAGES ON MODEL FRAME

Fig. 7.9

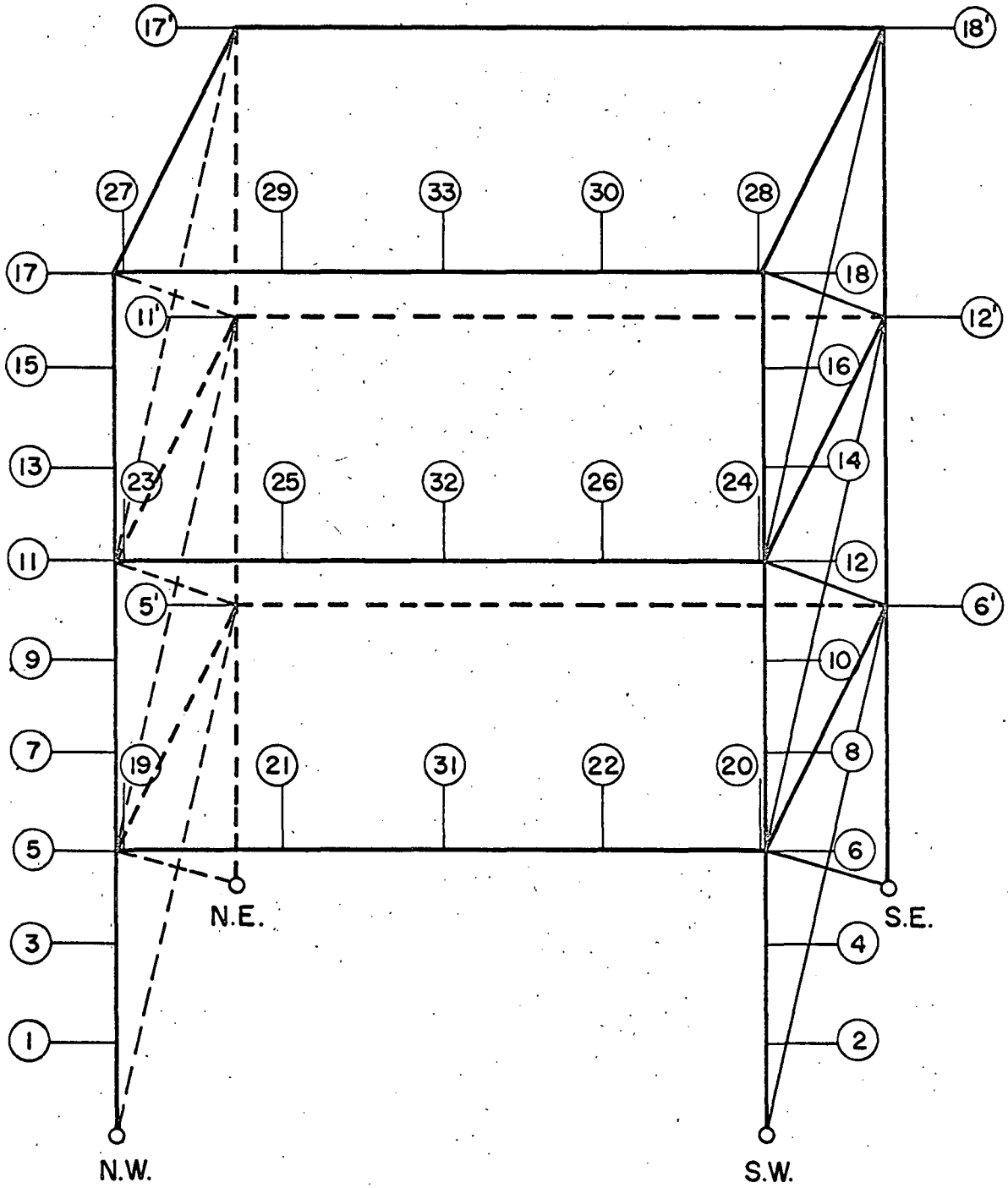

Fig. 7.9 HORIZONTAL AND VERTICAL DEFLECTION MEASUREMENT ON MODEL FRAME

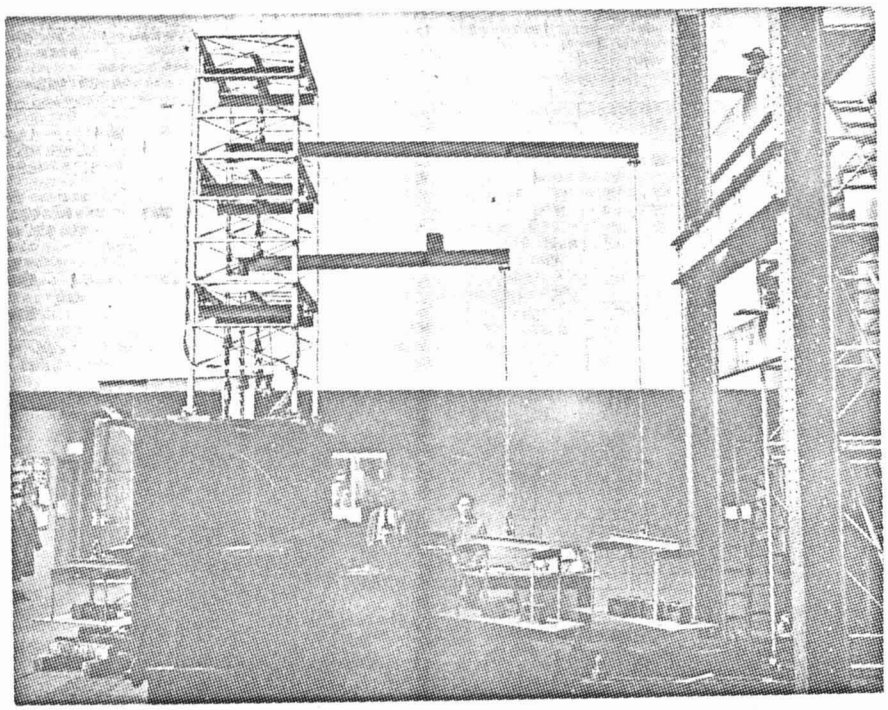

Fig. 7.10 SCAFFOLD AND TRANSITS ON THE RIGHT SIDE FOR DEFLECTION MEASUREMENT OF TEST FRAME DEFLECTION

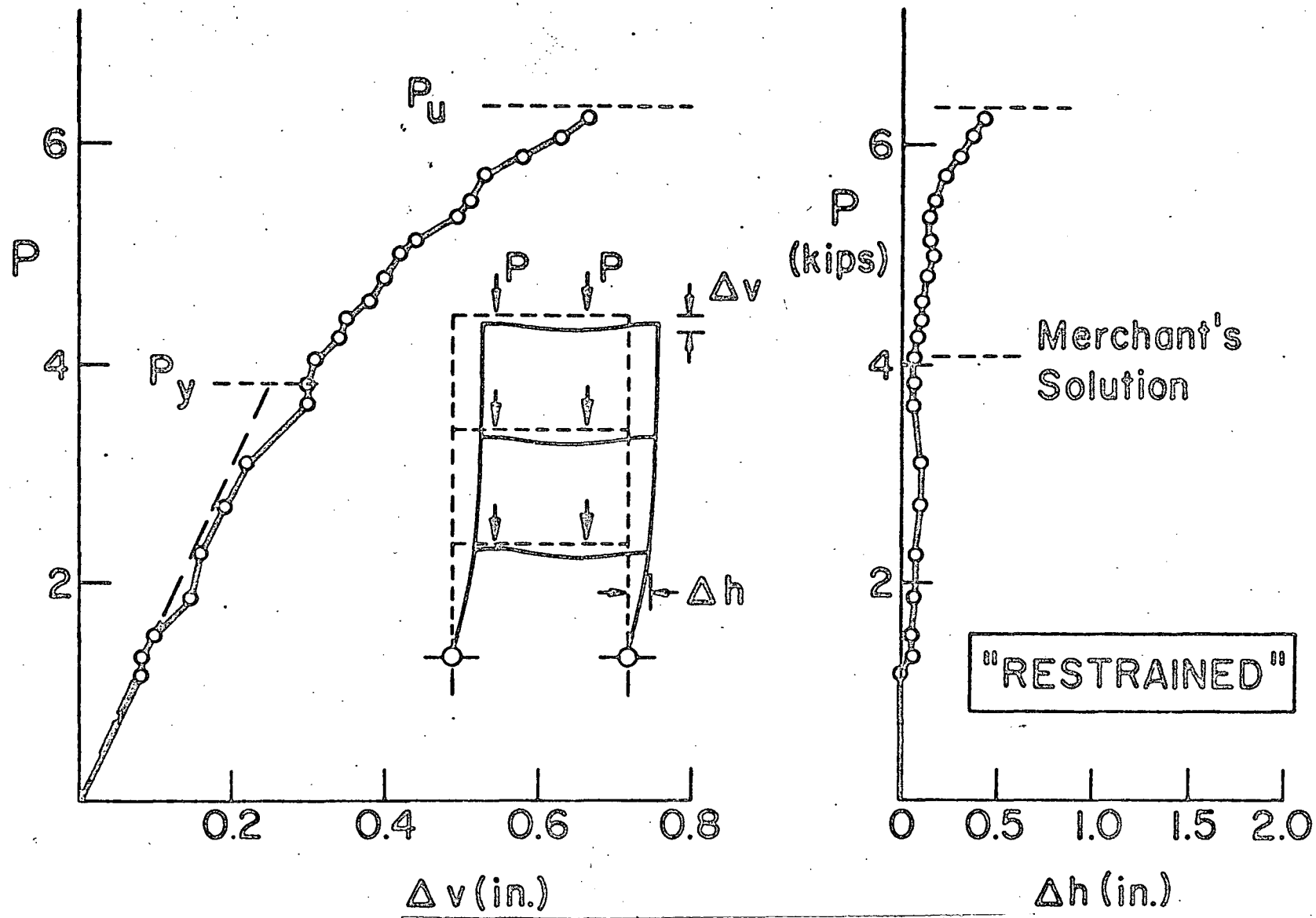

Fig. 7.11 LOAD-DEFLECTION CURVES FOR TEST U-2

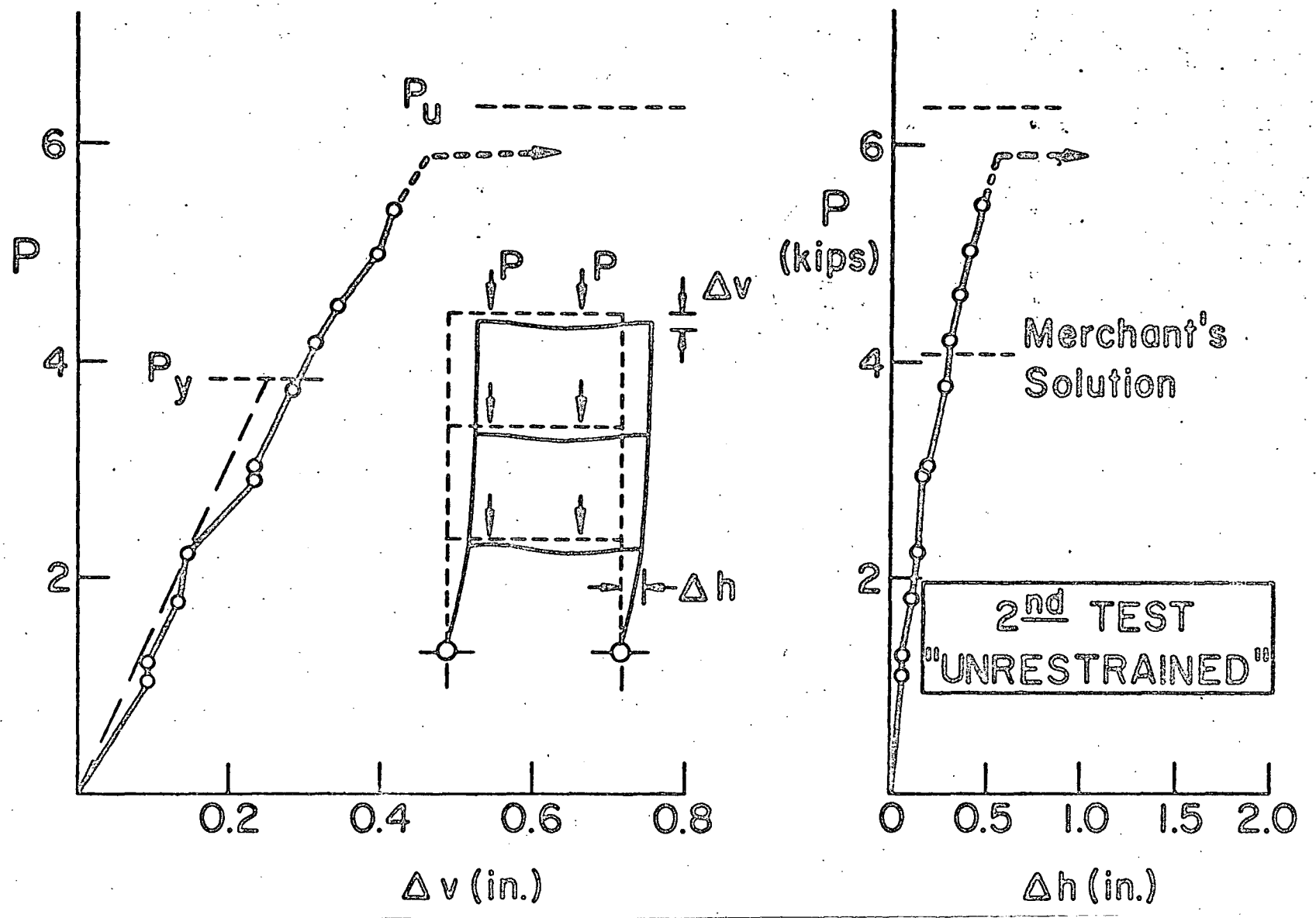

Fig. 7.12 REVISED LOAD-DEFLECTION CURVES FOR TEST U-2

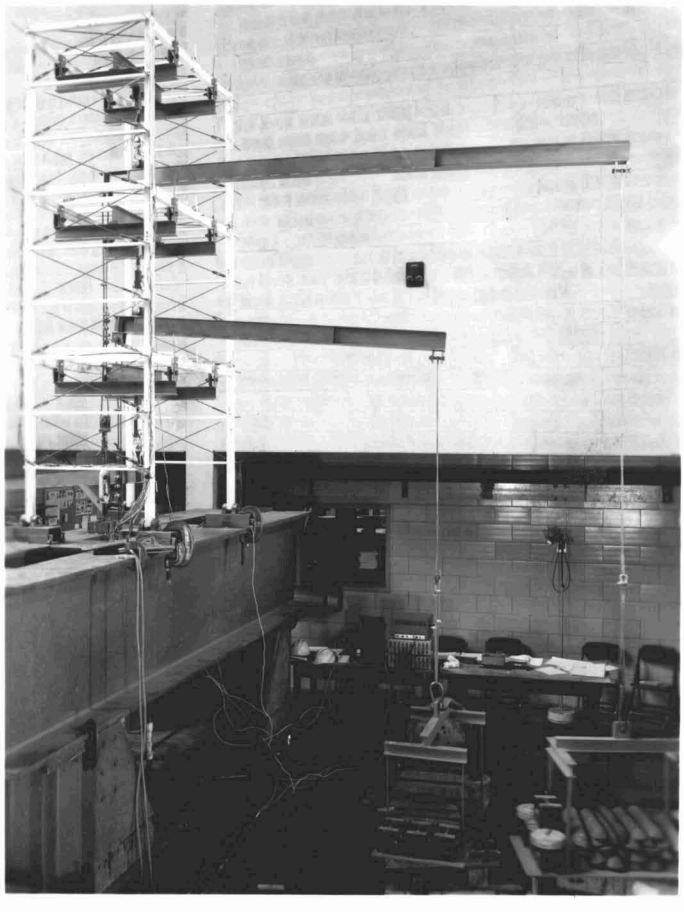

Fig. 7.13 SECOND TEST OF FRAME U-2 IN PROGRESS

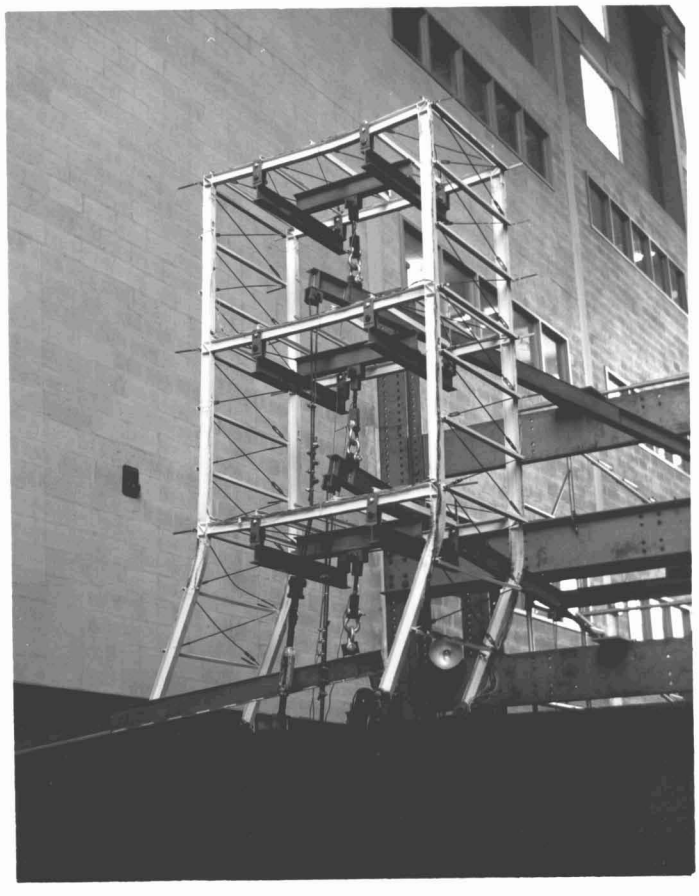

Fig. 7.14 SECOND TEST IMMEDIATELY AFTER BIFURCATION OF FRAME U-2

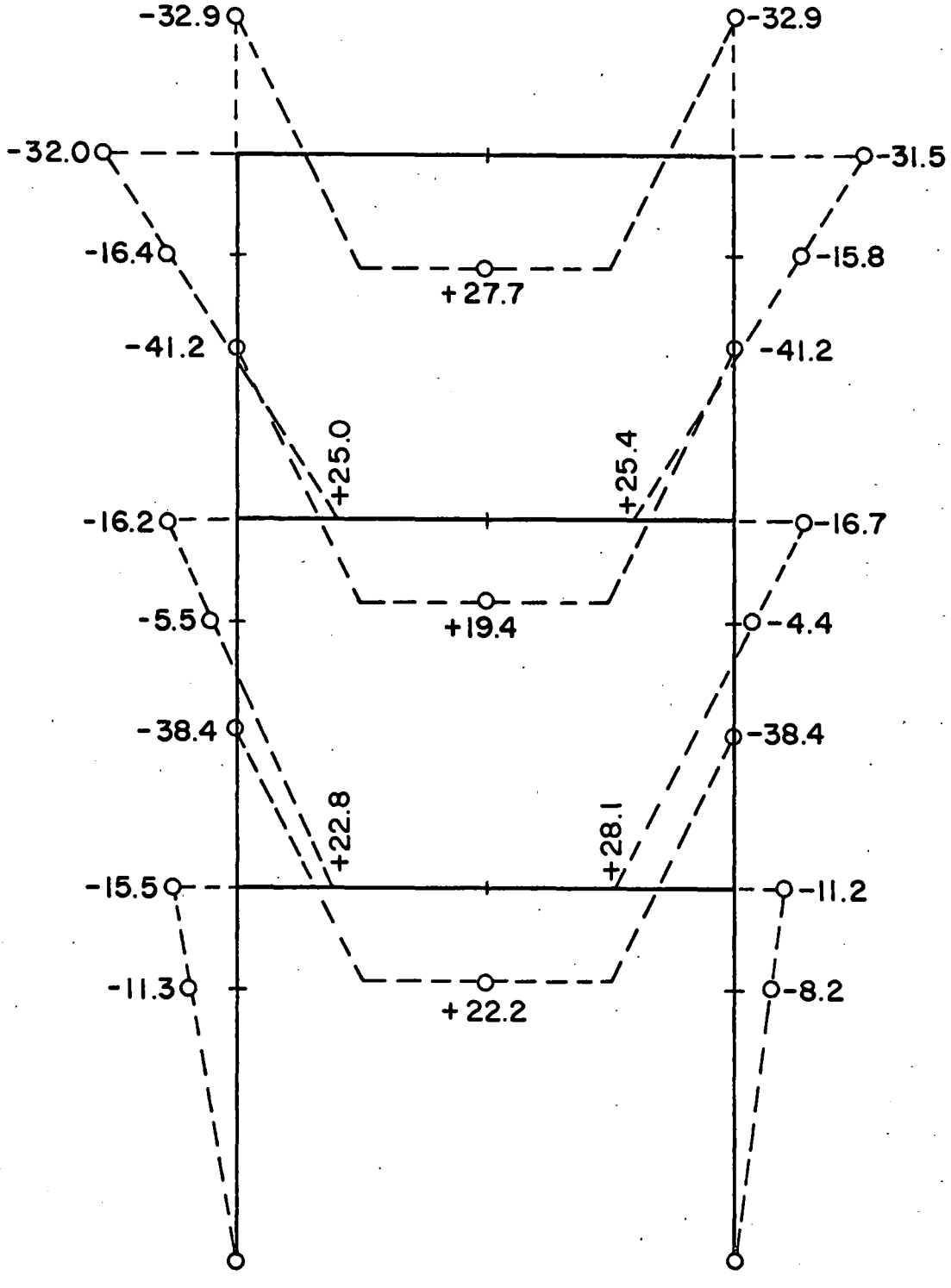

Fig. 7.15 MOMENT DIAGRAM OF WEST FRAME U-2 AT LOAD 53.16 KIPS

Fig. 7.16

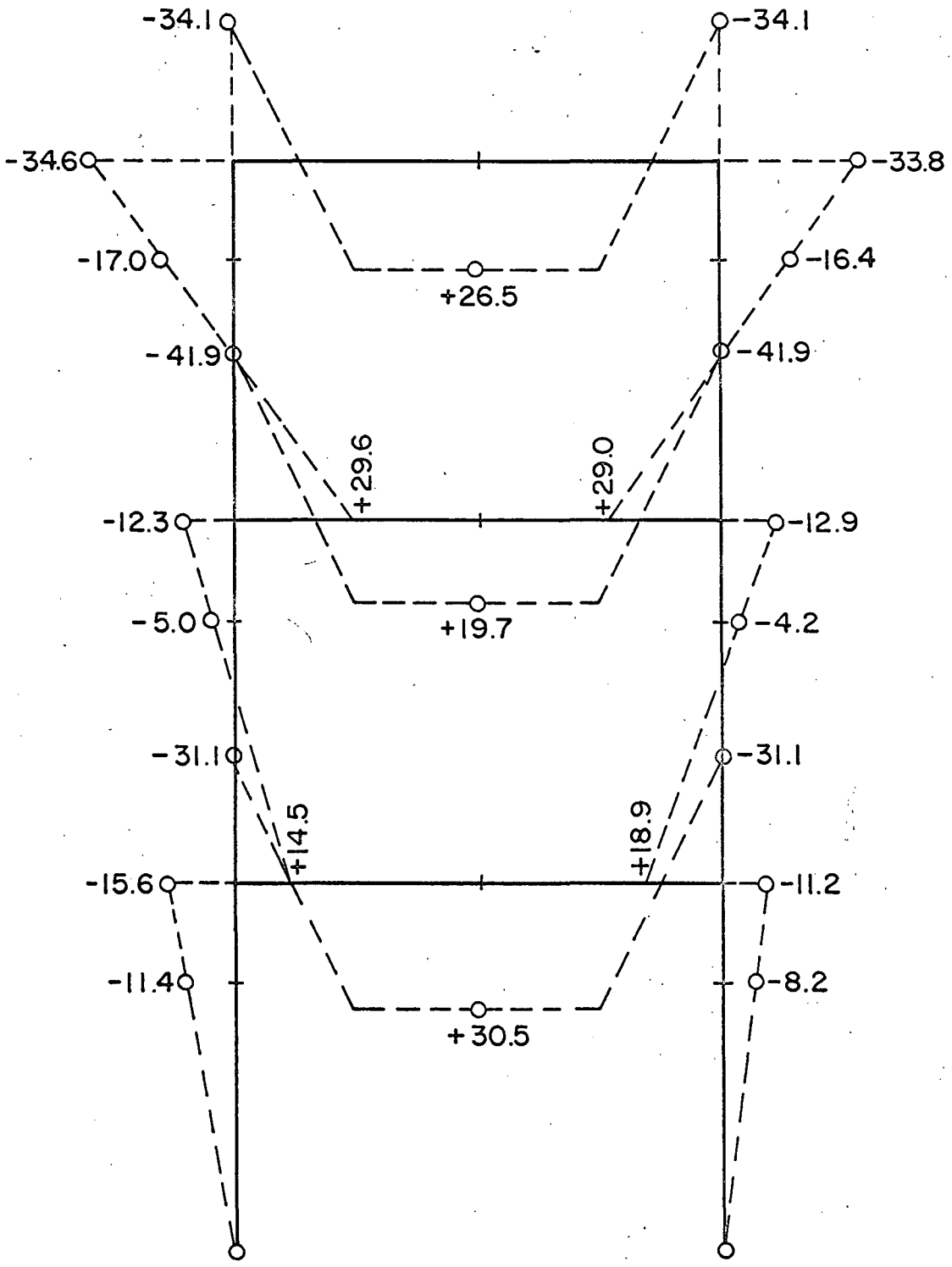

Fig. 7.16 MOMENT DIAGRAM OF EAST FRAME U-2 AT LOAD 53.16 KIPS

Fig. 7.17

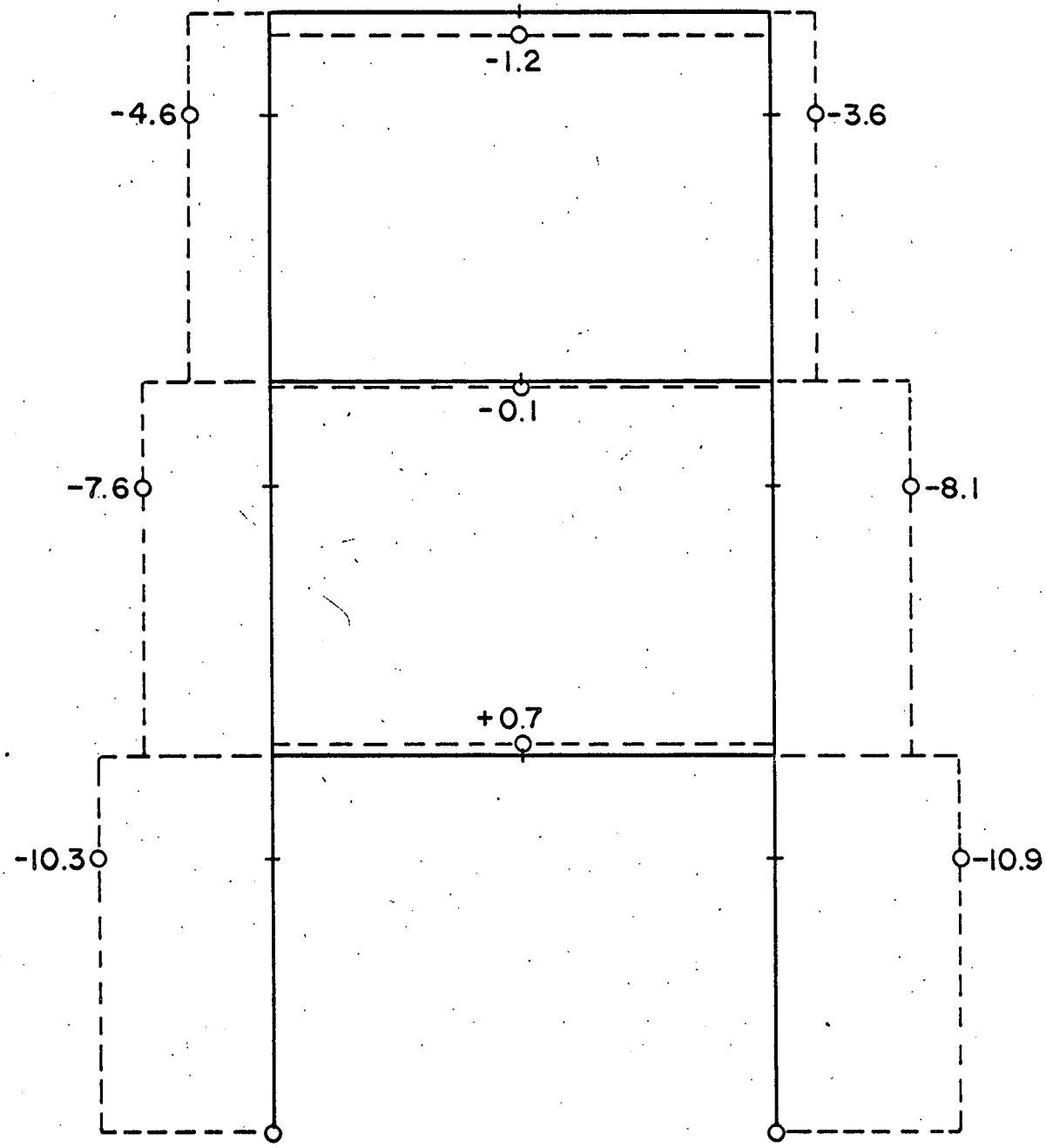

Fig. 7.17 THRUST DIAGRAM OF WEST FRAME U-2 AT LOAD 53.16 KIPS

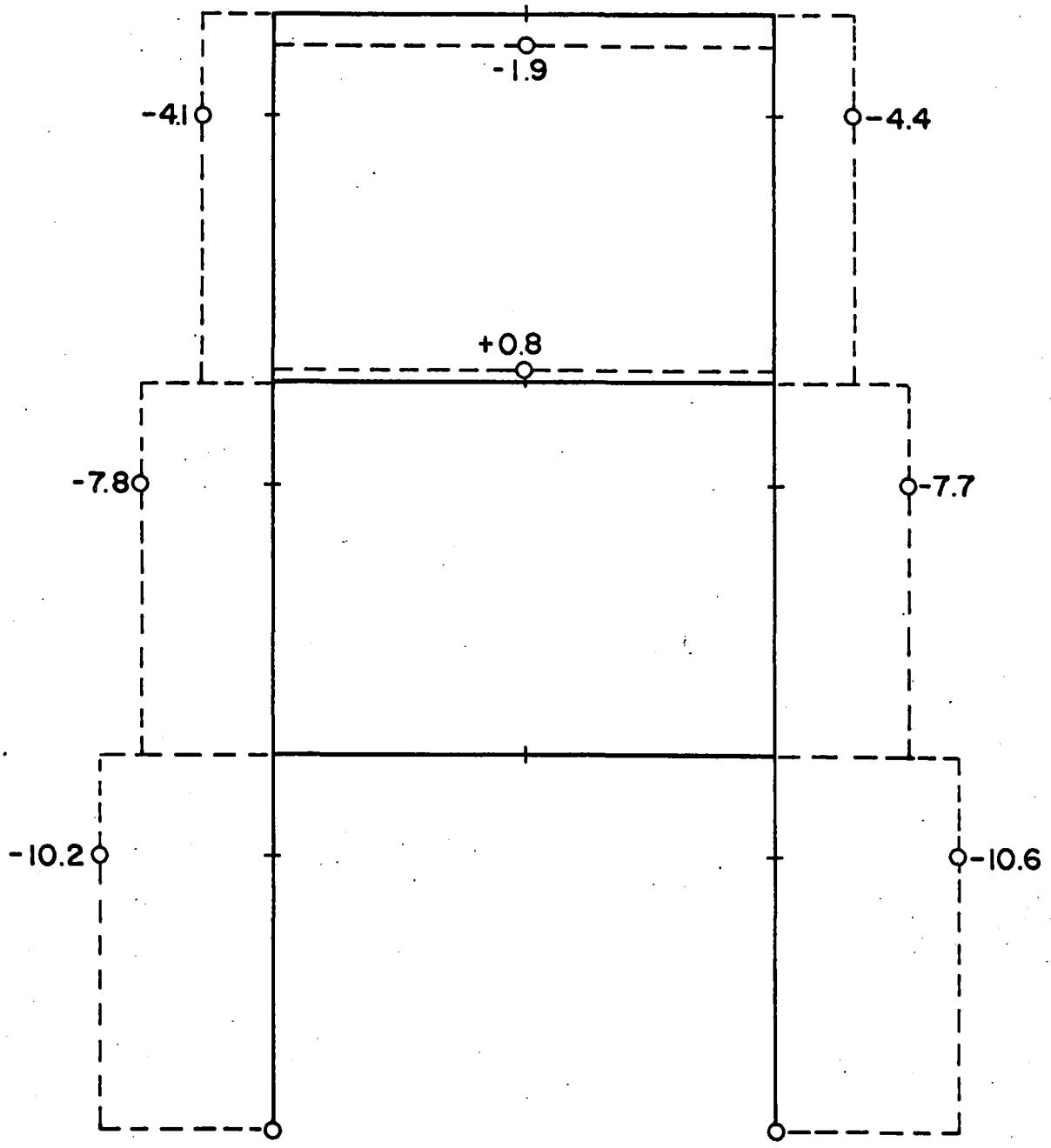

EAST FRAME
Load 53.16 kips (Rdngs. in kips)

Fig. 7.18 THRUST DIAGRAM OF EAST FRAME U-2 AT LOAD 53.16 KIPS

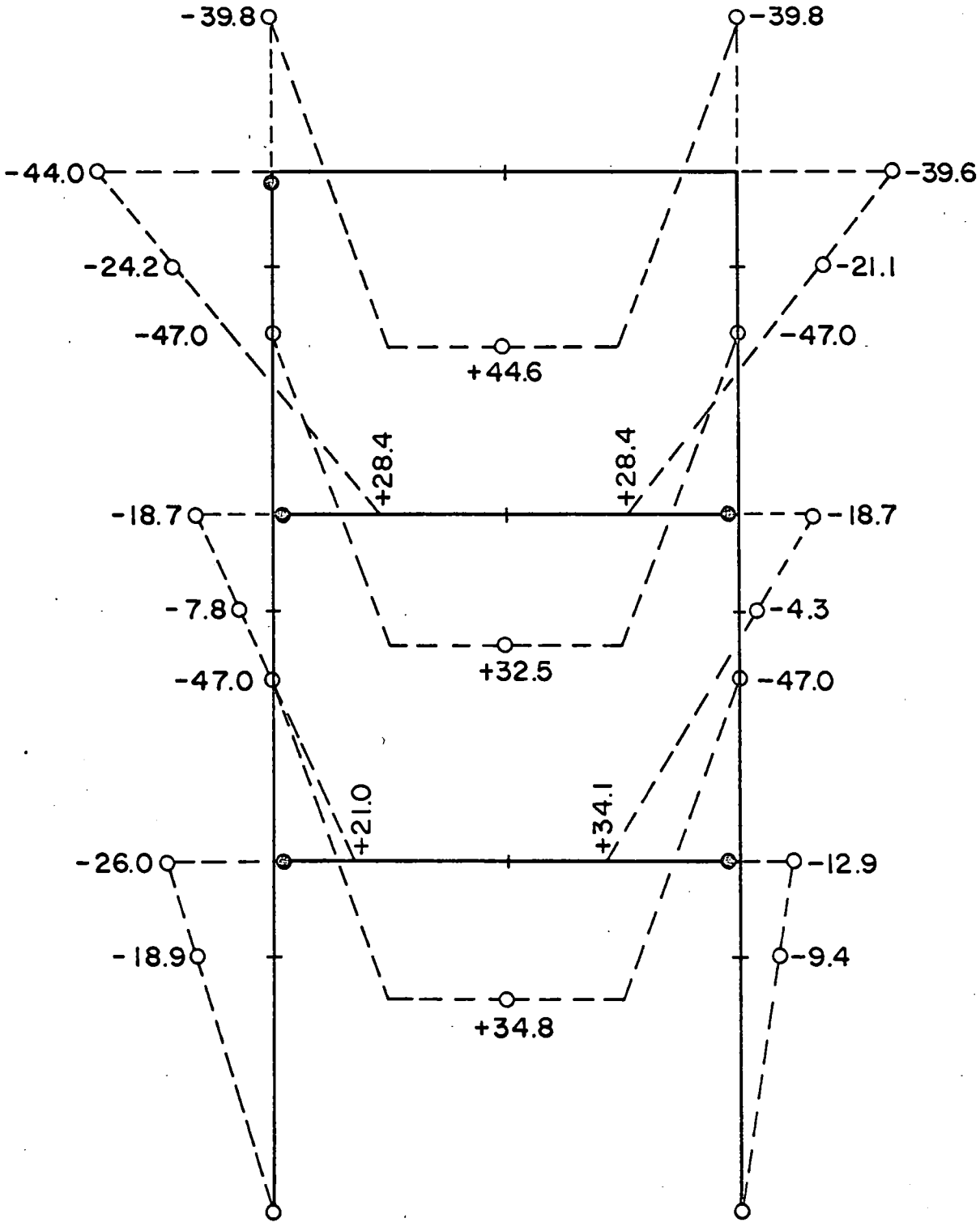

Fig. 7.19 MOMENT DIAGRAM OF WEST FRAME U-2 AT LOAD 70.9 KIPS

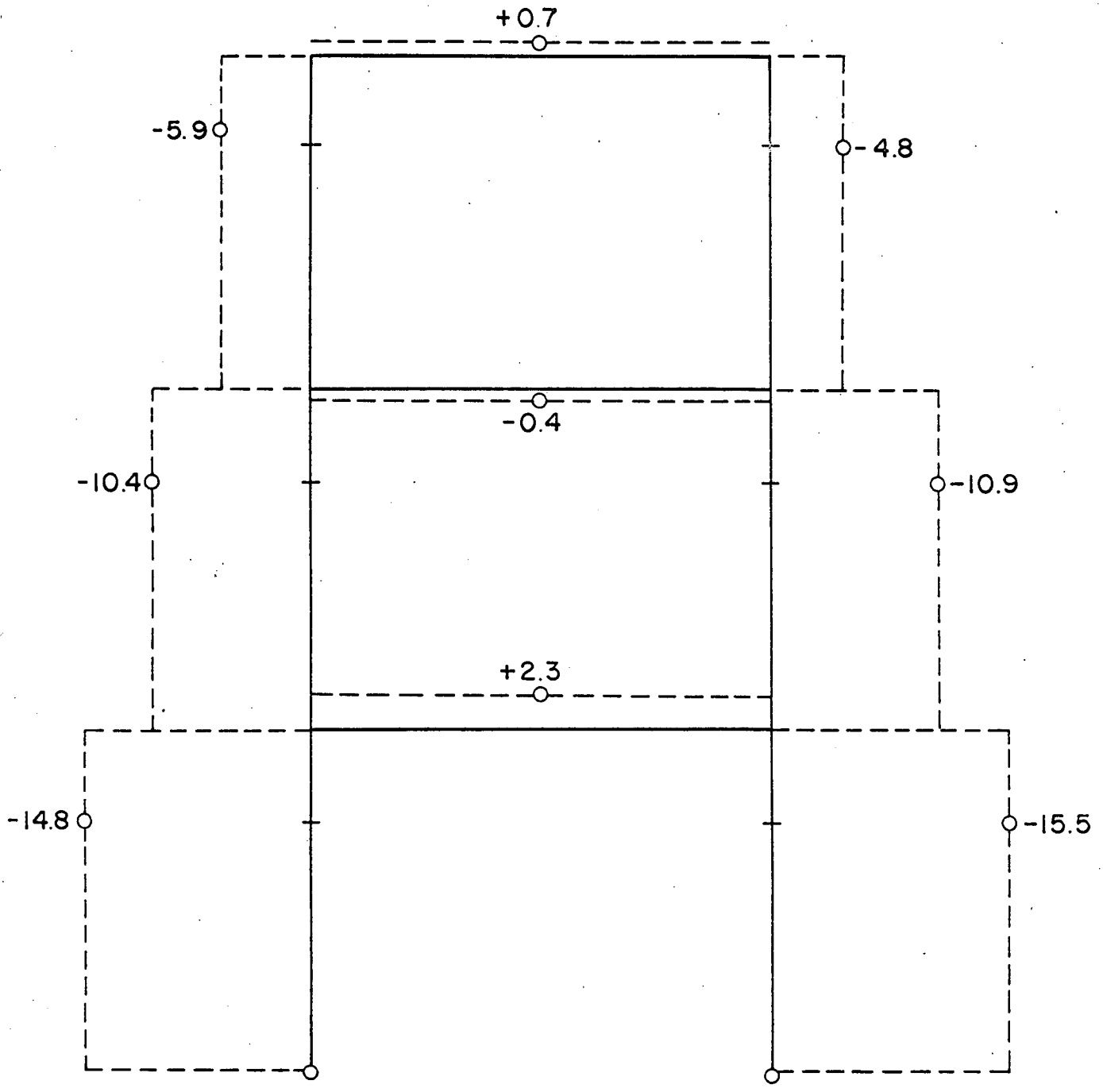

WEST FRAME

Load 70.90 kips (Rdngs. in kip-in)

Fig. 7.20 - THRUST DIAGRAM OF TEST FRAME U-2 AT LOAD 70.9 KIPS

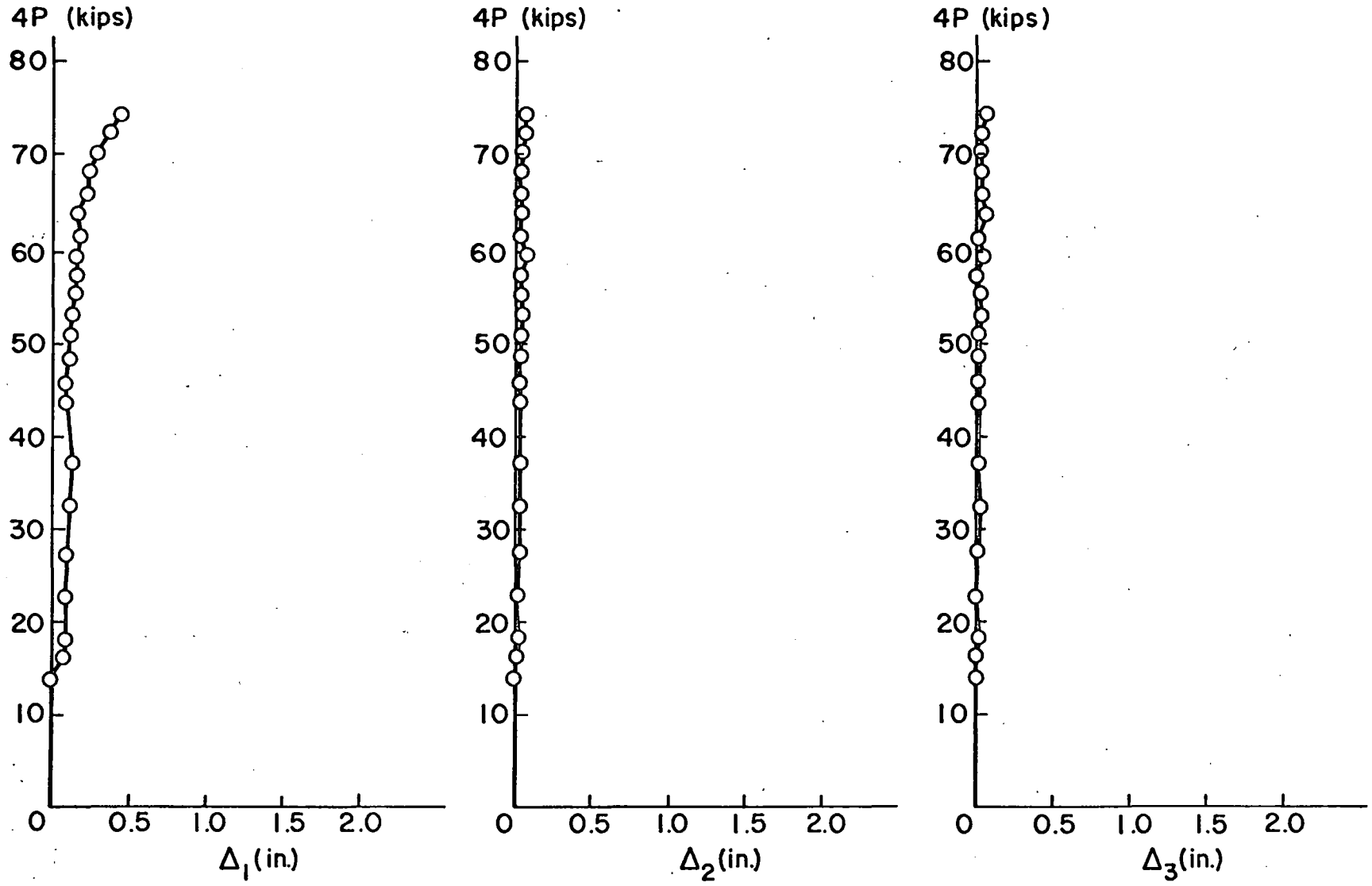

Fig. 7.21 LOAD VS. SIDESWAY OF N. W. COLUMN

Fig. 7.22

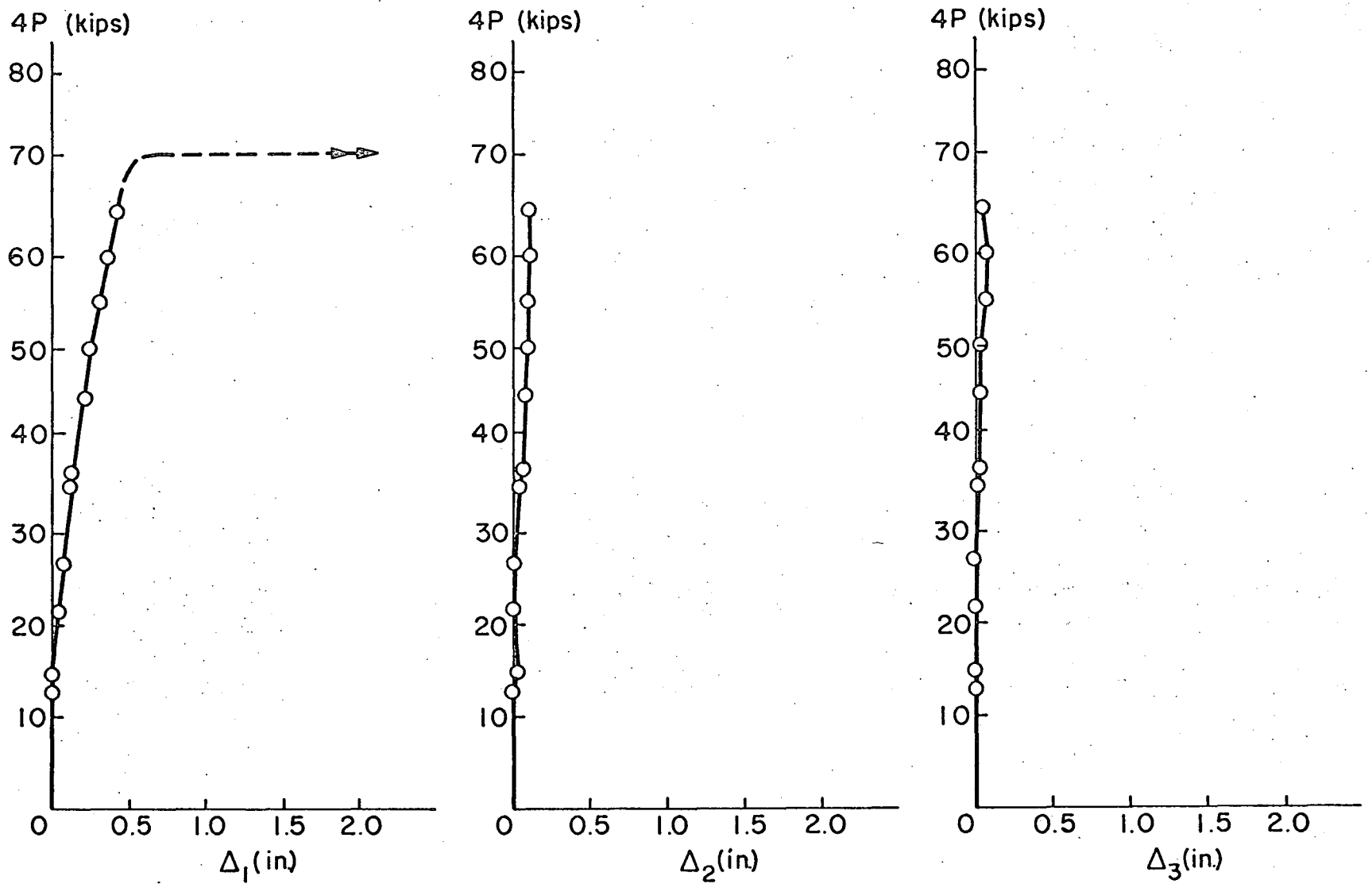

Fig. 7.22 REVISED LOAD VS. SIDESWAY OF N. W. COLUMN

Fig. 7.23

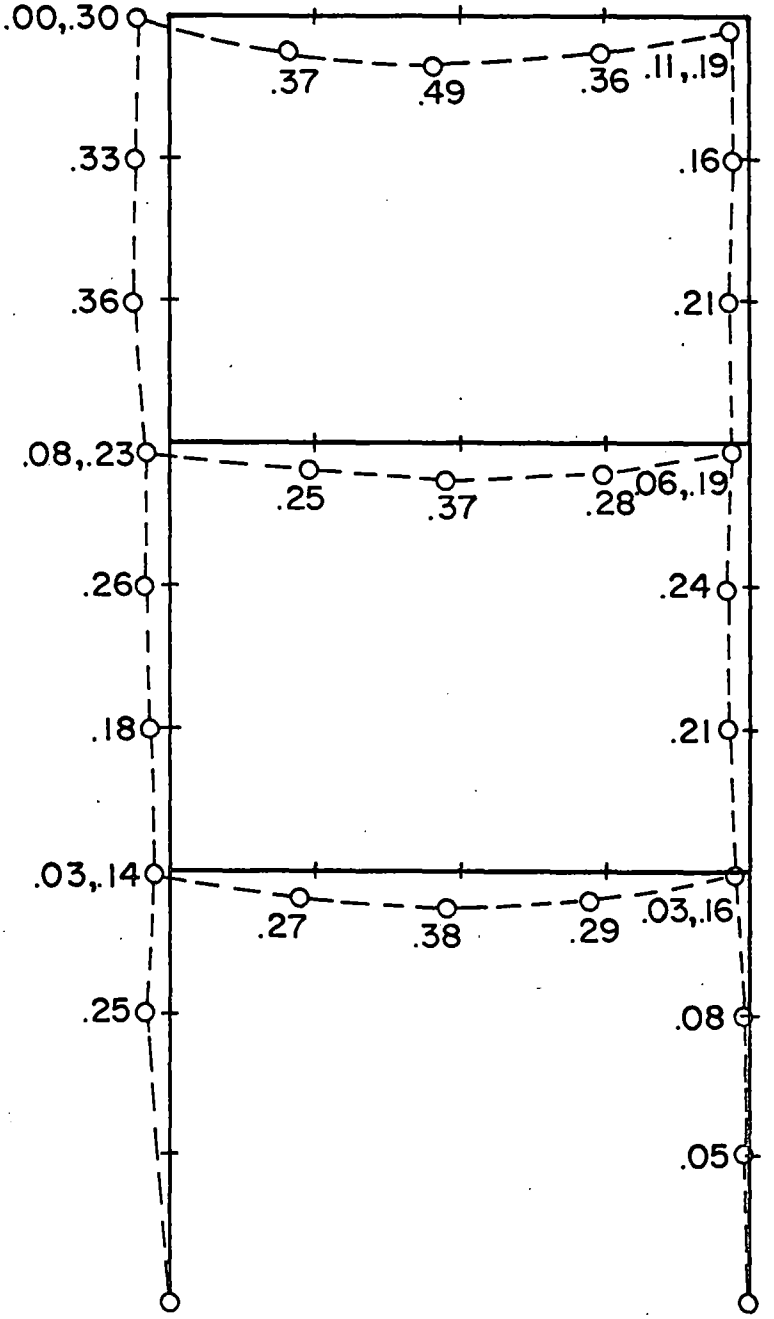

WEST FRAME

Load 64.03 kips (Rdngs. in in.)

Fig. 7.23 DEFORMATION OF FRAME U-2 AT LOAD 64.03 KIPS

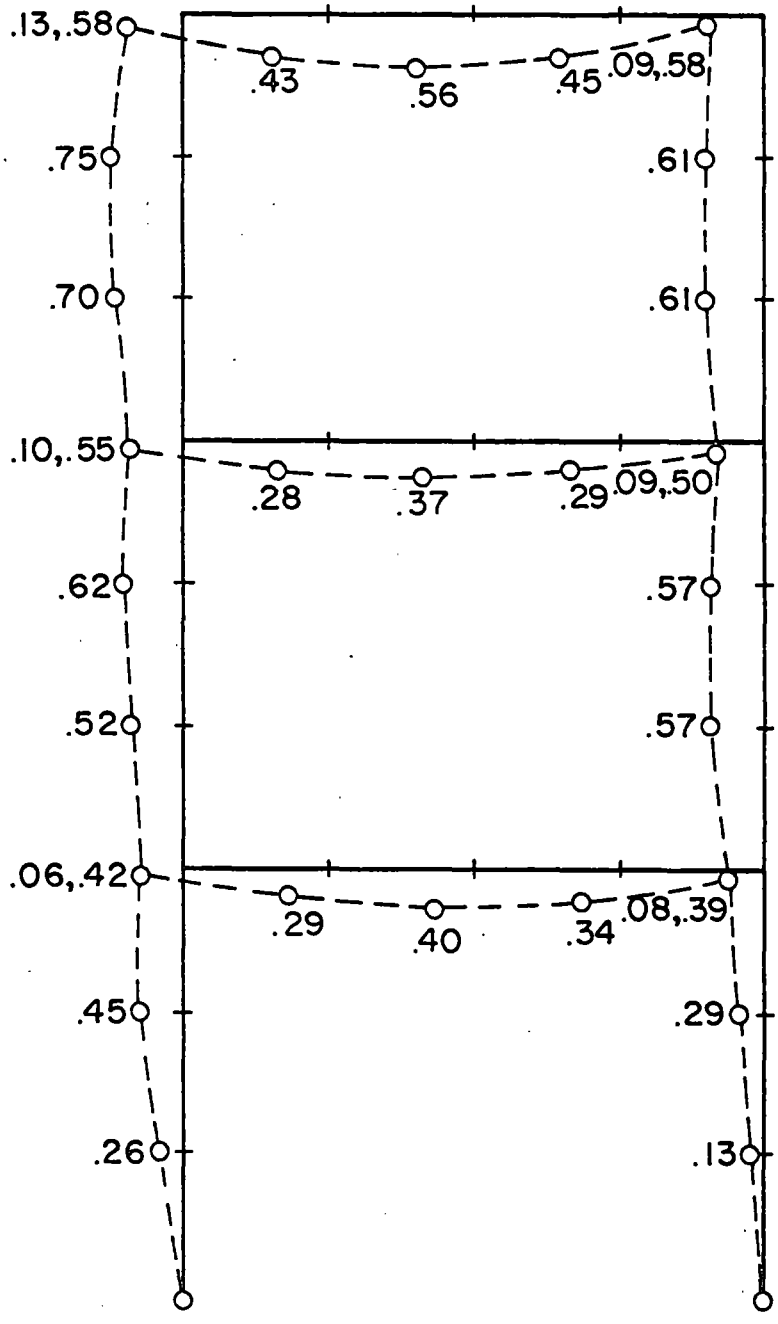

WEST FRAME

Load 64.93 kips (Rdngs. in in.)

Fig. 7.24 — DEFORMATION OF FRAME U-2 AT REVISED LOAD 64.93 KIPS

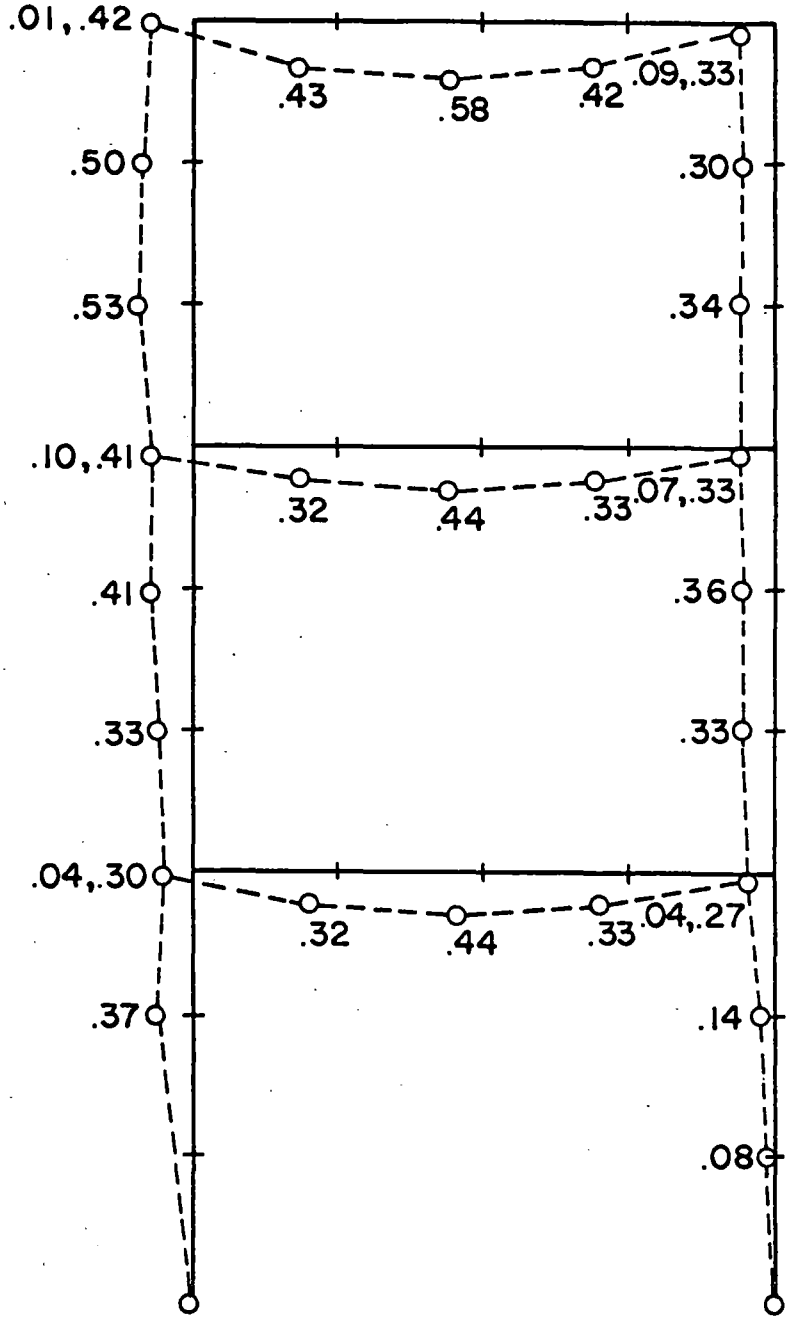

WEST FRAME
Load 70.9 kips (Rdngs. in in.)

Fig. 7.25 DEFORMATION OF FRAME U-2 AT LOAD 70.90 KIPS

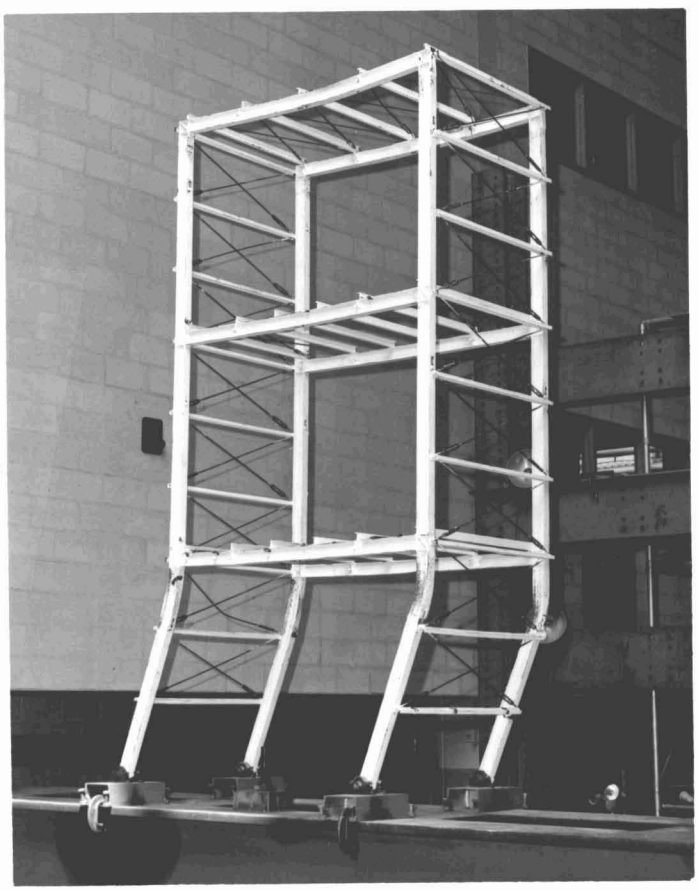

Fig. 7.26 FRAME U-2 AFTER TESTING

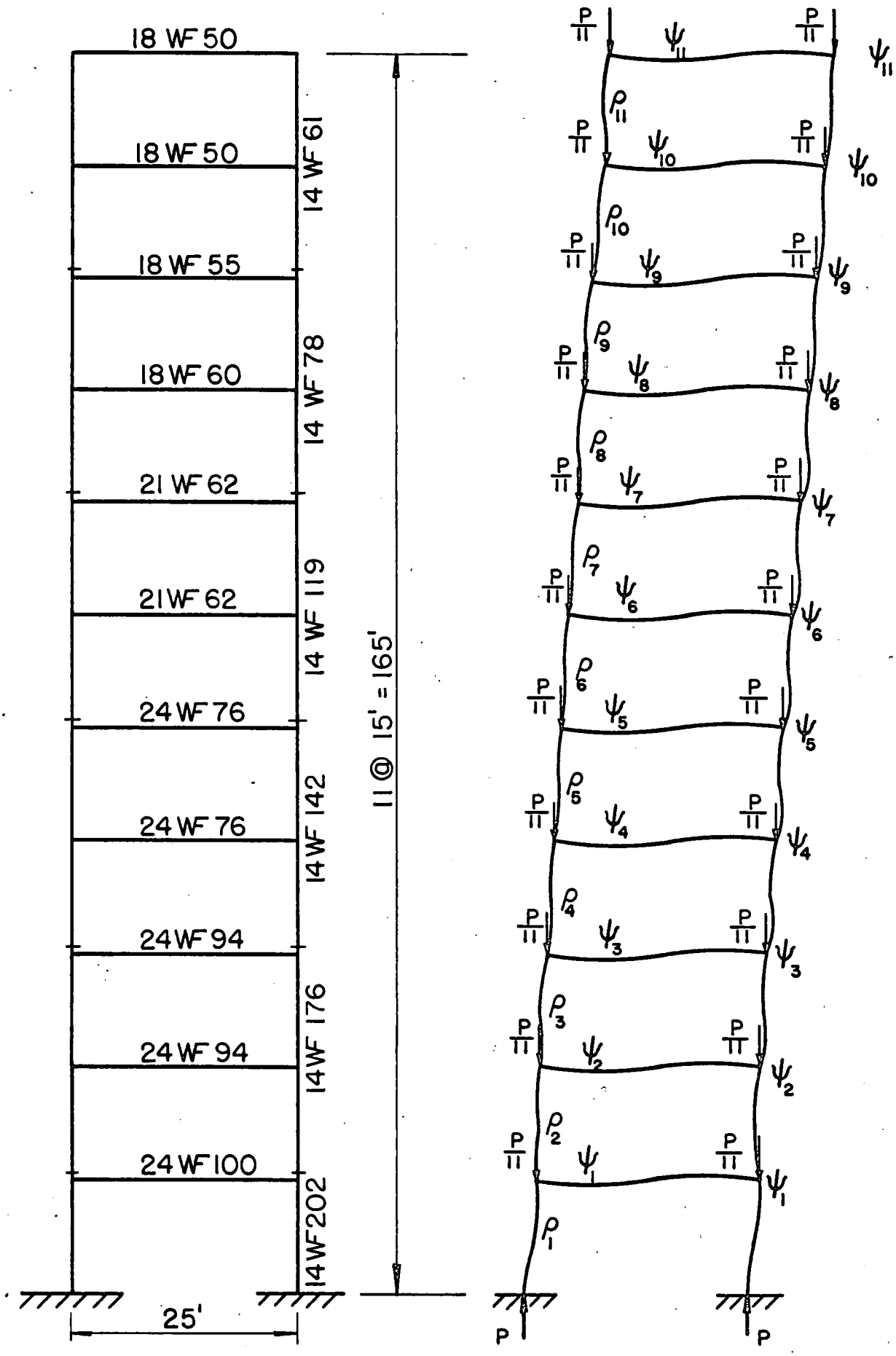

Fig. 8.1 AN ELEVEN-STORY BUILDING FRAME

Fig. 8.2

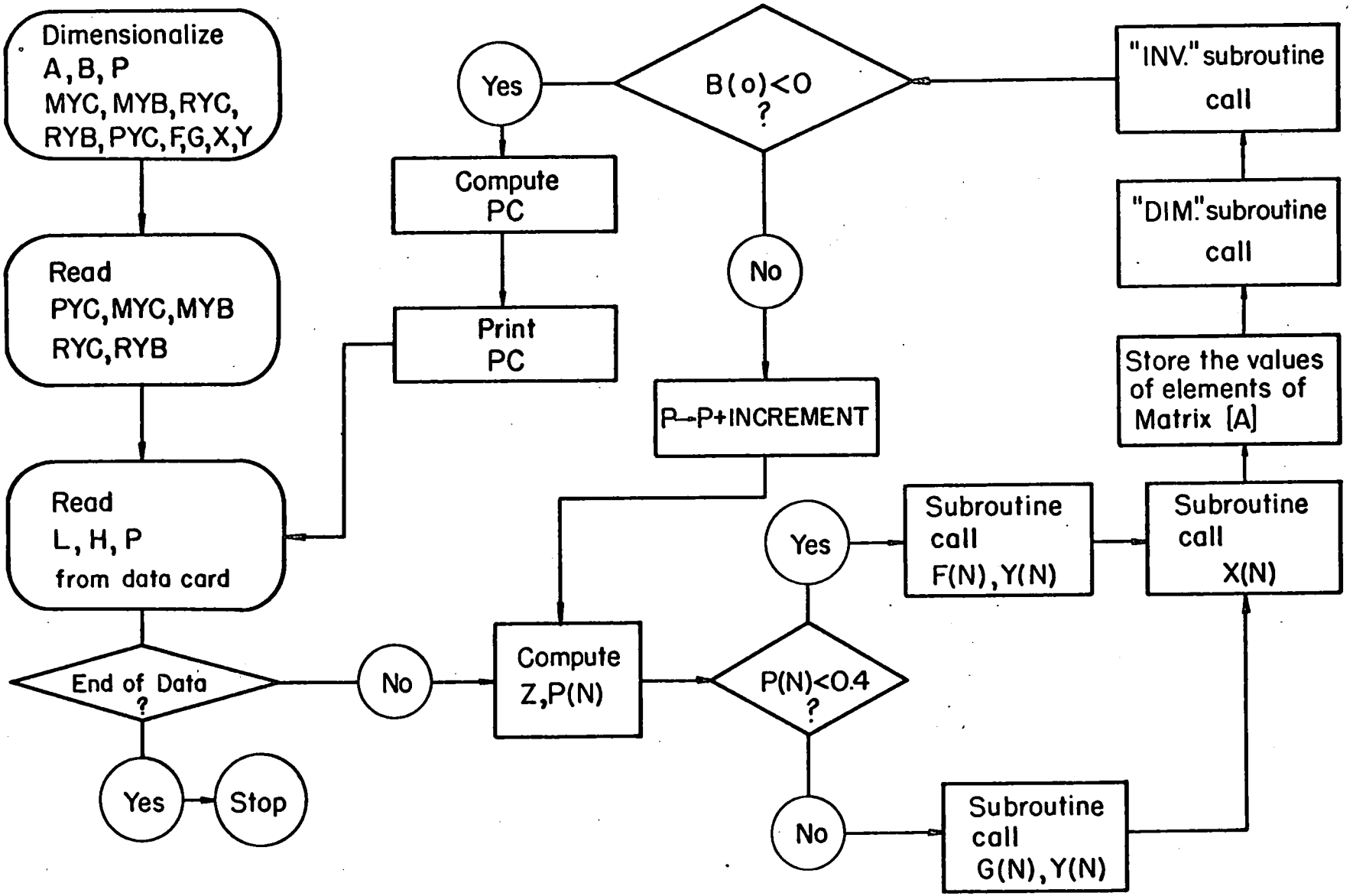

Fig. 8.2 FLOW CHART FOR BUCKLING ANALYSIS OF AN ELEVEN-STORY FRAME

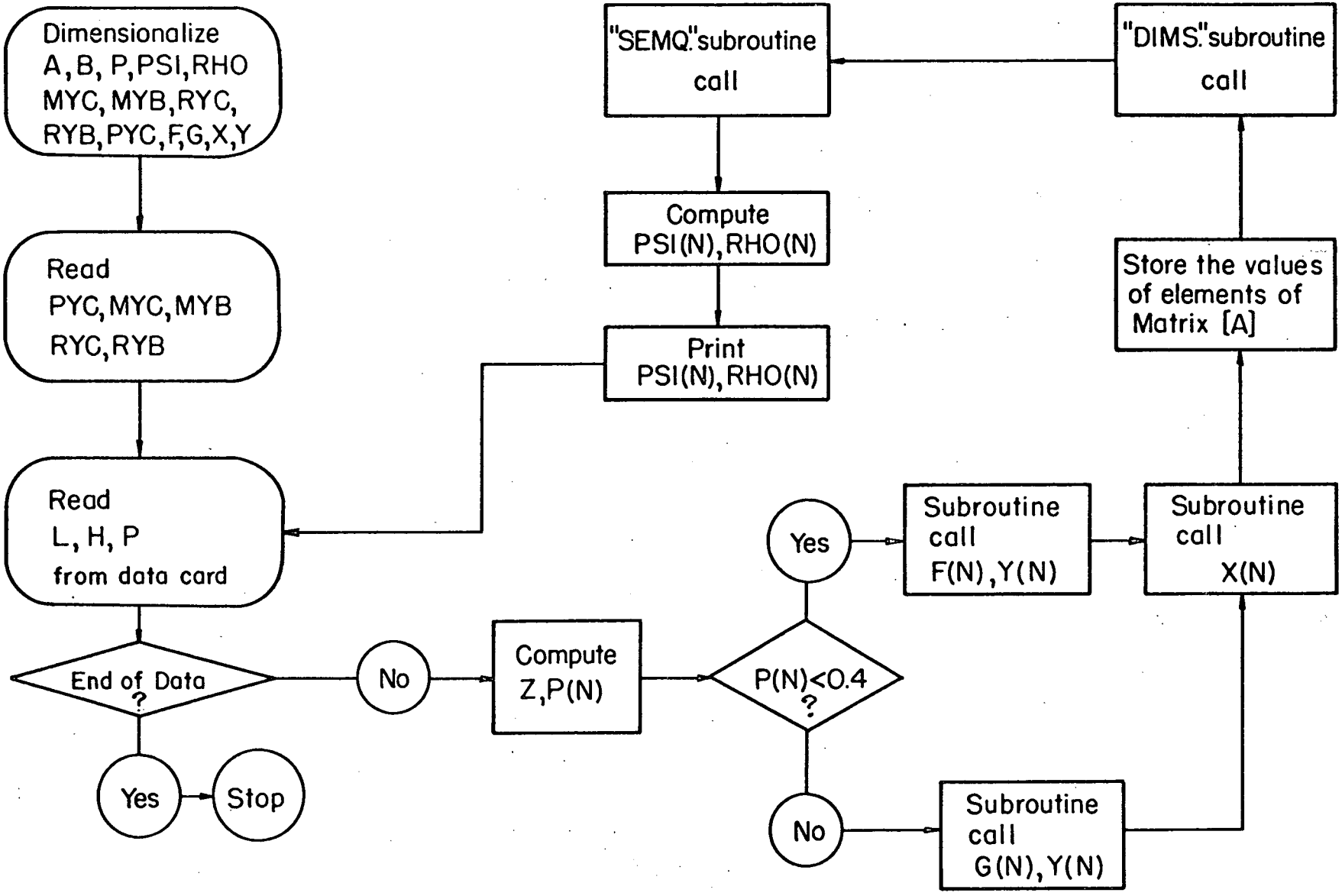

Fig. 8.3 FLOW CHART FOR DEFORMATION ANALYSIS OF ELEVEN-STORY FRAME

Fig. 8.4

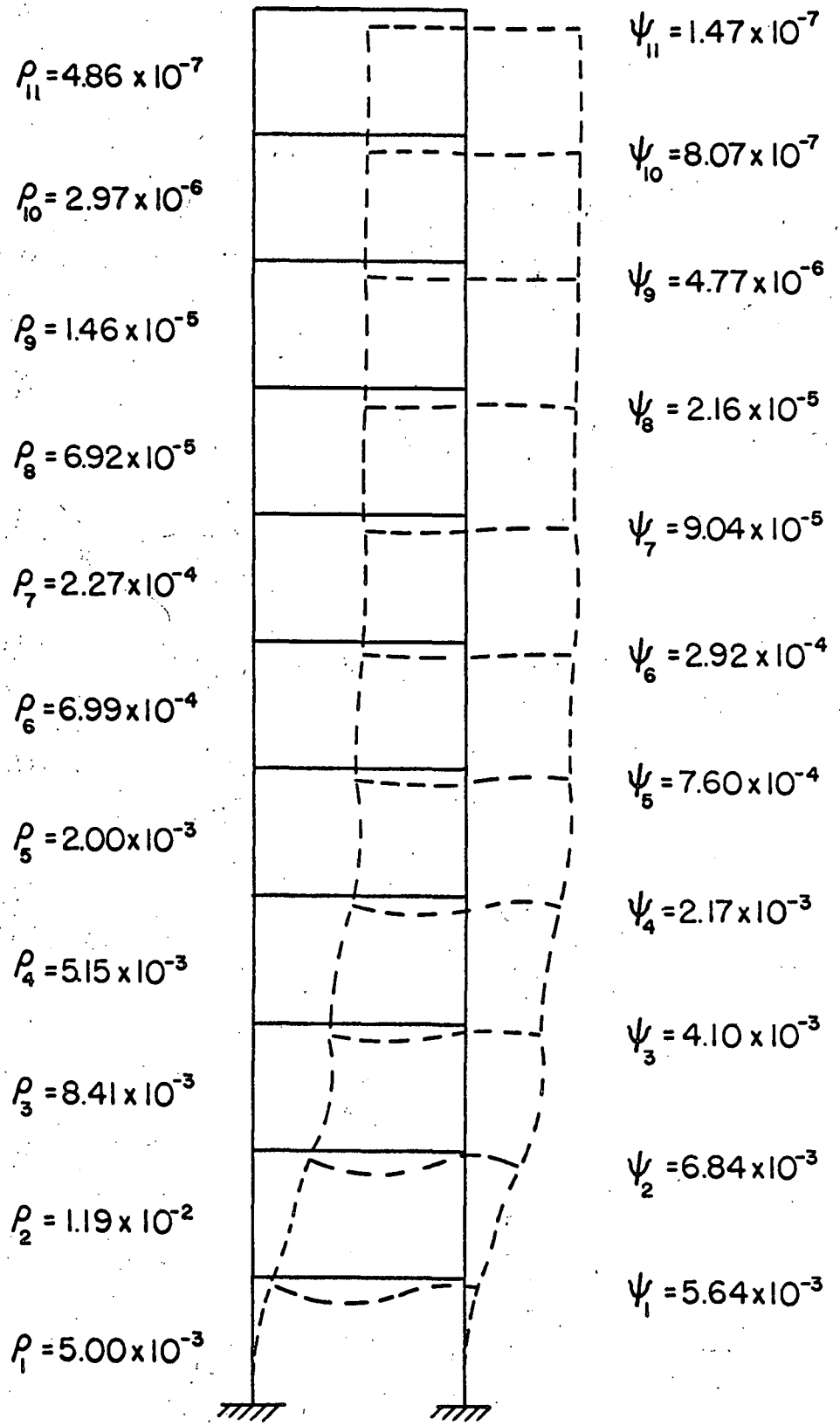

Fig. 8.4 BUCKLING MODE OF AN ELEVEN-STORY FRAME

Fig.8.5

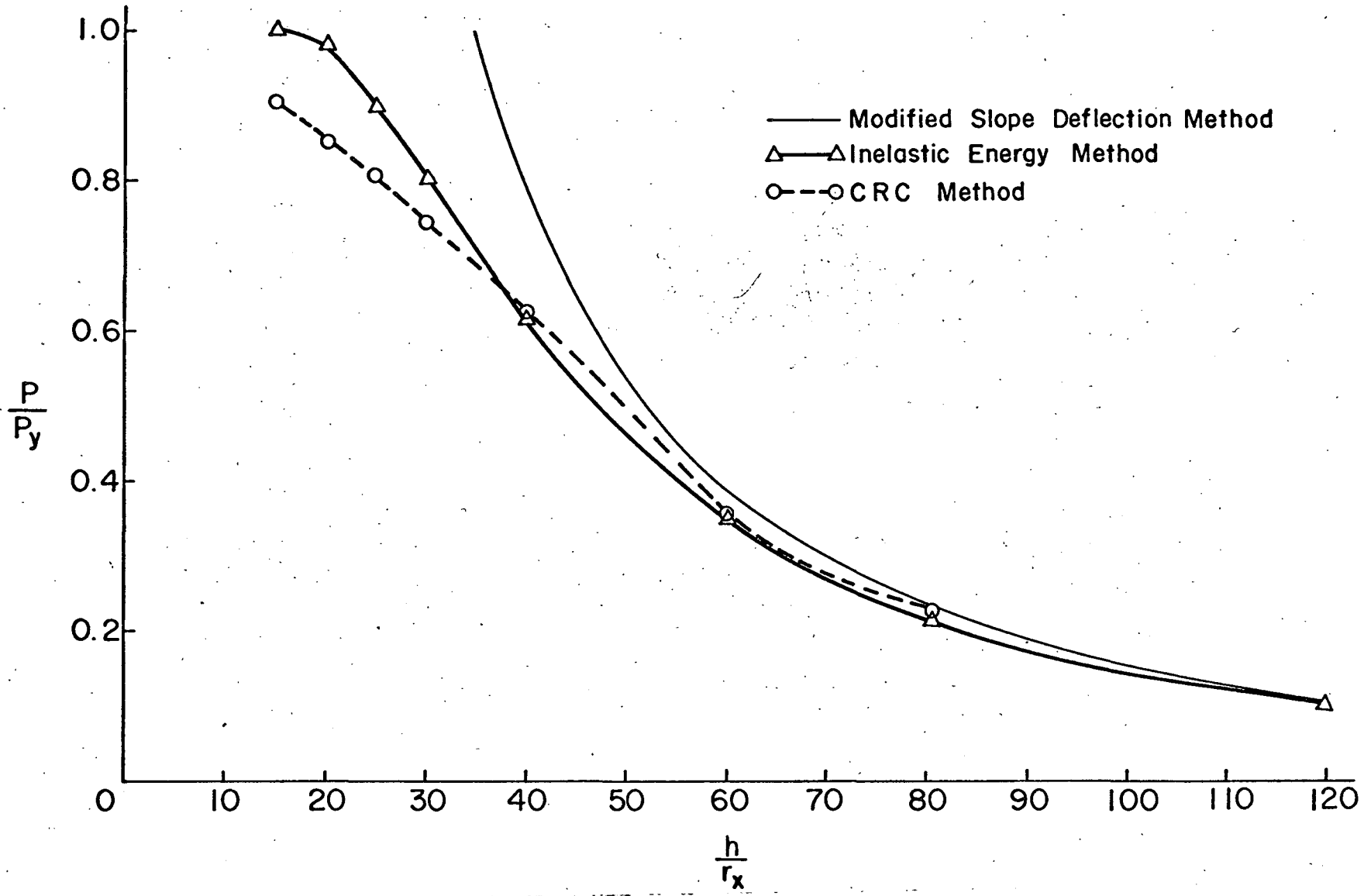

Fig. 8.5 COMPARISON BETWEEN INELASTIC ENERGY METHOD AND CRC METHOD FOR BUCKLING LOADS OF THREE-STORY FRAMES

12. APPENDICES

APPENDIX A

```
265    Y.C.YEN   ANTISYMMETRIC BUCKLING OF ELEVEN-STORY FRAMES
NOV 21 63        10 11.3

010             $ WIZ PROGRAM, NOVEMBER,1963. Y.C.YEN
020             $ ANTISYMMETRIC BUCKLING OF ELEVEN-STORY
                $ FRAMES,ELASTIC AND INELASTIC,FIXED ENDS.
030          D  DIM.(16),INV.(502),A(484),B(484),P(11)
             D  MYC(11),MYB(11),RYC(11),RYB(11),F(11),G(11)
             D  X(11),Y(11),PYC(11)
040             PYC(1)=1960, PYC(2)=PYC(3)=1707
                PYC(4)=PYC(5)=1381, PYC(6)=PYC(7)=1154
                PYC(8)=PYC(9)=757, PYC(10)=PYC(11)=592
050             MYC(1)=10722, MYC(2)=MYC(3)=9303
                MYC(4)=MYC(5)=7481, MYC(6)=MYC(7)=6250
                MYC(8)=MYC(9)=3996, MYC(10)=MYC(11)=3043
060             MYB(1)=8214, MYB(2)=MYB(3)=7289
                MYB(4)=MYB(5)=5788, MYB(6)=MYB(7)=4171
                MYB(8)=3557,MYB(9)=3241,MYB(10)=MYB(11)=2937
070             RYC(1)=1.40764E-4,RYC(2)=RYC(3)=1.44277E-4
                RYC(4)=RYC(5)=1.49143E-4
                RYC(6)=RYC(7)=1.51736E-4
                RYC(8)=RYC(9)=1.56460E-4
                RYC(10)=RYC(11)=1.58160E-4
080             RYB(1)=0.91674E-4, RYB(2)=RYB(3)=0.90569E-4
                RYB(4)=RYB(5)=0.92004E-4
                RYB(6)=RYB(7)=1.04825E-4
                RYB(8)=1.20535E-4, RYB(9)=1.21431E-4
                RYB(10)=RYB(11)=1.22222E-4
090    BACK CRDL,H,P
100             INCREMENT=0.02  $ FOR P ONLY
110    BEGN     N=1
120    10       (P(N)=(12-N)*P*PYC(1)/(11*PYC(N)))-0.4
130             F(N)=FS.(P(N))
140             Y(N)=F(N)*YS.(MYC(N),RYC(N))
150    HIGH     G(N)=GS.(P(N))
160             Y(N)=G(N)*YS.(MYC(N),RYC(N))
170    TRAS     X(N)=XS.(MYB(N),RYB(N))
180             (N=N+1)-12
190             Z=P*PYC(1)*H/165
200             I=1
```

HIGH

TRAS

(10

```
210     20      A(I)=0                                                  (     ) (     ) (     ) (     ) (     ) (     )
220             (I=I+1)-485                                             (     ) (     ) (     ) (20   ) (     ) (     )
230             A(2)=A(23)=Y(2)+55*Z                                    (     ) (     ) (     ) (     ) (     ) (     )
240             A(25)=A(46)=Y(3)+45*Z                                   (     ) (     ) (     ) (     ) (     ) (     )
250             A(48)=A(69)=Y(4)+36*Z                                   (     ) (     ) (     ) (     ) (     ) (     )
260             A(71)=A(92)=Y(5)+28*Z                                   (     ) (     ) (     ) (     ) (     ) (     )
270             A(94)=A(115)=Y(6)+21*Z                                  (     ) (     ) (     ) (     ) (     ) (     )
280             A(117)=A(138)=Y(7)+15*Z                                 (     ) (     ) (     ) (     ) (     ) (     )
290             A(140)=A(161)=Y(8)+10*Z                                 (     ) (     ) (     ) (     ) (     ) (     )
300             A(163)=A(184)=Y(9)+6*Z                                  (     ) (     ) (     ) (     ) (     ) (     )
310             A(186)=A(207)=Y(10)+3*Z                                 (     ) (     ) (     ) (     ) (     ) (     )
320             A(209)=A(230)=Y(11)+Z                                   (     ) (     ) (     ) (     ) (     ) (     )
330             A(12)=A(243)=-3*Y(1)+198*Z                              (     ) (     ) (     ) (     ) (     ) (     )
340             A(13)=A(35)=A(265)=A(266)=3*Y(2)+165*Z                  (     ) (     ) (     ) (     ) (     ) (     )
350             A(36)=A(58)=A(288)=A(289)=-3*Y(3)+135*Z                 (     ) (     ) (     ) (     ) (     ) (     )
360             A(59)=A(81)=A(311)=A(312)=-3*Y(4)+108*Z                 (     ) (     ) (     ) (     ) (     ) (     )
370             A(82)=A(104)=A(334)=A(335)=-3*Y(5)+84*Z                 (     ) (     ) (     ) (     ) (     ) (     )
380             A(105)=A(127=A(357)=A(358)=-3*Y(6)+63*Z                 (     ) (     ) (     ) (     ) (     ) (     )
390             A(128)=A(150)=A(380)=A(381)=-3*Y(7)+45*Z                (     ) (     ) (     ) (     ) (     ) (     )
400             A(151)=A(173)=A(403)=A(404)=-3*Y(8)+30*Z                (     ) (     ) (     ) (     ) (     ) (     )
410             A(174)=A(196)=A(426)=A(427)=-3*Y(9)+18*Z                (     ) (     ) (     ) (     ) (     ) (     )
420             A(197)=A(219)=A(449)=A(450)=-3*Y(10)+9*Z                (     ) (     ) (     ) (     ) (     ) (     )
430             A(220)=A(242)=A(472)=A(473)=-3*Y(11)+3*Z                (     ) (     ) (     ) (     ) (     ) (     )
440             A(1)=X(1)+2*Y(1)+2*Y(2)-484*Z                           (     ) (     ) (     ) (     ) (     ) (     )
450             A(24)=X(2)+2*Y(2)+2*Y(3)-400*Z                          (     ) (     ) (     ) (     ) (     ) (     )
460             A(47)=X(3)+2*Y(3)+2*Y(4)-324*Z                          (     ) (     ) (     ) (     ) (     ) (     )
470             A(70)=X(4)+2*Y(4)+2*Y(5)-256*Z                          (     ) (     ) (     ) (     ) (     ) (     )
480             A(93)=X(5)+2*Y(5)+2*Y(6)-196*Z                          (     ) (     ) (     ) (     ) (     ) (     )
490             A(116)=X(6)+2*Y(6)+2*Y(7)-144*Z                         (     ) (     ) (     ) (     ) (     ) (     )
500             A(139)=X(7)+2*Y(7)+2*Y(8)-100*Z                         (     ) (     ) (     ) (     ) (     ) (     )
510             A(162)=X(8)+2*Y(8)+2*Y(9)-64*Z                          (     ) (     ) (     ) (     ) (     ) (     )
520             A(185)=X(9)+2*Y(9)+2*Y(10)-36*Z                         (     ) (     ) (     ) (     ) (     ) (     )
530             A(208)=X(10)+2*Y(10)+2*Y(11)-16*Z                       (     ) (     ) (     ) (     ) (     ) (     )
```

```
540             A(231)=X(11)+2*Y(11)-4*Z                                ( ) ( ) ( ) ( ) ( )
550             A(254)=6*Y(1)-2376*Z                                    ( ) ( ) ( ) ( ) ( )
560             A(277)=6*Y(2)-1980*Z                                    ( ) ( ) ( ) ( ) ( )
570             A(300)=6*Y(3)-1620*Z                                    ( ) ( ) ( ) ( ) ( )
580             A(323)=6*Y(4)-1296*Z                                    ( ) ( ) ( ) ( ) ( )
590             A(346)=6*Y(5)-1008*Z                                    ( ) ( ) ( ) ( ) ( )
600             A(369)=6*Y(6)-756*Z                                     ( ) ( ) ( ) ( ) ( )
610             A(392)=6*Y(7)-540*Z                                     ( ) ( ) ( ) ( ) ( )
620             A(415)=6*Y(8)-360*Z                                     ( ) ( ) ( ) ( ) ( )
630             A(438)=6*Y(9)-216*Z                                     ( ) ( ) ( ) ( ) ( )
640             A(461)=6*Y(10)-108*Z                                    ( ) ( ) ( ) ( ) ( )
650             A(484)=6*Y(11)-36*Z                                     ( ) ( ) ( ) ( ) ( )
660             A=DIM,(22,22)                                           ( ) ( ) ( ) ( ) ( )
670             B=INV,(A)                                               ( ) ( ) ( ) ( ) ( )
680             B(0)   STHE VALUE OF DETERMINANT                        ( ) ( ) ( ) (30 ) ( )
690             D=B(0)                                                  ( ) ( ) ( ) ( ) ( )
700             P=P+INCREMENT                                           ( ) ( ) ( ) ( ) (BEGN)
710     30      PC=P+0.02*B(0)/(D-B(0)                                  ( ) ( ) ( ) ( ) ( )
720         PVLH,P,D,B(0),PC                                            ( ) ( ) ( ) ( ) (BACK)
730     FS  .   $FS-SUBROUTINE STARTS HERE                              ( ) ( ) ( ) ( ) ( )     FS .
740             FS(1)=-0.0425*FS(1)*FS(1)-0.1363*FS(1)+0.4509           ( ) ( ) ( ) ( ) (.  )   FS .
750             $FS-SUBROUTINE ENDS.                                    ( ) ( ) ( ) ( ) ( )     FS .
760     GS  .   $GS-SUBROUTNIE STARTS HERE                              ( ) ( ) ( ) ( ) ( )     GS .
770             GS(1)=-0.34713*GS(1)*GS(1)+0.2423*GS(1)+0.43C
            ###543                                                      ( ) ( ) ( ) ( ) (.  )   GS .
780             $GS-SUBROUTINE ENDS.                                    ( ) ( ) ( ) ( ) ( )     GS .
790     XS  .   $XS-SUBROUTINE STARTS HERE                              ( ) ( ) ( ) ( ) ( )     XS .
800             XS(1)=10.8216*XS(1)/(XS(2)*L)                           ( ) ( ) ( ) ( ) (.  )   XS .
810             $XS-SUBROUTINE ENDS.                                    ( ) ( ) ( ) ( ) ( )     XS .
820     YS      $YS-SUBROUTINE STARTS HERE                              ( ) ( ) ( ) ( ) ( )     YS .
830             YS(1)=8*YS(1)/(YS(2)*H)                                 ( ) ( ) ( ) ( ) (.  )   YS .
840             $YS-SUBROUTINE ENDS.                                    ( ) ( ) ( ) ( ) ( )     YS .
850         END$END OF THE PROGRAM.                                     ( ) ( ) ( ) ( ) ( )     YS .
            180 $H  6.4000000-01 $P  2.3389992-17 $D -9.3653367-18 $B(0)
  6.3428164-01 $PC
#END OF DATA# CARD READ AS DATA
NOV 21 63       10 14.7
```

APPENDIX B

```
265  Y.C.YEN   DEFORMATION ANALYSIS OF ELEVEN-STORY FRAMES
DEC 03 63      10 58.3

0100           $ WIZ PROGRAM, DECEMBER,1963.  Y.C.YEN
0200           $ DEFORMATION ANALYSIS OF ELEVEN-STORY FRAMES
               $ ELASTIC AND INELASTIC, FIXED ENDS.
030       D    DIMS.(14), SMEQ.(273), A(462), B(21) ,P(11)
          D    MYC(11),MYB(11),RYC(11),RYB(11),F(11),G(11)
          D    PYC(11),X(11),Y(11),PSI(11),RHO(11)
040            PYC(1)=1960, PYC(2)=PYC(3)=1707
               PYC(4)=PYC(5)=1381, PYC(6)=PYC(7)=1154
               PYC(8)=PYC(9)=757, PYC(10)=PYC(11)=592
050            MYC(1)=10722, MYC(2)=MYC(3)=9303
               MYC(3)=MYC(5)=7381, MYC(6)=MYC(7)=6250
               MYC(8)=MYC(9)=3996, MYC(10)MYC(11)=3043.
060            MYB(1)=8214, MYB(2)=MYB(3)=7289
               MYB(4)=MYB(5)=5788, MYB(6)=MYB(7)=4171
               MYB(8)=3557,MYB(9)=3241,MYB(10)=MYB(11)=2937
070            RYC(1)=1.40764E-4,RYC(2)=RYC(3)=1.44277E-4
               RYC(4)=RYC(5)=1.49143E-4
               RYC(6)=RYC(7)=1.51736E-4
               RYC(8)=RYC(9)=1.56460E-4
               RYC(10)=RYC(11)=1.58160E-4
080            RYB(1)=0.91674E-4, RYB(2)=RYB(3)=0.90569E-4
               RYB(4)=RYB(5)=0.92004E-4
               RYB(6)=RYB(7)=1.04825E-4
               RYB(8)=1.20535E-4, RYB(9)=1.21431E-4
               RYB(10)=RYB(11)=1.22222E-4
090    BACK CRDL,H,P
110            N=1
120    10      (P(N)=(12-N)*P*PYC(1)/(11*PYC(N)))-0.4
130            F(N)=FS.(P(N))
```

```
140             Y(N)=F(N)*YS.(MYC(N),RYC(N))                    ( TRAS )
150     HIGH    G(N)=GS.(P(N))
160             Y(N)=G(N)*YS.(MYC(N),RYC(N))
170     TRAS    X(N)=XS.(MYB(N),RYB(N))
180             (N=N+1)-12                                      ( 10 )
190             Z=P*PYC(1)*H/165
200             I=1
210     20      A(I)=0
220             (I=I+1)-463                                     ( 20 )
230             A(1)=X(1)+2*Y(1)+2*Y(2)-484*Z
240             A(24)=X(2)+2*Y(2)+2*Y(3)-400*Z
250             A(47)=X(3)+2*Y(3)+2*Y(4)-324*Z
260             A(70)=X(4)+2*Y(4)+2*Y(5)-256*Z
270             A(93)=X(5)+2*Y(5)+2*Y(6)-196*Z
280             A(116)=X(6)+2*Y(6)+2*Y(7)-144*Z
290             A(139)=X(7)+2*Y(7)+2*Y(8)-100*Z
300             A(162)=X(8)+2*Y(8)+2*Y(9)-64*Z
310             A(185)=X(9)+2*Y(9)+2*Y(10)-36*Z
320             A(208)=X(10)+2*Y(10)+2*Y(11)-16*Z
330             A(231)=X(11)+2*Y(11)-4*Z
340             A(254)=6*Y(2)-1980*Z
350             A(277)=6*Y(3)-1620*Z
360             A(300)=6*Y(4)-1296*Z
370             A(323)=6*Y(5)-1008*Z
380             A(346)=6*Y(6)-756*Z
390             A(369)=6*Y(7)-540*Z
400             A(392)=6*Y(8)-360*Z
410             A(415)=6*Y(9)-216*Z
420             A(438)=6*Y(10)-108*Z
430             A(461)=6*Y(11)-36*Z
440             A(2)=A(23)=Y(2)+55*Z
450             A(25)=A(46)=Y(3)+45*Z
460             A(48)=A(69)=Y(4)+36*Z
```

```
470             A(71)=A(92)=Y(5)+28*Z                                    ( ) ( ) ( ) ( ) ( )
480             A(94)=A(115)=Y(6)+21*Z                                   ( ) ( ) ( ) ( ) ( )
490             A(117)=A(138)=Y(7)+15*Z                                  ( ) ( ) ( ) ( ) ( )
500             A(140)=A(161)=Y(8)+10*Z                                  ( ) ( ) ( ) ( ) ( )
510             A(163)=A(184)=Y(9)+6*Z                                   ( ) ( ) ( ) ( ) ( )
520             A(186)=A(207)=Y(10)+3*Z                                  ( ) ( ) ( ) ( ) ( )
530             A(209)=A(230)=Y(11)+Z                                    ( ) ( ) ( ) ( ) ( )
540             A(12)=A(34)=A(243)=A(244)=-3*Y(2)+165*Z                  ( ) ( ) ( ) ( ) ( )
550             A(35)=A(57)=A(266)=A(267)=-3*Y(3)+135*Z                  ( ) ( ) ( ) ( ) ( )
560             A(58)=A(80)=A(289)=A(290)=-3*Y(4)+108*Z                  ( ) ( ) ( ) ( ) ( )
570             A(81)=A(103)=A(312)=A(313)=-3*Y(5)+84*Z                  ( ) ( ) ( ) ( ) ( )
580             A(104)=A(126)=A(335)=A(336)=-3*Y(6)+63*Z                 ( ) ( ) ( ) ( ) ( )
590             A(127)=A(149)=A(358)=A(359)=-3*Y(7)+45*Z                 ( ) ( ) ( ) ( ) ( )
600             A(150)=A(172)=A(381)=A(382)=-3*Y(8)+30*Z                 ( ) ( ) ( ) ( ) ( )
610             A(173)=A(195)=A(404)=A(405)=-3*Y(9)+18*Z                 ( ) ( ) ( ) ( ) ( )
620             A(196)=A(218)=A(427)=A(428)=-3*Y(10)+9*Z                 ( ) ( ) ( ) ( ) ( )
630             A(219)=A(241)=A(450)=A(451)=-3*Y(11)+3*Z                 ( ) ( ) ( ) ( ) ( )
640             A(22)=(-3*Y(1)+198*Z)*(-0.005)                           ( ) ( ) ( ) ( ) ( )
650             A=DIMS.(21,22)                                           ( ) ( ) ( ) ( ) ( )
660             B=SMEQ.(A)                                               ( ) ( ) ( ) ( ) ( )
670             M=1                                                      ( ) ( ) ( ) ( ) ( )
680     30      PSI(M)=B(M), RHO(M+1)=B(M+11),PSI(11)=B(11)              ( ) ( ) ( ) ( ) ( )
690             (M=M+1)-11                                               ( ) ( ) ( ) 30  ( )
700           PVLPSI(1),PSI(2),PSI(3),PSI(4),PSI(5),PSI(6)               ( ) ( ) ( ) ( ) ( )
710           PVLPSI(7),PSI(8),PSI(9),PSI(10),PSI(11)                    ( ) ( ) ( ) ( ) ( )
720           PVLRHO(2),RHO(3),RHO(4),RHO(5),RHO(6)                      ( ) ( ) ( ) ( ) ( )
725           PVLRHO(7),RHO(8),RHO(9),RHO(10),RHO(11)                    ( ) ( ) ( ) ( ) (BACK)
730     FS .    $FS-SUBROUTINE STARTS HERE                               ( ) ( ) ( ) ( ) ( ) FS .
740             FS(1)=-0.0425*FS(1)*FS(1)-0.1363*FS(1)+0.4509            ( ) ( ) ( ) ( ) ( ) FS .
750             $FS-SUBROUTINE ENDS.                                     ( ) ( ) ( ) ( ) ( ) FS .
760     GS .    $GS-SUBROUTINE STARTS HERE                               ( ) ( ) ( ) ( ) ( ) GS .
770             GS(1)=-0.34713*GS(1)*GS(1)+0.02423*GS(1)+0.43C           ( ) ( ) ( ) ( ) ( ) GS .
              ###543
780             $GS-SUBROUTINE ENDS.                                     ( ) ( ) ( ) ( ) ( ) GS .
```

```
 790    XS  .   $XS-SUBROUTINE STARTS HERE                    (     ) (     ) (     ) (     ) (     )  XS .
 800            XS(1)=10.8216*XS(1)/(XS(2)*L)                 (     ) (     ) (     ) (     ) (     )  XS .
 810            $XS-SUBROUTINE ENDS.                          (     ) (     ) (     ) (     ) (     )  XS .
 820    YS  .   $YS-SUBROUTINE STARTS HERE                    (     ) (     ) (     ) (     ) (     )  YS .
 830            YS(1)=8*YS(1)/(YS(2)*H)                       (     ) (     ) (     ) (     ) (     )  YS .
 840            $YS-SUBROUTINE ENDS.                          (     ) (     ) (     ) (     ) (     )  YS .
 850          END$END OF THE PROGRAM.                         (     ) (     ) (     ) (     ) (     )  YS .
 5.6382421-03 $PSI(1)  6.8445603-03 $PSI(2)  4.1036291-03 $PSI(3)  2.1729242-03 $PSI(4)  7.6021378-04 $PSI(5)
 2.9195052-04 $PSI(6)
 9.0442619-05 $PSI(7)  2.1612172-05 $PSI(8)  4.7738616-06 $PSI(9)  8.0713221-07 $PSI(10)
 1.4672309-07 $PSI(11)
 1.1916090-02 $RHO(2)  8.4054896-03 $RHO(3)  5.1467406-03 $RHO(4)  2.0022059-03 $RHO(5)
 6.9914112-04 $RHO(6)
 2.2691887-04 $RHO(7)  6.9183010-05 $RHO(8)  1.4610377-05 $RHO(9)  2.9728182-06 $RHO(10)
 4.8606711-07 $RHO(11)
#END OF DATA# CARD READ AS DATA

DEC 03 63      11 00.2
```

APPENDIX C

```
265  Y. C. YEN  ANTISYMMETRIC BUCKLING OF MODEL FRAME U-2
JUL 17 64        10 11.3

010             $ WIZ PROGRAM Y. C. YEN
020             $ BUCKLING OF MODEL FRAME U-2
030          D  DIM. (16), INV. (502), A(289), B(289)
040             MY =40.5,R=1.023E-3,PY=44.26,L=60,H=44
050     BACK CRDP
060             INCREMENT=0.01  $ FOR P ONLY
070     BEGN    P-0.4
080             F1=-0.0425*P*P-0.1363*P+0.4509
090     10      F1=-0.34713*P*P+0.02423*P+0.43543
110     20      Y1=4*MY*F1/(R*H)
120             (S=2*P/3) -0.4
130             F2=-0.0425*S*S-0.1363*S+0.4509
140     30      F2=-0.34713*S*S+0.02423*S+0.43543
150     40      Y2=4*MY*F2/(R*H)
160             (T=P/3)-0.4
170             F3=-0.0425*T*T-0.1363*T+0.4509
180     50      F3=-0.34713*T*T+0.02423*T+0.43543
190     60      Y3=4*MY*F3/(R*H)
200             MB=P*PY*L/(12*MY)-1.16
205             T=28.8*MB**MB*-81.0*MB*MB+72.3*MB-19.8
210             X=3.1416*3.1416*MY*T/(16*R*L)
220             Z=P*PY*H/90
230             N=1
240     70      A(N)=0
250             (N=N+1)-290
260             A(1) =2*Y1-12*Z
270             A(19)=2*Y1+2*Y2-20*Z+26*X
280             A(37)=2*Y2+2*Y3-12*7+26*X
290             A(55)=2*Y 3-4*Z+26*X
300             A(73)=2*Y1-12*Z
310             A(91)=2*Y1+2*Y2-20*Z
320             A(109)=2*Y2+2*Y3-12*Z
330             A(127)=2*Y3-4*Z
340             A(145)=A(163)=A(281)=26*X
```

```
350          A(199)=12*Y1-216*Z                                    (     )  (     )  (     )  (     )  (     )
360          A(217)=12*Y2-144*Z                                    (     )  (     )  (     )  (     )  (     )
370          A(235)=12*Y3-72*Z                                     (     )  (     )  (     )  (     )  (     )
380          A(253)=A(271)=A(289)=80*3.1416*3.1416*X               (     )  (     )  (     )  (     )  (     )
390          A(2)=A(18)=A(74)=A(90)=Y1+3*Z                         (     )  (     )  (     )  (     )  (     )
400          A(20)=A(36)=A(92)=A(108)=Y2+2*z                       (     )  (     )  (     )  (     )  (     )
410          A(38)=A(54)=A(110)=A(126)=Y3+Z                        (     )  (     )  (     )  (     )  (     )
420          A(26)=A(44)=A(62)=A(138)=A(156)=A174)=-10*X           (     )  (     )  (     )  (     )  (     )
430          A(12)=A(29)=A(80)=A(97)=A(188)=A(189)=A(192)  C(     )  (     )  (     )  (     )  (     )
440       ###=A(193)= 3*Y1+9*7
             A(30)=A(47)=A(98)=A(115)=A(206)=A(207)=A(210)C (     )  (     )  (     )  (     )  (     )
          ###-A(211)= 3*Y2+6*Z
450          A(48)=A(65)=A(116)= A(133)=A(224)=A(225)      C (     )  (     )  (     )  (     )  (     )
          ###=A(228)=A(229)= 3*Y3+ 3*Z
460          A(32)=A(50)=A(68)=A(240)=A(258)               C (     )  (     )  (     )  (     )  (     )
          ###A(276)= 36*3.1416*X                             C
470          A(151)=A(169)=A(187)=A(247) =A(265)           C (     )  (     )  (     )  (     )  (     )
          ###=A(283)=#6*3.1416*X
480          A=DIM.(17,17)                                         (     )  (     )  (     )  (     )  (     )
490          B=INV.(A)                                             (     )  (     )  (     )  (     )  (     )
500          B(0)  $VALUE OF DET.                                  (     )  (     )  (80   )  (     )  (     )
510          D=B (0)                                               (     )  (     )  (     )  (     )  (     )
520          P=P+INCREMENT                                         (     )  (     )  (     )  (     )  (BEGN )
530    80    PC=P+0.01*B(0)/(D-B(0))                               (     )  (     )  (     )  (     )  (     )
540       PVLH,P,D,B(0),PC$                                       (     )  (     )  (     )  (     )  ( BACK)
550       END$END OF THE PROGRAM                                  (     )  (     )  (     )  (     )  (     )
          44 $H  4.2000000-01  $P  -1.1881061+60  $D  1.7558098+54  $B(0)     4.1999998-01 $PC
#END OF DATA# CARD READ AS DATA
JUL 17 64      13 52.5
```

13. REFERENCES

1.1 Yen, Y. C., Lu, L. W. and Driscoll, Jr., G. C.
TESTS ON THE STABILITY OF STEEL FRAMES, WRC Bulletin Series No. 81, (1962)

1.2 Driscoll, G. C., Jr.
ROTATION CAPACITY REQUIREMENTS FOR BEAMS AND FRAMES OF STRUCTURAL STEEL, Ph. D. Dissertation, Lehigh University, (1958)

1.3 Galambos, T. V.
INELASTIC LATERAL TORSIONAL BUCKLING OF WIDE-FLANGE COLUMNS, Ph. D. Dissertation, Lehigh University, (1959)

1.4 Levi, Victor
PLASTIC DESIGN OF BRACED MULTI-STORY FRAMES, Ph. D. Dissertation, Lehigh University, (1962)

1.5 Beedle, L. S.
PLASTIC DESIGN OF STEEL FRAMES, John Wiley & Sons, Inc., New York, (1958)

1.6 Members of the Fritz Engineering Laboratory
STRUCTURAL STEEL DESIGN, The Ronald Press Co., New York, (1964)

1.7 Muller-Breslau, H.
DIE NEVEREN METHODEN DER FESTIGKEITSLEHRE, 4 Aufl. Leipzig, (1913)

1.8 Bleich, F.
THEORIE UND BERECHNUNG DER EISERNEN BRUECKEN, Julius Springer, Berlin, (1924)

1.9 Bleich, F.
STAHLHOCHBAUTEN, Springer Wien, (1932)

1.10 Zimmerman, H.
DIE KNICKFESTIGKEIT DES GERADEN STABES MIT MEHREREN FELDERN, Sitzungsberichte der preussischen Akademie der Wissenschaften (1909)

1.11 Zimmerman, H.
DIE KNICKFESTIGKEIT DER DRUCKGURTE OFFENER BRUKEN, W. Ernst und Sohn, Berlin (1910)

1.12 Zimmerman, H.
DIE KNICKFESTIGKEIT DER STABVERBINDUNGEN, W. Ernst und Sohn, Berlin (1925)

1.13 Kasarnowsky, S. and Zetterholm, D.
ZUR THEORIE DER SEITENSTEIFIGKEIT OFFENER FACHWERKBRÜCKER, Der Bauingenier, Vol. 8, (1927)

1.14 Bleich, F. and Bleich, H.
BEITRAG ZUR STABILITATSUNTER SUCHUNG DES PUNKWEISE ELASTISCH GESTUTZTEN STABES, Der Stahlbau, Vol. 10, (1937)

1.15 Lundquist, E. E.
STABILITY OF STRUCTURAL MEMBERS UNDER AXIAL LOAD, NACA Tech. Note 617, (1937)

1.16 Hoff, N. J.
INSTABILITY OF AIRCRAFT FRAMEWORKS, Paper presented at the 2nd Annual Summer Meeting of the Institute of Aeronautical Science, California, (1940)

1.17 Hoff, N. J.
STABLE AND UNSTABLE EQUILIBRIUM OF PLANE FRAMEWORKS, Jour Aeronaut, Sci., Vol. 8, (1941)

1.18 Hoff, N. J.
THE PROPORTIONING OF AIRCRAFT FRAMEWORKS, Jour., Aeronaut., Sci., Vol. 8, (1941)

1.19 Hoff, N. J.
STRESS ANALYSIS OF AIRCRAFT FRAMEWORKS, Proc. Roy. Aeronaut., Soc., Vol. 45, (1941)

1.20 Chwalla, E.
DIE STABILITAET LOTRECHT BELASTETER RECHTECKRAHMEN, Der Bauingenieur 19, p. 69, (1938)

1.21 Loh, M. H.
BUCKLING OF RIGID FRAMES, Doctoral Thesis, Cornell University, (1946)

1.22 Winter, G., Hsu, P. T., Koo, B., and Loh, M. H.
BUCKLING OF TRUSSES AND RIGID FRAMES, Cornell University, Engrg. Exp., Sta. Bulletin No. 36, (1948)

1.23 Perri, J. G.
MODIFIED METHOD OF MOMENT DISTRIBUTION FOR RIGID FRAMES WITH SIDESWAY AND FOR ANALYZING COMPRESSION MEMBERS AS PARTS OF RIGID FRAMES, Doctoral Thesis, New York University, (1948)

1.24 Kavanagh, T. C.
INSTABILITY OF PLANE TRUSS FRAMEWORKS, Doctoral Thesis, New York University, (1948)

1.25 Masur, E. F.
ON THE LATERAL STABILITY OF MULTI-STORY BENTS, Proc. of the ASCE, 81, Separate No. 672, (April 1955)

1.26 Linesley, R. H., and Chandler, D. B.
STABILITY FUNCTIONS FOR STRUCTURAL FRAME-WORKS, Manchester University Press, (1956)

1.27 Wood, R. H.
THE STABILITY OF TALL BUILDINGS, The Institute of Civil Engineers, Vol. 11, p. 69, (September 1958)

1.28 Marchant, W. and Salem, A. H.
THE USE OF STABILITY FUNCTIONS IN THE ANALYSIS OF RIGID FRAMES, Preliminary Publication, Sixth Congress of IABSE, Stockholm, (1960)

1.29 Chwalla, E. and Jokisch, F.
UBER DAS EBENE KNICKPLOBLEM DES STOCKWERKRAHMENS, Der Stahlbau, 14, No. 8/9 and 10/11, p. 33 and p. 47, (April and May, 1941)

1.30 Galambos, T. V.
INFLUENCE OF PARTIAL BASE FIXITY ON FRAME STABILITY, Proc. of the ASCE, 86, (ST5), p. 85, (May 1960)

1.31 Ojalvo, M. and Lu, L. W.
ANALYSIS OF FRAMES LOADED INTO THE PLASTIC RANGE, Proc. of the ASCE, 87, (EM4), p. 35, (August 1961)

1.32 Lu, L. W.
STABILITY OF ELASTIC AND PARTIALLY PLASTIC FRAMES, Ph. D. Dissertation, Lehigh University, (1960)

1.33 Winter, G., Hsu, P. T., Koo, B. and Loh, M. H.
BUCKLING OF TRUSSES AND RIGID FRAMES, Cornell University Engineering Experiment Station Bulletin No. 36, (1948)

1.34 Johnson, D. E.
LATERAL STABILITY OF FRAMES BY ENERGY METHOD, Proc. of the ASCE, 86, (EM3), p. 23, (August 1960)

1.35 Masur, E. F., Chang, I. C. and Donnell, L. H.
STABILITY OF FRAMES IN THE PRESENCE OF PRIMARY BENDING MOMENTS, Proc. of the ASCE, 87, (EM4), p. 19 (August 1961)

1.36 Livesley, R. K.
THE APPLICATION OF AN ELECTRONIC DIGITAL COMPUTER TO SOME PROBLEMS OF STRUCTURAL ANALYSIS, The Structural Engineer, 34 No. 1, p. 1, (January 1956)

1.37 Livesley, R. K.
SYMPOSIUM ON THE USE OF ELECTRONIC COMPUTERS IN STRUCTURAL ENGINEERING, University of Southampton (1959)

1.38 Japanese Column Research Council
ELASTIC STABILITY FORMULAS, PART 3, Chapter 1, (1960)

1.39 Horne, M. R.
THE STABILITY OF ELASTIC-PLASTIC STRUCTURES in "Progress in Solid Mechanics" edited by I. N. Sneddon and R. Hill, North-Holland Publishing Co., Amsterdam, (1961)

1.40 Lu, L. W.
A SURVEY OF LITERATURE ON THE STABILITY OF FRAMES, Welding Research Council Bulletin, No. 81, (September 1962)

1.41 Rawlings, B.
ENERGY RELATIONSHIPS IN PLASTIC STEEL STRUCTURES, Proc. of the ASCE, 88, (ST4), p. 159, (August 1962)

1.42 Jennings, A.
THE ELASTIC STABILITY OF RIGIDLY JOINTED FRAMES, International Journal of Mechanical Sciences, Vol. 5, pp. 99-113, (1963)

1.43 Temple, G. and Bickley, W. G.
RAYLEIGH'S PRINCIPLE, Oxford University Press (1933)

1.44 Timoshenko, S.
THEORY OF ELASTIC STABILITY, McGraw Hill Book Co., New York, (1936)

1.45 Bleich, F.
BUCKLING STRENGTH OF METAL STRUCTURES, McGraw-Hill Book Co., New York, (1952)

1.46 Hoff, N. J.
THE ANALYSIS OF STRUCTURES, John Wiley and Sons, Inc., New York, (1956)

1.47 LaSalle, J. and Lefschetz, S.
STABILITY BY LIAPUNOV'S DIRECT METHOD, Academic Press, New York, (1961)

1.48 Chwalla, E. and Kollbrunner, C. F.
BEITRAEGE ZUM KNICKPROBLEM DES BOGENTRAEGERS UND DES RAHMENS, Der Stahlbau, 11, No. 12, p. 94 (June 1938)

1.49 Lu, L. W. and G. C. Driscoll, Jr.
BUCKLING TESTS ON MODEL FRAMES, Report 276.4 Fritz Engrg. Lab., Lehigh University, Bethlehem, Pa. (1963)

1.50 Bolton, A.
STRUCTURAL FRAMEWORK, Ph. D. Dissertation, Manchester University, (1947)

1.51 Gurney, T. R.
FRAME INSTABILITY OF PARTIALLY PLASTIC STRUCTURES, British Welding Research Association, Report FE 1/56/68, (1947)

1.52 Salem, A.
FRAME INSTABILITY IN THE PLASTIC RANGE, Ph. D. Dissertation, Manchester University, (1958)

1.53 Wood, R. H.
THE STABILITY OF TALL BUILDINGS, Proc. Instn. Civ. Engrgs., 11, p. 69, (September 1958)

1.54 Low, M. W.
SOME MODEL TESTS ON MULTI-STORY RIGID STEEL FRAMES, Proc., Institution of Civil Engineering, Vol. 13, p. 287, (1959)

2.1 Ojalvo, M.
RESTRAINED COLUMNS, Ph. D. Dissertation, Lehigh University, (1960)

2.2 Ketter, R. L., Kaminsky, E. L. and Beedle, L. S.
PLASTIC DEFORMATION OF WIDE-FLANGE BEAM COLUMNS, ASCE Transactions, Vol. 120, (1955)

2.3 Lay, Maxwell G.
THE STATIC LOAD-DEFORMATION BEHAVIOR OF PLANAR STEEL STRUCTURES, Ph. D. Dissertation, Lehigh University, (1964)

3.1 Tall, L. Huber, A. W. and Beedle, L. S.
RESIDUAL STRESS AND THE INSTABILITY OF AXIALLY LOADED COLUMNS, Fritz Laboratory Report No. 220A.35, Lehigh University (1960)

3.2 Fukumoto, Yuhshi
MOMENT-CURVATURE-THRUST PROGRAM FOR WIDE-FLANGE SHAPES, Fritz Engineering Laboratory Report No. 205A.37, (1963)

5.1 Yen, Yu-Chin, Lu, Le-Wu and Driscoll, Jr. G. C.
PROPOSAL FOR INVESTIGATION OF INSTABILITY OF MULTI-STORY FRAMES, Fritz Laboratory Report No. 276.11, (October 1962)

5.2 Computing Laboratory, Lehigh University
WIZ COMPILER LANGUAGE, (September 1963)

6.1 Merchant, W.
THE FAILURE LOAD OF RIGID JOINTED FRAMEWORKS AS INFLUENCED BY STABILITY, The Structural Engineering, 32, No. 7, p. 185, (July 1954)

7.1 WRC and ASCE
COMMENTARY ON PLASTIC DESIGN IN STEEL, ASCE Manual (1961)

8.1 Column Research Council
GUIDE TO DESIGN CRITERIA FOR METAL COMPRESSION MEMBERS (1960)

14. VITA

The author was born as the second child of Yon-shi and Chong-Tien Yen on February 16, 1931 in Taiwan, China.

He attended Taiwan Cheng Kung University, Tainan, Taiwan from September 1949 to July 1953. There he received the degree of Bachelor of Science in Civil Engineering.

After graduation he taught one year in the School of Technology, affiliated with the University. In September 1954 he joined the Wu-Sheh Dam Project, Taiwan Power Company as a design engineer. In 1957 he was appointed the head of the Dam Design Section, Design Division of the Wu-Sheh Dam Project.

He came to the United States in September 1959 after he was awarded the Henry Marison Byllesby Memorial Fellowship by Lehigh University.

In February 1960 he was appointed research assistant and completed his Master's Degree in October 1961.